NONLINEAR VIBRATION OF CYLINDRICAL SHELLS

Thesis by

Jay-Chung Chen

In Partial Fulfillment of the Requirements

For the Degree of

Doctor of Philosophy

California Institute of Technology

Pasadena, California

1972

(Submitted December 14, 1971)

ACKNOWLEDGMENT

The author is sincerely grateful to Dr. C. D. Babcock for the patient guidance and endless discussions provided by him during the course of this investigation. Throughout his graduate study, the author has benefited from the advice and counsel of Dr. E. E. Sechler; his continuous support is sincerely appreciated. The author is also indebted to Dr. D. A. Evensen of TRW, who made many helpful comments and suggestions. Thanks are also due Messrs. C. B. Hemphill and M. E. Jessey for their support in the experimental study, Mrs. Elizabeth Fox for typing the manuscript and Mrs. Betty Wood for the graphs and figures.

The author is employed by the Structures, Dynamics and Materials Section (formerly Applied Mechanics Section) of the Jet Propulsion Laboratory. Their permission to undertake this study, financial support and understanding are gratefully acknowledged.

Finally, the author is indebted to his wife, Christina, who has provided continuing encouragement throughout this study.

ABSTRACT

The large amplitude vibrations of a thin-walled cylindrical shell are analyzed using the Donnell's shallow-shell equations. A perturbation method is applied to reduce the nonlinear partial differential equations into a system of linear partial differential equations. The simply-supported boundary condition and the circumferential periodicity condition are satisfied. The resulting solution indicates that in addition to the fundamental modes, the response contains asymmetric modes as well as axisymmetric modes with the frequency twice that of the fundamental modes. In the previous investigations in which the Galerkins procedure was applied, only the additional axisymmetric modes were assumed.

Vibrations involving a single driven mode response are investigated. The results indicate that the nonlinearity is either softening or hardening depending on the mode. The vibrations involving both a driven mode and a companion mode are also investigated. The region where the companion mode participates in the vibration is obtained and the effects due to the participation of the companion mode are studied.

An experimental investigation is also conducted. The results are generally in agreement with the theory. "Non-stationary" response is detected at some frequencies for large amplitude response where the amplitude drifts from one value to another. Various nonlinear phenomena are observed and quantitative comparisons with the theoretical results are made.

TABLE OF CONTENTS

TABLE OF CONTENTS (Cont'd)

LIST OF FIGURES

LIST OF FIGURES (Cont'd)

LIST OF FIGURES (Cont'd)

NOMENCLATURE

SYMBOLS	DEFINITION
a	Amplitude of the driven mode
$A(\tau)$	Driven mode
b	Amplitude of the companion mode
$B(\tau)$	Companion mode
C	Coefficient of viscous damping
C_c	Critical damping
$c_1 \cdots c_8$	Constant coefficients of first order particular solution
D	Plate bending rigidity
E	Young's modulus
f	Amplitude of external forcing function
F	Stress function
$G_1 \text{---} G_4$ $\overline{G}_1 \text{---} \overline{G}_4$	Constants in the second order equations
$g_0 \text{----} g_6$ $\overline{g}_0 \text{----} \overline{g}_6$	First order complementary solution
h	Shell thickness
k	Length to radius ratio
L	Length of the shell
M_x, M_y, M_{xy}	Bending moment
m	Half axial wave number
n	Circumferential wave number
N_x, N_y, N_{xy}	Stress resultant
q(x, y, t)	External forcing function
r	Nondimensional bending rigidity = $\frac{h}{\sqrt{12}\,R}$

NOMENCLATURE (Cont'd)

SYMBOL	DEFINITION
R	Shell radius
S	Nondimensional axial coordinate
t	Time
T	Period of vibration
u	Axial displacement
U	Nondimensional axial displacement
v	Circumferential displacement
V	Nondimensional circumferential displacement
w	Radial displacement
w_m	Maximum radial displacement
W	Nondimensional radial displacement
W_1^p	First order particular solution
W_1^c	First order complementary solution
x	Longitudinal coordinate
y	Circumferential coordinate
z	Radial coordinate
X, Y	Constants
α	Nonlinear parameter
β, σ, η	Constants in the second order equations
a_1---a_3	First order particular solution
γ	Percentage of critical damping
ϕ	Nondimensional stress function
ρ	Density
ξ	Coefficient of Fourier expansion

NOMENCLATURE (Cont'd)

SYMBOL	DEFINITION
λ	Nondimensional frequency parameter
λ_c	Circumferential wave length
λ_o---λ_2	Perturbation values of nondimensional frequency parameter
ω	Frequency
Ω	Normalized frequency
ζ	Aspect ratio
ϵ	Small perturbation parameter
$\sigma_x, \sigma_y, \sigma_{xy}$	Stresses
$\epsilon_x, \epsilon_y, \epsilon_{xy}$	Strains
ν	Poisson's ratio
∇^4	Biharmonic operator
δ_a	Phase angle of the driven mode
δ_b	Phase angle of the companion mode
Γ	Constant
τ	Nondimensional time
θ	Nondimensional circumferential coordinate
ϕ_1^p	First order particular solution for stress function
ϕ_1^c	First order complementary solution for stress function

I. INTRODUCTION

Thin walled cylindrical shells have a wide application in modern aerospace vehicle structural design. With increasing vehicle speed and more powerful propulsion systems, the dynamic environment imposed on the vehicle structure becomes severe. Hence there is a growing appreciation of the importance of nonlinear effects in determining the stability and response of thin walled shells under dynamic loading. The nonlinearities considered here are of geometric nature, namely the large amplitude in the shell wall deformation makes the nonlinear relations between the strain and displacement necessary. However, the amplitude is small enough such that the strain itself is considered infinitesimal. Since the amplitude is of the order of shell thickness the nonlinear terms are small in the governing equation. But the effects due to this small nonlinearity can be quite pronounced as has been demonstrated in the buckling problem of cylindrical shells under axial compression.

The nonlinear effects of large amplitude vibration of cylindrical shells are demonstrated by two phenomena; namely, the response-frequency relationship in the vicinity of a resonant frequency and the occurrence of traveling wave response. Contrasted to the linear vibration in which the resonant frequency is independent of its amplitude of vibration, the resonant frequency in nonlinear vibration is a function of its amplitude. The response-frequency relationship will indicate whether the nonlinearity is of hardening type (frequency increasing with amplitude) or softening type (frequency decreasing with amplitude). Similar phenomenon can be observed on a much

simpler system such as a spring-mass system with a nonlinear characteristic in the spring (Ref. 1).

In the linear vibration of cylindrical shells, the response to a stationary periodic excitation is in the form of a standing wave. This standing wave will be in conformity with the distribution of the external excitation. In case of the external force applied on a discrete point, the standing wave will be symmetrical with respect to the point of application. In other words, the response will be a cosine function in both circumferential and axial direction with the origin at point of application. In the present investigation this standing wave will be referred to as a "driven mode."

A striking feature of the results of experimental observation of supersonic cylindrical shell flutter (Ref. 2) is the fact that "almost all the flutter modes observed in these experiments were of the circumferentially traveling-wave type." Such traveling waves are not predicted by linear theory and it was suggested in Ref. 2 that nonlinearities in the shell were responsible for the phenomenon. A circumferentially traveling wave in cylindrical shell response can be decomposed into a driven mode standing wave and another standing wave which is circumferentially 90 degrees out of phase with the driven mode (which will be referred to as a "companion mode" in this investigation). Therefore, the occurrence of the circumferentially traveling wave is a result of the companion mode being excited due to the nonlinearities in the shell response. Related studies on nonlinear vibrations of circular rings (Ref. 3) and circular plates (Ref. 4) have shown the need for including these companion modes in the study of

nonlinear forced vibrations of axisymmetric structures. In addition to the supersonic cylindrical shell flutter, the traveling wave responses have been observed in the sloshing-vibration of thin cylindrical shells (Ref. 5).

The problem of large amplitude vibration of cylindrical shells has given rise to a number of theoretical studies (Refs. 7 to 17). The basic approach used in these studies (except Ref. 17) is to assume the shape of the deflection in space, that is, the shape of the vibration mode, sometimes referred to as generalized coordinates, and then to derive a set of nonlinear ordinary differential equations by using Galerkin's approximation procedure. Subsequently, the nonlinear ordinary differential equations are solved to obtain the response-frequency relationship.

The Galerkin's method is a very powerful approximation method that reduces a system of nonlinear partial differential equations into a system of nonlinear ordinary differential equations which become manageable. Also the Galerkin's method provides insight to the nonlinear coupling of various vibration modes during the solution procedure. However, its results are highly dependent on the assumed deflection shape. Completely different results could be obtained by a small difference in the assumed deflection shape as can be seen from the previous investigations on this subject. Evensen (Ref. 18) and Dowell (Ref. 13) have pointed out that the axisymmetric modes in the assumed deflection shape play an important role in the outcome of the results. Yet there is no standard for selecting particular axisymmetric modes for the assumed deflection shape.

There is another constraint to the solutions of nonlinear vibration equations of cylindrical shells, namely the midplane circumferential displacement must satisfy the periodicity condition in the circumferential direction. This periodicity condition assures that the circumferential displacement will be continuous and single-valued whenever the circumferential coordinate moves by 2π. This constraint is identically satisfied in the linear cylindrical shell theory once the periodicity condition is satisfied by the radial (lateral) displacement due to the linear relation between the circumferential displacement and radial displacement. However, in the nonlinear theory of cylindrical shells, the circumferential and radial displacements are nonlinearly related and circumferentially periodicity of radial displacement does not necessarily enforce the same condition on the circumferential displacement. In general, for nonlinear vibrations of cylindrical shells the radial displacement is solved directly from the equations of motion and then the circumferential displacement is calculated as a function of the radial displacement. Therefore, in the Galerkin's procedure, the satisfaction of the circumferential periodicity condition by the circumferential displacement is solely dependent on the assumed deflection shape. Evensen (Ref. 3) has pointed out that violation of this circumferential periodicity condition may give incorrect results. It may be noted in passing that nonlinear static stability analyses have made use of this circumferentially periodicity condition since the 1941 paper by von Karman and Tsien (Ref. 6).

The present investigation will apply a perturbation technique using the ratio of maximum radial displacement to the radius of the shell as a small parameter to reduce the nonlinear partial differential equations into a system of linear partial differential equations. Then the solutions may be obtained without the handicap of selecting a particular set of deflections in the analysis. The usual response-frequency relationship will be calculated and the occurrence of traveling wave response will also be investigated. The resulting deflection shape will be discussed and compared with the previous studies to establish the important axisymmetric modes participating in the nonlinear vibration. This may provide a reasonable method for selecting the assumed deflection shape in future analyses using Galerkin's method which by far is the simplest method used by previous investigations in nonlinear vibration of shells.

In the following, a brief summary of previous investigations will be given and then the present investigation will be described. For the convenience of summary, the equations of motion will be discussed first. Finally an experimental investigation will be described.

II. DISCUSSIONS OF EQUATIONS OF MOTION

In most of the analyses of nonlinear vibration of cylindrical shells, the well-known Donnell's shallow-shell equations have been used because of their simplicity. However, the Donnell's equations are of an approximate nature, a simplification of the full nonlinear shell equations in which the following quantities are neglected:

1. Inplane displacements in the curvature relations
2. Transverse shear force in the inplane equilibrium equations
3. Order $(\frac{h}{R})^2$ in the inplane shear force

   (i.e., $N_{xy} = N_{yx}$)
4. Tangential inertia
5. Rotary inertia

The Donnell's shallow-shell equations are often derived (Refs. 7 and 8) and are simply summarized here: The coordinate system, displacements and the resultant forces, moments are shown in Fig. 1 and Fig. 2 respectively. The equilibrium equations are:

$$\frac{\partial N_x}{\partial x} + \frac{\partial N_{xy}}{\partial y} = 0 \tag{2.1}$$

$$\frac{\partial N_{xy}}{\partial x} + \frac{\partial N_y}{\partial y} = 0 \tag{2.2}$$

$$\frac{\partial^2 M_x}{\partial x^2} + 2\frac{\partial^2 M_{xy}}{\partial x \partial y} + \frac{\partial^2 M_y}{\partial y^2} + \frac{\partial}{\partial x}\left(N_x \frac{\partial w}{\partial x} + N_{xy}\frac{\partial w}{\partial y}\right) - \frac{\partial}{\partial y}\left(N_x \frac{\partial w}{\partial y} + N_{xy}\frac{\partial w}{\partial x}\right) + \frac{N_y}{R} + q(x,y,t) = \rho h \frac{\partial^2 w}{\partial t^2} \tag{2.3}$$

The resultant forces and moments per unit length are defined in terms of the stresses as follows:

$$N_x = \int_{-h/2}^{h/2} \sigma_{xx} dz, \quad N_{xy} = \int_{-h/2}^{h/2} \sigma_{xy} dz, \quad N_y = \int_{-h/2}^{h/2} \sigma_{yy} dz$$

$$M_x = \int_{-h/2}^{h/2} \sigma_{xx} z dz, \quad M_{xy} = \int_{-h/2}^{h/2} \sigma_{xy} z dz, \quad M_y = \int_{-h/2}^{h/2} \sigma_{yy} z dz \tag{2.4}$$

The applied external load $q(x, y, t)$ acts in the radial direction.

The constitutive law for the cylindrical shell of isotropic linear elastic material is as follows:

$$\sigma_{xx} = \frac{E}{1-\nu^2} (\epsilon_{xx} + \nu \epsilon_{yy})$$

$$\sigma_{yy} = \frac{E}{1-\nu^2} (\epsilon_{yy} + \nu \epsilon_{xx}) \tag{2.5}$$

$$\sigma_{xy} = \frac{E}{2(1+\nu)} \epsilon_{xy}$$

where E is Young's modulus and ν is Poisson's ratio. The strain-displacement relations are approximated by

$$\epsilon_{xx} = \frac{\partial u}{\partial x} + \frac{1}{2} \left(\frac{\partial w}{\partial x}\right)^2 - z \frac{\partial^2 w}{\partial x^2}$$

$$\epsilon_{yy} = \frac{\partial v}{\partial y} - \frac{w}{R} + \frac{1}{2} \left(\frac{\partial w}{\partial y}\right)^2 - z \frac{\partial^2 w}{\partial y^2} \tag{2.6}$$

$$\epsilon_{xy} = \frac{\partial v}{\partial x} + \frac{\partial u}{\partial y} + \frac{\partial w}{\partial x} \frac{\partial w}{\partial y} - 2z \frac{\partial^2 w}{\partial x \partial y}$$

Using the constitutive law (eqs. 2.5) and the strain-displacement relation (eqs. 2.6), the resultant forces and moments (eqs. 2.4) can be written in terms of displacements:

$$N_x = \frac{Eh}{1-\nu^2}\{\frac{\partial u}{\partial x} + \nu[\frac{\partial v}{\partial y} - \frac{w}{R}] + \frac{1}{2}[(\frac{\partial w}{\partial x})^2 + \nu(\frac{\partial w}{\partial y})^2]\}$$

$$N_y = \frac{Eh}{1-\nu^2}\{\frac{\partial v}{\partial y} - \frac{w}{R} + \nu\frac{\partial u}{\partial x} + \frac{1}{2}[(\frac{\partial w}{\partial y})^2 + \nu(\frac{\partial w}{\partial x})^2]\} \qquad (2.7)$$

$$N_{xy} = \frac{Eh}{2(1+\nu)}(\frac{\partial v}{\partial x} + \frac{\partial u}{\partial y} + \frac{\partial w}{\partial x}\frac{\partial w}{\partial y})$$

$$M_x = -D(\frac{\partial^2 w}{\partial x^2} + \nu\frac{\partial^2 w}{\partial y^2})$$

$$M_y = -D(\frac{\partial^2 w}{\partial y^2} + \nu\frac{\partial^2 w}{\partial x^2}) \qquad (2.8)$$

$$M_{xy} = -D(1-\nu)\frac{\partial^2 w}{\partial x \partial y}$$

where the shell bending rigidity $D = \frac{Eh^3}{12(1-\nu^2)}$

Using eqs. (2.1), (2.2) and (2.8), eq. (2.3) can be rewritten as

$$D\nabla^4 w + \rho h\frac{\partial^2 w}{\partial t^2} = q(x, y, t) + \frac{N_y}{R} + N_x\frac{\partial^2 w}{\partial x} + 2N_{xy}\frac{\partial^2 w}{\partial x \partial y} + N_y\frac{\partial^2 w}{\partial y} \qquad (2.9)$$

where ∇^4 is a biharmonic operator $\nabla^4 = \frac{\partial^4}{\partial x^4} + 2\frac{\partial^4}{\partial x^2 \partial y^2} + \frac{\partial^4}{\partial y^4}$

Now by assuming a stress function $F(x, y, t)$

$$N_x = \frac{\partial^2 F}{\partial y^2}$$
$$N_y = \frac{\partial^2 F}{\partial x^2} \qquad (2.10)$$
$$N_{xy} = - \frac{\partial^2 F}{\partial x \partial y}$$

The equilibrium equations (2.1) and (2.2) are identically satisfied and eq. (2.9) becomes

$$D\nabla^4 w + \rho h \frac{\partial^2 w}{\partial t^2} = q(x, y, t) + \frac{1}{R} \frac{\partial^2 F}{\partial x^2} + \left(\frac{\partial^2 F}{\partial y^2} \frac{\partial^2 w}{\partial x^2}\right.$$
$$\left. -2 \frac{\partial^2 F}{\partial x \partial y} \frac{\partial^2 w}{\partial x \partial y} + \frac{\partial^2 F}{\partial x^2} \frac{\partial^2 w}{\partial y^2}\right) = 0 \qquad (2.11)$$

On the other hand, from eqs. (2.7) the compatibility equation can be obtained by eliminating the inplane displacements u, v as follows

$$\frac{1}{Eh} \nabla^4 F = - \frac{1}{R} \frac{\partial^2 w}{\partial x^2} + \left[\left(\frac{\partial^2 w}{\partial x \partial y}\right)^2 - \frac{\partial^2 w}{\partial x^2} \frac{\partial^2 w}{\partial y^2}\right] \qquad (2.12)$$

Equations (2.11) and (2.12) are generally referred to as Donnell's shallow-shell equations which have been used in the previous investigation of nonlinear vibrations (except Refs. 11, 17).

The boundary conditions in this investigation are assumed to be the "classical simply-supported" conditions, sometimes referred to as SS1/SS1 conditions. Mathematically, they can be expressed as:

$$w = M_x = N_x = v = 0 \quad \text{at} \quad x = 0, L \qquad (2.13)$$

For a complete cylindrical shell such as is considered here,

it is apparent that the displacements, slope, moments, shears and stresses must all satisfy the periodicity condition in the circumferential direction. The dependent variables w and F in equations (2. 11) and (2. 12) can be enforced to satisfy this periodicity condition during the solution procedure. However the periodicity of w and F is not sufficient for the other physical quantities to satisfy the periodicity condition as can be shown from eqs. (2. 7) and (2. 8). Therefore it is necessary that in addition to w and F, the circumferential displacement v must also be enforced to satisfy the circumferential periodicity condition. (Note from eq. (2. 7) that axial displacement u satisfies the circumferential periodicity condition whenever the circumferential displacement satisfies the same condition.)

Hence

$$w(x, y, t) = w(x, y + 2\pi R, t)$$

$$F(x, y, t) = F(x, y+2\pi R, t) \qquad (2.14a)$$

$$v(x, y, t) = v(x, y+2\pi R, t) \qquad (2.14b)$$

are the additional constraints that the solutions of differential equations (2. 11) and (2. 12) must satisfy. This circumferential periodicity condition is sometimes referred to as the continuity condition (Refs. 13, 14).

For simplicity, the radial external loading q has been taken to be

$$q(x, y, t) = \bar{f}\cos\omega t\cos\frac{ny}{R}\sin\frac{m\pi x}{L} \tag{2.15}$$

since a "steady state" solution (note that "steady state" means periodic in time) is sought, no initial conditions are necessary.

In Donnell's shallow-shell equations the neglecting of inplane displacements in the curvature relations and transverse shear force in the inplane equilibrium equations is the result of shallow-shell approximation in which the circumferential wave length $\frac{2\pi R}{n}$ (n is the circumferential wave number) of the deformation pattern is always small compared with the radius R. Essentially, it is saying that the curvature and inplane equilibrium of the cylindrical shell are the same as a flat plate. Tangential inertias $\frac{\partial^2 u}{\partial t^2}$, $\frac{\partial^2 v}{\partial t^2}$ are neglected because of the assumption that the flexural motion is predominant in the present investigation. Rotary inertia is neglected because the wave lengths $\frac{2\pi R}{n}$ and $\frac{2L}{m}$ (m is the half axial wave number) are large compared to the shell thickness h.

El Raheb (Ref. 19) has made a detailed comparison for linear vibration between the results of Donnell's equations and the "exact" equations of motion derived by Koiter (Ref. 20) based on the Love-Kirchhoff hypothesis for shell theory in which all the quantities neglected in the Donnell's equations have been retained. He defined that the errors in frequency obtained by approximation as

$$e = \frac{\omega_{approx.}}{\omega_{exact}} - 1 \tag{2.16}$$

and concluded that:

1. Maximum error due to neglecting inplane displacements in curvature and transverse shear in inplane equilibrium is

$$(e_1)_{max} \simeq \frac{3^{3/4} \cdot r^{1/2}}{4(1-\nu^2)^{1/4} \cdot S} \qquad (2.17)$$

where $r = \frac{h}{\sqrt{12}\,R}$, $S = \frac{m\pi R}{L}$

m is half axial wave number.

2. Maximum error due to neglecting tangential inertia is

$$e_2 \simeq \frac{1}{2n^2} \quad \text{for} \quad n >> 3 \qquad (2.18)$$

This error is more pronounced for small n which is the circumferential wave number.

3. Error due to neglecting rotary inertia is

$$e_3 = \frac{r^2(S^2+n^2)}{2} \qquad (2.19)$$

With these estimations in errors due to the approximations in Donnell's shallow-shell equations, the present investigation will be limited to shells with the following configuration:

$$\frac{h}{\sqrt{12}R} \leqslant \frac{1}{100} , \quad \frac{L}{R} \leqslant 10 \qquad (2.20)$$

Also the deformation pattern will be limited to

$$4 \leqslant n \leqslant 30 , \qquad 1 \leqslant m \leqslant 6 \qquad (2.21)$$

so as to keep the errors within the acceptable range.

For example, the typical error for a shell having $\frac{h}{R} = \frac{1}{400}$, $\frac{L}{R} = 2$, m = 1, n = 5, will be

$$e_T = e_1 + e_2 + e_3 = 0.009979 + 0.02 + 0.0000072 \qquad (2.22)$$

$$\cong 3\%$$

As can be seen, the largest error is caused by neglecting the tangential inertia. However, this error will be rapidly reduced for larger circumferential wave number n.

Although El Raheb's error estimation for Donnell's shallow-shell equation has been made for the linear vibration, it is assumed that it will also be applicable to nonlinear vibrations. This will be true as long as the nonlinearity is small, as will be demonstrated later for the present investigation. Therefore the Donnell's shallow-shell equations will be used for the analysis of nonlinear vibration of cylindrical shells within the limits specified by (2. 20) and (2. 21).

III. SUMMARY OF PREVIOUS INVESTIGATIONS

In a pioneering work, Reissner (Ref. 7) analyzed the problem of nonlinear vibration of cylindrical shell using Donnell's shallow-shell equations (2.11) and (2.12) by assuming the deflection shape of the linear vibration. His results indicated that the nonlinearity could be either of the hardening or softening type, depending upon the geometry of the single half-wave or lobe chosen to be analyzed. Chu (Ref. 8) employed the same assumed mode shape as that of Reissner's but analyzed somewhat differently. His results indicated that the nonlinearity was always of the hardening type and could be strong in some cases. Cummings (Ref. 9) employed a Galerkin procedure and found that the results varied with the region of integration. The results over a single half-wave or lobe were the same as those of Reissner. The results for a complete shell were similar to those of Chu. Thus, it appeared that Reissner's results were characteristic of curved panels whereas Chu's calculations were apparently applicable to complete cylindrical shells. These three analyses did not investigate the traveling wave solution and the boundary conditions were partially satisfied; also the circumferential periodicity condition was violated by Chu (Ref. 8).

Nowinski (Ref. 10) applied Galerkin's procedure with an additional axisymmetric term in the assumed deflection shape. Thus the circumferential continuity condition was satisfied. His results were virtually identical to those of Chu in the isotropic case. However, his assumed deflection shape did not satisfy $w = 0$ at both ends of the shell.

Evensen solved a ring problem in considerable detail (Ref. 3) and subsequently investigated a cylindrical shell (Ref. 12). The mode shape Evensen assumed in his Galerkin procedure satisfied the circumferential periodicity condition but the boundary conditions were partially satisfied as long as a simply supported condition was considered. His results for the shell included the traveling wave response and a stability analysis which indicated the stability region of standing wave response and traveling wave response.

Dowell (Ref. 13) made a similar analysis to that of Evensen with a slightly different axisymmetric mode term in the assumed deflection shape. In his analysis all the simply supported boundary conditions and circumferentially periodicity conditions were satisfied "on the average." Although no numerical results were given, the modal equations obtained in the limiting case of $L/R \to \infty$ agreed with that of ring equations and $L/R \to 0$ agreed with that of plate equation.

Matsuzaki and Kobayashi (Refs. 15 and 16) carried out an analysis on a cylindrical shell with clamped ends. The method was similar to that of Evensen (Ref. 12). The results showed the nonlinearity being of the softening type.

Mayers and Wrenn (Ref. 11) used a more general assumed deflection shape than that of Evensen which satisfied all the out of plane boundary conditions but the inplane boundary conditions were not satisfied. Also in Ref. 11 more accurate shell equations (Sander's theory) were considered.

Bleich and Ginsberg (Ref. 17) recently considered an infinitely long cylindrical shell (periodic in axial direction). Their approach was to express three displacements in complete sets of normal mode series and then the energy expression was obtained in terms of these series. Lagrange equations were used to establish the equilibrium conditions and a perturbation method was employed to determine the truncation of the infinite series. Response-frequency relationship traveling wave response and stability analysis were included in the results. Tangential inertia and transverse shear deformation were included in the energy expression.

It is of interest to contrast and compare the analyses of Refs. 8, 10, 12 and 13, since these studies used the same Donnell's shallow shell equations (eqs. 2.11 and 2.12) and considered the simply supported end conditions (eq. 2.13). Also these four studies represent the major effort in the previous investigation on the problem of nonlinear vibration of cylindrical shells. In the following, their approach, satisfaction of boundary conditions and circumferential periodicity condition, and results will be summarized.

1. Chu (Ref. 8)

   a) Assumed deflection shape:

$$w(x, y, t) = AH(t)\sin\left(\frac{\pi x}{L}\right)\cos\left(\frac{ny}{R}\right) \qquad (3.1)$$

   This is the mode shape of linear vibration.

   b) Approach:

   Substituting eq. (3.1) into eq. (2.12), a particular solution of the stress function F can be obtained. The assumed

deflection w and the solution of stress function F are substituted into eq. (2.11) and the collection of the first harmonic terms gives a nonlinear ordinary differential equation which is subsequently solved by using elliptic integrals to obtain the response-frequency relationship.

c) Boundary conditions: (at x = 0 and L)

Out of plane boundary conditions,

$$w = 0, \quad M_x = 0$$

Inplane boundary conditions

$$N_x \neq 0, \quad v \neq 0$$

d) Circumferential periodicity condition: not satisfied.

e) Results: hardening type of nonlinearity is found.

2. Nowinski (Ref. 10)

a) Assumed deflection shape:

$$w(x, y, t) = f(t)\sin\frac{m\pi x}{L}\sin\frac{ny}{R} + f_o(t) \qquad (3.2)$$

An axisymmetric term is added to the assumed deflection shape. Stress function is obtained in a similar fashion as that of Chu.

b) Approach:

Eq. (3.2) and stress function F are substituted into eq. (2.11) and then a Galerkin procedure is applied to reduce eq. (2.11) into an ordinary equation. The weighting function chosen for the Galerkin procedure is $\sin\frac{m\pi x}{L}\sin\frac{ny}{R}$ which effectively eliminates the coupling effect of $f_o(t)$ from the problem.

c) Boundary conditions: (at x = 0 and L)

Out of plane boundary conditions

$$w \neq 0, \quad M_x = 0$$

Inplane boundary conditions

$$N_x \neq 0, \quad v \neq 0$$

d) Circumferential periodicity condition:

This condition is satisfied by determining $f_o(t)$ in terms of $f(t)$.

e) Results: hardening type of nonlinearity is found.

3. Evensen (Ref. 12):

a) Assumed deflection shape:

$$w(x, y, t) = \left[A(t)\cos\frac{ny}{R} + B(t)\sin\frac{ny}{R}\right]\sin\frac{m\pi x}{R} + \frac{n^2}{4R}\left[A^2(t) + B^2(t)\right]\sin^2\frac{m\pi x}{L} \tag{3.3}$$

The companion mode as well as the driven mode are considered. Also there are two terms in the axisymmetric mode since $\sin^2\frac{m\pi x}{L} = \frac{1}{2}\left(1-\cos\frac{2m\pi x}{L}\right)$

b) Approach:

Stress function F is obtained as a particular solution to eq. (2.12) which is substituted into eq. (2.11) together with eq. (3.3). Galerkin procedure is employed to reduce eq. (2.11) into two nonlinear ordinary equations. Choice of weighting functions are made such that the resulting equations are the same as would be obtained using Hamilton's principle, namely, $\frac{\partial w}{\partial A}$ and $\frac{\partial w}{\partial B}$.

This provides the coupling effect of the axisymmetric modes to the fundamental modes.

c) Boundary conditions: (at x = 0 and L)

Out of plane boundary conditions:

$w = 0, \quad M_x \neq 0$

Inplane boundary conditions:

$N_x \neq 0, \quad v \neq 0$

d) Circumferential periodicity conditions: satisfied.

e) Results:

Type of nonlinearity is found depending on the "Aspect Ratio" (ratio of circumferential wave length to axial wave length). For small aspect ratio, the nonlinearity is of the softening type, for large aspect ratio the nonlinearity is of the hardening type. The traveling wave response and the stability problem are also studied.

4. Dowell (Ref. 13):

a) Assumed deflection shape:

$$w(x, y, t) = \left[A(t)\cos\frac{ny}{R} + B(t)\sin\frac{ny}{R}\right]\sin\frac{m\pi x}{L} + A_o(t)\sin\frac{m\pi x}{L} \tag{3.4}$$

Here the coefficient of the axisymmetric mode is considered as independent of the driven mode A(t) and companion mode B(t).

b) Approach:

The stress function F is solved from eq. (2.12) by using eq. (3.4). A homogeneous solution is included in the

following form:

$$F_{homo} = \frac{1}{2}\overline{N}_x + \frac{1}{2}\overline{N}_y x^2 - \overline{N}_{xy}\, xy \qquad (3.5)$$

This satisfies the equation $\nabla^4 F = 0$. $\overline{N}_x$, $\overline{N}_y$ and $\overline{N}_{xy}$ are functions of time t only and are to be determined by considering the inplane boundary condition and circumferential periodicity conditions. Three nonlinear ordinary differential equations are obtained after employing the Galerkin procedure. The choice of the weighting functions is the same as that of Evensen.

c) Boundary conditions:

Out of plane boundary conditions:

$w = 0, \quad M_x = 0$

Inplane boundary conditions are satisfied "on the average;"

$$\int_0^{2\pi R}\int_0^{L} \frac{\partial u}{\partial x}\, dxdy = 0, \quad \int_0^{2\pi R} N_{xy}\, dxdy = 0$$

d) Circumferential periodicity condition is satisfied "on the average;"

$$\int_0^{L}\int_0^{2\pi R} \frac{\partial v}{\partial y}\, dydx = \int_0^{L} [v(x, 2\pi R) - v(x, 0)]\, dx = 0$$

e) Results:

Numerical results are not given. But, in the limiting cases, the resulting differential equations converge to the equation of a plate for $\frac{L}{R} \to 0$ and the equation of a ring for $\frac{L}{R} \to \infty$. However, for $\frac{L}{R} \to \infty$ and m even, the reduced ring equation loses the coupling effect

between A(t), B(t) and $A_o(t)$ and leads to a hardening type nonlinearity. This is in contrast to the findings by Evensen (Ref. 3).

The conclusion emerging from these four previous studies clearly indicates the following:

1) The assumed deflection shape plays an important role in the analysis and the results are somewhat dictated by the assumed deflection shape.
2) Specified boundary conditions are not enforced strictly in the previous studies. Evensen (Ref. 21) has shown that added inplane restraints may alter the response-frequency relationship.
3) Circumferential periodicity condition must be satisfied. One of the purposes of the present investigation is to avoid the necessity of assuming the deflection shape, instead the deflection shape will be obtained as a result of the perturbation technique. Boundary conditions and circumferential periodicity conditions will be satisfied asymptotically with respect to a small parameter in the present investigation.

IV. PERTURBATION METHOD

One of the important methods for solving nonlinear differential equations is the perturbation method. The use of this method was, in the early days, limited to astronomical calculations. But the important contributions of Poincaré and later mathematicians have broadened the capability of the method to include a more general field of nonlinear mechanics.

This method is applicable to equations in which a small parameter is associated with nonlinear terms. In application, it consists of developing the desired quantities in powers of the small parameter multiplied by coefficients which are functions of the independent variable and determining the coefficients of the developments one by one, usually by solving a sequence of linear equations.

In nonlinear vibration of cylindrical shells, it would be natural to regard the amplitude of response as a quantity to be determined by the power series expansion of the small parameter. However by proceeding in this way a serious difficulty may be encountered in the form of the so-called "secular terms," i.e., terms which grow up indefinitely as $t \to \infty$. The appearance of the secular terms shows that the expansion of response is asymptotically valid only for a finite time. Previous experience has indicated that the essential feature omitted from the expansion of response in a power series of small parameter is the dependence of the frequency on the response amplitude. Therefore, the frequency as well as the amplitude of the response must be expressed in the power series of

a small parameter in the perturbation method. Then, elimination of secular terms in the solution will provide the frequency-response relationship.

First the small nondimensional parameter used in the power series expansion must be determined. In the vibration of cylindrical shells the maximum amplitude of response is of the order of shell thickness h. Since thin-walled shells ($\frac{h}{R} << 1$) are considered, it seems natural that the small parameter ϵ be chosen as $\frac{w_m}{R}$ where w_m is the maximum radial displacement of the shell.

4.1 Nondimensionalization and Systems of Linear Equations

Before proceeding in applying the perturbation method, the differential equations must be rewritten in the nondimensional form. Also the effect of damping will be included in the analysis by inducing a viscous damping term in the equilibrium equation:

$$D\nabla^4 w + \rho h \frac{\partial^2 w}{\partial t^2} + Ch \frac{\partial w}{\partial t} = q(x, y, t) + \frac{1}{R} \frac{\partial^2 F}{\partial x^2}$$

$$+\left(\frac{\partial^2 F}{\partial y^2} \frac{\partial^2 w}{\partial x^2} - 2 \frac{\partial^2 F}{\partial x \partial y} \frac{\partial^2 w}{\partial x \partial y} + \frac{\partial^2 F}{\partial x^2} \frac{\partial^2 w}{\partial y^2}\right) = 0 \qquad (4.1)$$

$$\frac{1}{Eh} \nabla^4 F = -\frac{1}{R} \frac{\partial^2 w}{\partial x^2} + \left[\left(\frac{\partial^2 w}{\partial x \partial y}\right)^2 - \frac{\partial^2 w}{\partial x^2} \frac{\partial^2 w}{\partial y^2}\right] \qquad (4.2)$$

where C is the coefficient of linear viscous damping.

Next, let the nondimensional independent variables be defined as follows:

$$s = \frac{x}{L}, \quad \theta = \frac{y}{R} \qquad \tau = \omega t \qquad (4.3)$$

where ω is the frequency of the system.

Next, the nondimensional displacements and stress functions are defined as follows:

$$\left.\begin{aligned} W(s,\theta,\tau) &= \frac{w(x,y,t)}{w_m} \\ U(s,\theta,\tau) &= \frac{u(x,y,t)}{w_m} \\ V(s,\theta,\tau) &= \frac{v(x,y,t)}{w_m} \end{aligned}\right\} \qquad (4.4)$$

$$\phi(s,\theta,\tau) = \frac{1-\nu^2}{Ehw_m R} F(x,y,t) \qquad (4.5)$$

where w_m is the maximum radial displacement. Also the following nondimensional quantities are defined:

$$k = \frac{L}{R}, \quad \epsilon = \frac{w_m}{R}, \quad r = \frac{1}{\sqrt{12}} \frac{h}{R}$$

$$\lambda = \frac{(1-\nu^2)\rho R^2 \omega^2}{E}, \quad Q(s,\theta,\tau) = \frac{(1-\nu^2)R^2}{Eh^2} q(x,y,t) \qquad (4.6)$$

$$\gamma = \frac{C}{C_c}, \qquad C_c = \rho\omega_o, \qquad \bar{q}(s,\theta,\tau) = \frac{h}{w_m} Q(s,\theta,\tau)$$

where ω_o is the frequency of linear vibration of a cylindrical shell to be defined later.

Upon substituting eqs. (4.3), (4.4), (4.5) and (4.6) into eqs. (4.1) and (4.2), the nondimensional Donnell's shallow-shell equation can be written as

$$r^2\left[\frac{1}{k^4}\frac{\partial^4 W}{\partial s^4} + \frac{2}{k^2}\frac{\partial^4 W}{\partial s^2 \partial\theta^2} + \frac{\partial^4 W}{\partial\theta^4}\right] + \lambda\frac{\partial^2 W}{\partial\tau^2} + 2\sqrt{\lambda}\sqrt{\lambda_o}\gamma'\frac{\partial W}{\partial\tau}$$

$$= \bar{q}(s,\theta,\tau) + \frac{1}{k^2}\frac{\partial^2 W}{\partial s^2} + \frac{\epsilon}{k^2}\left(\frac{\partial^2\phi}{\partial\theta^2}\frac{\partial W}{\partial s^2} - 2\frac{\partial^2\phi}{\partial\theta\partial s}\frac{\partial^2 W}{\partial\theta\partial s} + \frac{\partial^2\phi}{\partial s^2}\frac{\partial^2 W}{\partial\theta^2}\right) \qquad (4.7)$$

$$\frac{1}{1-\nu^2}\left[\frac{1}{k^4}\frac{\partial^4\phi}{\partial s^4}+\frac{2}{k^2}\frac{\partial^4\phi}{\partial s^2\partial\theta^2}+\frac{\partial^4\phi}{\partial\theta^4}\right]=-\frac{1}{k^2}\frac{\partial^2 W}{\partial s^2}+\frac{\epsilon}{k^2}\left[\left(\frac{\partial^2 W}{\partial\theta\partial s}\right)^2-\frac{\partial^2 W}{\partial s^2}\frac{\partial^2 W}{\partial\theta^2}\right] \tag{4.8}$$

The boundary condition can be obtained as:

$$W=\left(\frac{1}{k^2}\frac{\partial^2 W}{\partial s^2}+\nu\frac{\partial^2 W}{\partial\theta^2}\right)=\frac{\partial^2\phi}{\partial\theta^2}=V=0 \quad \text{at } s=0,1 \tag{4.9}$$

The circumferential periodicity condition,

$$\int_0^{2\pi}\frac{\partial V}{\partial\theta}\,d\theta=\int_0^{2\pi}\left\{\frac{1}{1-\nu^2}\left[\frac{1}{k^2}\frac{\partial^2\phi}{\partial s^2}-\nu\frac{\partial^2\phi}{\partial\theta^2}\right]+\left[W-\tfrac{1}{2}\epsilon\left(\frac{\partial W}{\partial\theta}\right)^2\right]\right\}d\theta=0, \tag{4.10}$$

eq. (4.10), is obtained from the first two equations of (2.7) by eliminating $\frac{\partial u}{\partial x}$.

From equation (2.15), it is obvious that

$$\bar{q}(s,\theta,\tau)=f\cos\tau\cos n\theta\sin m\pi s \tag{4.11}$$

$$\text{where } f=\frac{(1-\nu^2)R^2}{Eh^2}\quad \bar{f}=\frac{h}{w_m}G \tag{4.12}$$

It is clear now that the nonlinear terms in eqs. (4.7), (4.8) and (4.10) are multiplied by a small parameter ϵ. The dependent variable and nondimensional frequency parameter λ will be expanded into a power series of ϵ as follows:

$$W(s,\theta,\tau,\epsilon)=W_o(s,\theta,\tau)+\epsilon W_1(s,\theta,\tau)+\epsilon^2 W_2(s,\theta,\tau)+\cdots$$
$$\phi(s,\theta,\tau,\epsilon)=\phi_o(s,\theta,\tau)+\epsilon\phi_1(s,\theta,\tau)+\epsilon^2\phi_2(s,\theta,\tau)+\cdots \tag{4.13}$$

$$V(s,\theta,\tau,\epsilon) = V_o(s,\theta,\tau)+\epsilon V_1(s,\theta,\tau)+\epsilon^2 V_2(s,\theta,\tau) + \text{---}$$

(4.13) Cont'd

$$\lambda = \lambda_o + \epsilon\lambda_1 + \epsilon^2\lambda_2 + \text{---}$$

Substituting eq. (4.13) into eqs. (4.7), (4.8) and (4.10) and equating the terms with equal powers of ϵ, a system of linear equations may be obtained. However two assumptions will be made before the linearization, namely,

1) the amplitude of the periodical external forcing function q is small such that $f = \epsilon^2 f'$

2) the damping of the shell is also small such that $\gamma = \epsilon^2\bar{\gamma}$

Now the linearized system of equations are as follows; order of ϵ°

$$r^2\left[\frac{1}{k^4}\frac{\partial^4 W_o}{\partial s^4} + \frac{2}{k^2}\frac{\partial^4 W_o}{\partial s^2\partial\theta^2} + \frac{\partial^4 W_o}{\partial\theta^4}\right] + \lambda_o\frac{\partial^2 W_o}{\partial\tau^2} - \frac{1}{k^2}\frac{\partial^2\phi_o}{\partial s^2} = 0 \tag{4.14}$$

$$\frac{1}{1-\nu^2}\left[\frac{1}{k^4}\frac{\partial^4\phi_o}{\partial s^4} + \frac{2}{k^2}\frac{\partial^4\phi_o}{\partial s^2\partial\theta^2} + \frac{\partial^4\phi_o}{\partial\theta^4}\right] + \frac{1}{k^2}\frac{\partial^2 W_o}{\partial s^2} = 0 \tag{4.15}$$

boundary condition:

$$W_o = \frac{1}{k^2}\frac{\partial^2 W_o}{\partial s^2} + \nu\frac{\partial^2 W_o}{\partial\theta^2} = \frac{\partial^2\phi_o}{\partial\theta^2} = V_o = 0 \quad \text{at } s = 0, 1 \tag{4.16}$$

circumferential periodicity condition

$$\int_0^{2\pi}\frac{\partial V_o}{\partial\theta}\,d\theta = \int_0^{2\pi}\left\{\frac{1}{1-\nu^2}\left[\frac{1}{k^2}\frac{\partial^2\phi_o}{\partial s^2} - \nu\frac{\partial^2\phi_o}{\partial\theta^2}\right] + W_o\right\}d\theta = 0 \tag{4.17}$$

Order of ϵ

$$\left.\begin{aligned} & r^2\left[\frac{1}{k^4}\frac{\partial^4 W_1}{\partial s^4}+\frac{2}{k^2}\frac{\partial^4 W_1}{\partial s^2\partial\theta^2}+\frac{\partial^4 W_1}{\partial\theta^4}\right]+\lambda_o\frac{\partial^2 W_1}{\partial\tau^2}-\frac{1}{k^2}\frac{\partial^2\phi_1}{\partial s^2} \\ & =-\lambda_1\frac{\partial^2 W_o}{\partial\tau^2}+\frac{1}{k^2}\left(\frac{\partial^2\phi_o}{\partial\theta^2}\frac{\partial^2 W_o}{\partial s^2}-2\frac{\partial^2\phi_o}{\partial s\,\partial\theta}\frac{\partial^2 W_o}{\partial s\,\partial\theta}+\frac{\partial^2\phi_o}{\partial s^2}\frac{\partial^2 W_o}{\partial\theta^2}\right) \end{aligned}\right\} \quad (4.18)$$

$$\left.\begin{aligned} & \frac{1}{1-\nu^2}\left[\frac{1}{k^4}\frac{\partial^4\phi_1}{\partial s^4}+\frac{2}{k^2}\frac{\partial^4\phi_1}{\partial s^2\partial\theta^2}+\frac{\partial^4\phi_1}{\partial\theta^4}\right] \\ & \quad +\frac{1}{k^2}\frac{\partial^2 W_1}{\partial s^2}=\frac{1}{k^2}\left[\left(\frac{\partial^2 W_o}{\partial\theta\,\partial s}\right)^2-\frac{\partial^2 W_o}{\partial s^2}\frac{\partial^2 W_o}{\partial\theta^2}\right] \end{aligned}\right\} \quad (4.19)$$

boundary conditions:

$$W_1=\frac{1}{k^2}\frac{\partial^2 W_1}{\partial s^2}+\nu\frac{\partial^2 W_1}{\partial\theta^2}=\frac{\partial^2\phi_1}{\partial\theta^2}=V_1=0 \quad \text{at} \quad s=0,1 \quad (4.20)$$

circumferential periodicity condition,

$$\left.\begin{aligned} & \int_0^{2\pi}\frac{\partial V_1}{\partial\theta}d\theta=\int_0^{2\pi}\left\{\frac{1}{1-\nu^2}\left[\frac{1}{k^2}\frac{\partial^2\phi_1}{\partial s^2}-\nu\frac{\partial^2\phi_1}{\partial\theta^2}\right]\right. \\ & \quad \left.+\left[W_1-\tfrac{1}{2}\left(\frac{\partial W_o}{\partial\theta}\right)^2\right]\right\}d\theta=0 \end{aligned}\right\} \quad (4.21)$$

order of ϵ^2

$$\begin{aligned} & r^2\left[\frac{1}{k^2}\frac{\partial^4 W_2}{\partial s^4}+\frac{2}{k}\frac{\partial^4 W_2}{\partial s^2\partial\theta^2}+\frac{\partial^4 W_2}{\partial\theta^4}\right]+\lambda_o\frac{\partial^2 W_2}{\partial\tau^2}-\frac{1}{k^2}\frac{\partial\phi_2}{\partial s^2} \\ & =f\cos\tau\cos(n\theta)\sin(m\pi s)-\lambda_1\frac{\partial^2 W_1}{\partial\tau^2}-\lambda_2\frac{\partial^2 W_o}{\partial\tau^2}-\bar{\gamma}\sqrt{\lambda_o}\sqrt{\lambda}\frac{\partial W_o}{\partial\tau} \end{aligned} \quad (4.22)$$

$$+\frac{1}{k^2}\left[\frac{\partial^2\phi_o}{\partial\theta^2}\frac{\partial^2 W_1}{\partial s^2}+\frac{\partial^2\phi_1}{\partial\theta^2}\frac{\partial^2 W_o}{\partial s^2}-2\frac{\partial^2\phi_o}{\partial\theta\,\partial s}\frac{\partial^2 W_1}{\partial\theta\,\partial s}-\right.$$

$$\left.-2\frac{\partial^2\phi_1}{\partial\theta\,\partial s}\frac{\partial^2 W_o}{\partial\theta\,\partial s}+\frac{\partial^2\phi_o}{\partial s^2}\frac{\partial^2 W_1}{\partial\theta^2}+\frac{\partial^2\phi_1}{\partial s^2}\frac{\partial^2 W_o}{\partial\theta^2}\right] \qquad (4.22)\ \text{Cont'd}$$

$$\frac{1}{1-\nu^2}\left[\frac{1}{k^4}\frac{\partial^4\phi_2}{\partial s^4}+\frac{2}{k^2}\frac{\partial^4\phi_2}{\partial s^2\partial\theta^2}+\frac{\partial^4\phi_2}{\partial\theta^4}\right]+\frac{1}{k^2}\frac{\partial^2 W_2}{\partial s^2} \qquad (4.23$$

$$=\frac{1}{k^2}\left[2\frac{\partial^2 W_o}{\partial\theta\,\partial s}\frac{\partial^2 W_1}{\partial\theta\,\partial s}-\frac{\partial^2 W_o}{\partial\theta^2}\frac{\partial^2 W_1}{\partial\theta^2}\frac{\partial^2 W_o}{\partial\theta^2}\frac{\partial^2 W_1}{\partial s^2}\right]$$

boundary conditions

$$W_2=\frac{1}{k^2}\frac{\partial^2 W_2}{\partial s^2}+\nu\frac{\partial^2 W_2}{\partial\theta^2}=\frac{\partial^2\phi_2}{\partial\theta^2}=V_2=0 \text{ at } s=0,1 \qquad (4.24)$$

circumferential periodicity condition

$$\int_0^{2\pi}\frac{\partial V_2}{\partial\theta}\,d\theta=\int_0^{2\pi}\left\{\frac{1}{1-\nu^2}\left[\frac{1}{k^2}\frac{\partial^2\phi_2}{\partial s^2}-\nu\frac{\partial^2\phi_2}{\partial\theta^2}\right]+\right. \qquad (4.25)$$

$$\left.+\left[W_2-\frac{\partial W_o}{\partial\theta}\frac{\partial W_1}{\partial\theta}\right]\right\}d\theta=0$$

Similarly, the linearized equations for the order of ϵ^3 and higher can be written. In the following sections the equations for zero order, first order and second order of ϵ will be solved.

4.2 Solutions of Zero Order Equations

Equations (4.14) and (4.15) are the zero order equations which are identical to the linear equations of free vibration of cylindrical shells (see Appendix A). The solution can be readily obtained as:

$$W_o = \sum_{m=1}^{\infty} \sum_{n=1}^{\infty} [A_{mn}(\tau)\cos(n\theta) + B_{mn}(\tau)\sin(n\theta)] \sin(m\pi s) \qquad (4.26)$$

As indicated by the results of linear vibration (Appendix A), with an external forcing function of the form $f\cos\tau\cos n\theta \sin m\pi s$, the response at the vicinity of a resonance can be expressed as

$$W_o = a\cos\tau\cos(n\theta)\sin(m\pi s) \qquad (4.26a)$$

In nonlinear vibration of cylindrical shells, the circumferentially traveling wave response must be included. The traveling wave response may be expressed as:

$$W_{o_{(\text{traveling wave})}} = c\cos(\tau - n\theta)\sin(m\pi s)$$

$$= c[\cos\tau\cos(n\theta) + \sin\tau\sin(n\theta)] \sin(m\pi s) \qquad (4.27)$$

Combining the standing wave response, eq. (4.26) and traveling wave response, eq. (4.27), the zero order solution will be

$$W_o(s, \theta, \tau) = [A(\tau)\cos(n\theta) + B(\tau)\sin(n\theta)] \sin(m\pi s) \qquad (4.28)$$

where

$$\left.\begin{aligned} A(\tau) &= a\cos(\tau + \delta_a) \text{ and} \\ B(\tau) &= b\sin(\tau + \delta_b) \end{aligned}\right| \qquad (4.29)$$

where δ_a and δ_b are the phase angles which are included in the response due to the damping and nonlinear effects.

Comparing eqs. (4.28) and (4.26) indicates that the zero order solution is one of the solutions of the linear free vibration of

cylindrical shells.

Here $A(\tau)\cos(n\theta)\sin(m\pi s)$ will be referred to as the driven mode since it is spatially similar to the external forcing function. $B(\tau)\sin(n\theta)\sin(m\pi s)$ will be referred to as the companion mode since it is excited indirectly.

Substituting eq. (4.28) into eq. (4.15), the zero order stress function can be obtained as:

$$\phi_o = \Gamma[A(\tau)\cos(n\theta)+B(\tau)\sin(n\theta)]\sin(m\pi s) \tag{4.30}$$

where

$$\Gamma = \frac{(1-\nu^2)\zeta^2}{n^2(1+\zeta^2)^2} \quad , \qquad \zeta = \frac{m\pi}{nk} \tag{4.31}$$

With eq. (4.28) and eq. (4.30), it can be shown that the boundary conditions, eq. (4.16) and the circumferential periodicity condition are satisfied.

Substituting eqs. (14.28) and (4.30) into eq. (4.14), the zero order frequency parameter λ_o may be obtained as,

$$\lambda_o = r^2\left[\left(\frac{m\pi}{k}\right)^2+n^2\right]^2 + \frac{(1-\nu^2)\left(\frac{m\pi}{k}\right)^4}{\left[\left(\frac{m\pi}{k}\right)^2+n^2\right]^2} \tag{4.32}$$

This zero order nondimensional frequency parameter is identical to the resonance frequency of linear vibration.

The amplitudes and phase angles of the driven mode and companion mode are not determined by this zero order solution. Subsequent solutions of higher order equations will determine these values.

4.3 Solutions of First Order Equations

With the results of the zero order solution, the first order equations (4.18) and (4.19) can be written as

$$r^2\left[\frac{1}{k^4}\frac{\partial^4 W_1}{\partial s^4}+\frac{2}{k^2}\frac{\partial^4 W_1}{\partial s^2\partial\theta^2}+\frac{\partial^4 W_1}{\partial\theta^4}\right]+\lambda_o\frac{\partial^2 W_1}{\partial\tau^2}-\frac{1}{k^2}\frac{\partial^2\phi_1}{\partial s^2}$$

$$=-\lambda_1\left[\ddot{A}\cos(n\theta)+\ddot{B}\sin(n\theta)\right]\sin(m\pi s) \qquad (4.33)$$

$$+\left(\frac{mn\pi}{k}\right)^2\Gamma\left[(A^2+B^2)\cos 2m\pi s+(A^2-B^2)\cos 2n\theta+2AB\sin 2n\theta\right]$$

$$\frac{1}{1\nu^2}\left[\frac{1}{k^4}\frac{\partial^4\phi_1}{\partial s^4}+\frac{2}{k^2}\frac{\partial^4\phi_1}{\partial s^2\partial\theta^2}+\frac{\partial^4\phi_1}{\partial\theta^4}\right]+\frac{1}{k^2}\frac{\partial^2 W_1}{\partial s^2} \qquad (4.34)$$

$$=\left(\frac{mn\pi}{k}\right)^2\left[\tfrac{1}{2}(A^2+B^2)\cos 2m\pi s-\tfrac{1}{2}(A^2-B^2)\cos 2n\theta-AB\sin 2n\theta\right]$$

The right hand side of eqs. (4.33) and (4.34) are the results of the right hand side of eqs. (4.18) and (4.19) by substituting the zero order solutions and using trigonometric relations. The dot means differentiation with respect to time τ, hence $\ddot{A}=\frac{\partial^2 A}{\partial\tau^2}$.

Since eqs. (4.33) and (4.34) are inhomogeneous, the solutions of these equations are decomposed into two parts, the particular solution W_1^P, ϕ_1^P and the homogeneous solutions W_1^c, ϕ_1^c. Therefore the complete solution can be written as:

$$\left.\begin{aligned} W_1 &= W_1^P + W_1^c \\ \phi_1 &= \phi_1^P + \phi_1^c \end{aligned}\right\} \qquad (4.35)$$

W_1^P and ϕ_1^P satisfy the equations (4.33) and (4.34) and W_1^c

and $\phi_1{}^c$ satisfy the homogeneous equations of (4. 33) and (4. 34);

$$\left.\begin{aligned} r^2\left[\frac{1}{k^4}\frac{\partial^4 W_1{}^c}{\partial s^4}+\frac{2}{k^2}\frac{\partial^4 W_1{}^c}{\partial s^2\partial\theta^2}+\frac{\partial^4 W_1{}^c}{\partial\theta^4}\right] \\ +\lambda_2\frac{\partial^2 W_1{}^c}{\partial\tau^2}-\frac{1}{k^2}\frac{\partial^2\phi_1{}^c}{\partial s^2}=0 \end{aligned}\right\} \qquad (4.36)$$

$$\frac{1}{1-\nu^2}\left[\frac{1}{k^4}\frac{\partial^4\phi_1{}^c}{\partial s^4}+\frac{2}{k^2}\frac{\partial^4\phi_1{}^c}{\partial s^2\partial\theta^2}+\frac{\partial^4\phi_1{}^c}{\partial\theta^4}\right]+\frac{1}{k^2}\frac{\partial^2 W_1{}^c}{\partial s^2}=0 \qquad (4.37)$$

and the complete solution (4. 35) must satisfy the boundary condition (4. 20) and the circumferential periodicity condition(4. 21).

Let the particular solutions $W_1{}^p$ and $\phi_1{}^p$ be as follows:

$$\begin{aligned} W_1{}^p(s,\theta,\tau) &= a_1(\tau)\cos 2m\pi s+a_2(\tau)\cos 2n\theta+a_3(\tau)\sin 2n\theta \\ &\quad+[A_1(\tau)\cos(n\theta)+B_1(\tau)\sin(n\theta)]\sin(m\pi s) \end{aligned} \qquad (4.38)$$

$$\begin{aligned} \phi_1{}^p(s,\theta,\tau) &= \bar{a}_1(\tau)\cos 2m\pi s+\bar{a}_2(\tau)\cos 2n\theta+\bar{a}_3(\tau)\sin 2n\theta \\ &\quad+[\bar{A}_1(\tau)\cos(n\theta)+\bar{B}_1(\tau)\sin(n\theta)]\sin(m\pi s) \end{aligned}$$

Substituting equations (4. 38) into (4. 33) and (4. 34) and equating the coefficients of $\cos 2m\pi s$, $\cos 2n\theta$, $\sin 2n\theta$, $\cos n\theta \sin m\pi s$ and $\sin n\theta \sin m\pi s$, five sets of ordinary differential equations may be obtained as follows:

$$\left.\begin{aligned} & r^2\left(\frac{2m\pi}{k}\right)^4 a_1 + \lambda \ddot{a}_1 + \left(\frac{2m\pi}{k}\right)^2 \bar{a}_1 = -\left(\frac{mn\pi}{k}\right)^2 \Gamma(A^2+B^2) \\ & \frac{1}{1-\nu^2}\left(\frac{2m\pi}{k}\right)^4 \bar{a}_1 - \left(\frac{2m\pi}{k}\right)^2 a_1 = \tfrac{1}{2}\left(\frac{mn\pi}{k}\right)^2 (A^2+B^2) \end{aligned}\right\} \quad (4.39)$$

$$\left.\begin{aligned} & 16r^2n^4 a_2 + \lambda_o \ddot{a}_2 = \left(\frac{mn\pi}{k}\right)^2 \Gamma(A^2-B^2) \\ & \frac{16n^4}{1-\nu^2}\bar{a}_2 = -\tfrac{1}{2}\left(\frac{mn\pi}{k}\right)^2 (A^2-B^2) \end{aligned}\right\} \quad (4.40)$$

$$\left.\begin{aligned} & 16r^2n^4 a_3 + \lambda_o \ddot{a}_3 = 2\left(\frac{mn\pi}{k}\right)^2 \Gamma AB \\ & \frac{16n^4}{1-\nu^2}\bar{a}_3 = -\left(\frac{mn\pi}{k}\right)^2 AB \end{aligned}\right\} \quad (4.41)$$

$$\left.\begin{aligned} & r^2\left[\left(\frac{m\pi}{k}\right)^2+n^2\right]^2 A_1 + \lambda_o \ddot{A}_1 + \left(\frac{m\pi}{k}\right)^2 \bar{A}_1 = -\lambda_1 \ddot{A} \\ & \frac{1}{1-\nu^2}\left[\left(\frac{m\pi}{k}\right)^2+n^2\right]^2 \bar{A}_1 - \left(\frac{m\pi}{k}\right)^2 A = 0 \end{aligned}\right\} \quad (4.42)$$

$$\left.\begin{aligned} & r^2\left[\left(\frac{m\pi}{k}\right)^2+n^2\right]^2 B_1 + \lambda_o \ddot{B}_1 + \left(\frac{m\pi}{k}\right)^2 \bar{B}_1 = -\lambda_1 \ddot{B} \\ & \frac{1}{1-\nu^2}\left[\left(\frac{m\pi}{k}\right)^2+n^2\right]^2 \bar{B}_1 - \left(\frac{m\pi}{k}\right)^2 B_1 = 0 \end{aligned}\right\} \quad (4.43)$$

The solutions of eqs. (4.39), (4.40) and (4.41) may be readily obtained as

$$\left.\begin{aligned} a_1 &= c_1(a^2+b^2)+c_2[a^2\cos 2(\tau+\delta_a)-b^2\cos 2(\tau+\delta_b)] \\ \bar{a}_1 &= \bar{c}_1(a^2+b^2)+\bar{c}_2[a^2\cos 2(\tau+\delta_a)-b^2\cos 2(\tau+\delta_b)] \end{aligned}\right\} \qquad (4.44)$$

$$\left.\begin{aligned} a_2 &= c_3(a^2-b^2)+c_4[a^2\cos 2(\tau+\delta_a)+b^2\cos 2(\tau+\delta_b)] \\ \bar{a}_2 &= \bar{c}_3(a^2-b^2)+\bar{c}_4[a^2\cos 2(\tau+\delta_a)+b^2\cos 2(\tau+\delta_b)] \end{aligned}\right\} \qquad (4.45)$$

$$\left.\begin{aligned} a_3 &= c_8 ab\sin(\delta_b-\delta_a)+c_7 ab\sin(2\tau+\delta_b+\delta_a) \\ \bar{a}_3 &= \bar{c}_8 ab\sin(\delta_b-\delta_a)+\bar{c}_7 ab\sin(2\tau+\delta_b+\delta_a) \end{aligned}\right\} \qquad (4.46)$$

where

$$c_1 = -\tfrac{1}{2}\frac{n^4\zeta^2\Gamma+(1-\nu^2)\frac{n^2}{8}}{16r^2n^4\zeta^4+(1-\nu^2)}, \qquad \bar{c}_1 = \frac{(1-\nu^2)}{4}\frac{1}{n^2\zeta^2}\left(\frac{n^2}{16}+c_1\right)$$

$$c_2 = -\tfrac{1}{2}\frac{n^4\zeta^2\Gamma+(1-\nu^2)\frac{n^2}{8}}{[16r^2n^4\zeta^4+(1-\nu^2)-4\lambda_o]}, \qquad \bar{c}_2 = \frac{(1-\nu^2)}{4}\frac{1}{n^2\zeta^2}\left(\frac{n^2}{16}+c_2\right)$$

$$c_3 = \frac{1}{32}\frac{\zeta^2\Gamma}{r^2}, \qquad \bar{c}_3 = -\frac{1}{64}(1-\nu^2)\zeta^2$$

$$c_4 = \tfrac{1}{2}\left[\frac{n^4\zeta^2\Gamma}{16r^2n^4-4\lambda_o}\right], \qquad \bar{c}_4 = -\frac{1}{64}(1-\nu^2)\zeta^3 \qquad (4.47)$$

$$c_7 = \frac{n^4\zeta^2\Gamma}{16r^2n^4-4\lambda_o}, \qquad \bar{c}_7 = -\frac{(1-\nu^2)}{32}\zeta^2$$

$$c_8 = \frac{1}{16}\frac{\zeta^2\Gamma}{r^2}, \qquad \bar{c}_8 = -\frac{1}{32}(1-\nu^2)\zeta^2$$

where Γ and ζ^2 are defined in eq. (4.31).

The solutions of equations (4.42) and (4.43) need special attention. By eliminating $\overline{A}_1(\tau)$, eq. (4.43) can be reduced to as the following equation

$$\ddot{A}_1 + A_1 = \frac{\lambda_1}{\lambda_o} a \cos(\tau+\delta_a) \tag{4.48}$$

The solution of the above equation is

$$A_1(\tau) = \tfrac{1}{2} \frac{\lambda_1}{\lambda_o} a \tau \sin(\tau+\delta_a) \tag{4.49}$$

$A_1(\tau)$ is the so-called "secular term" which grows indefinitely as $\tau \to \infty$. Since only the periodic solutions are sought, $A_1(\tau)$ can not be part of the solution. Therefore it is necessary to assign:

$$\lambda_1 \equiv 0 \tag{4.50}$$

which in turn makes:

$$A_1(\tau) = \overline{A}_1(\tau) = B_1(\tau) = \overline{B}_1(\tau) = 0 \tag{4.51}$$

Now the particular solution has been obtained and the first order frequency parameter has also been determined to be zero. This particular solution satisfies neither the boundary condition (4.20) nor the periodicity condition (4.21). Therefore the complementary solution is necessary to enforce these conditions.

After some observations, the homogeneous solution will be assumed as follows:

$$W_1^c(s,\theta,\tau) = g_o(\tau)+g_1(s)+g_2(s)[a^2\cos 2(\tau+\delta_a)-b^2\cos 2(\tau+\delta_b)]$$

$$+g_3(s)\cos 2n\theta+g_4(s)\cos 2n\theta[a^2\cos 2(\tau+\delta_a)+b^2\cos 2(\tau+\delta_b)]$$

$$+g_5(s)\sin 2n\theta\sin(2R+\delta_a+\delta_b)+g_6(s)\sin 2n\theta\sin(\delta_b-\delta_a) \qquad (4.52)$$

and

$$\phi_1^c(s,\theta,\tau) = \bar{g}_o(\tau)s^2+\bar{g}_1(s)+\bar{g}_2(s)[a^2\cos 2(\tau+\delta_a)-b^2\cos 2(\tau+\delta_b)]$$

$$+\bar{g}_3(s)\cos 2n\theta+\bar{g}_4(s)\cos 2n\theta[a^2\cos 2(\tau+\delta_a)+b^2\cos 2(\tau+\delta_b)]$$

$$+\bar{g}_5(s)\sin 2n\theta\sin(2\tau+\delta_a+\delta_b)+\bar{g}_6(s)\sin 2n\theta\sin(\delta_b-\delta_a) \qquad (4.53)$$

Substituting eqs. (4.52) and (4.53) into the homogeneous equations (4.36) and (4.37) and equating the coefficients of likely terms, a set of ordinary differential equations for the unknown functions may be obtained. The circumferential periodicity condition (4.21) must be satisfied by the complete solution (4.35) which is the sum of a particular solution and complementary solution. This provides an additional equation for the function $g_o(\tau)$ and $\bar{g}_o(\tau)$. The details of the circumferential periodicity condition are discussed in Appendix B. The satisfaction of boundary condition (4.20) by the complete solution provides the boundary conditions for the unknown functions in the complementary solutions. The details of the boundary conditions are discussed in Appendix C. In the following the differential equations for the undetermined functions and their

boundary conditions will be summarized. [Note $(\dot{}) = \frac{\partial}{\partial \tau}$, $(') = \frac{\partial}{\partial s}$]

$$\left.\begin{aligned} &\lambda_o \bar{g}_o - \frac{2}{k^2}\bar{g}_o = 0 \\ &g_o + \frac{1}{1-\nu^2}\frac{2}{k^2}\bar{g}_o = \frac{n^2}{8}(A^2+B^2) \end{aligned}\right\} \qquad (4.54)$$

The solutions are as follows:

$$\left.\begin{aligned} g_o(\tau) &= c_5(a^2+b^2)+c_6[a^2\cos 2(\tau+\delta_a)-b^2\cos 2(\tau+\delta_b)] \\ \bar{g}_o(\tau) &= \bar{c}_6[a^2\cos 2(\tau+\delta_a)-b^2\cos 2(\tau+\delta_b)] \end{aligned}\right\} \qquad (4.54a)$$

where

$$\left.\begin{aligned} c_5 &= \frac{n^2}{16}, \qquad c_6 = \frac{1-\nu^2}{(1-\nu^2-4\lambda_o)}\frac{n^2}{16} \\ \bar{c}_6 &= -\frac{(1-\nu^2)n^2k^2\lambda_o}{8(1-\nu^2-4\lambda_o)} \end{aligned}\right\} \qquad (4.54b)$$

$$\left.\begin{aligned} &\frac{r^2}{k^4} g_1'''' - \frac{1}{k^2}\bar{g}_1'' = 0 \\ &\frac{1}{1-\nu^2}\frac{1}{k^4}\bar{g}_1'''' + \frac{1}{k^2} g_1'' = 0 \end{aligned}\right\} \qquad (4.55)$$

The boundary conditions at s = 0, 1 are

$$\left.\begin{aligned} g_1(s=0,1) &= -(c_1+c_5)(a^2+b^2) \\ g_1''(s=0,1) &= (2m\pi)^2 c_1(a^2+b^2) \end{aligned}\right\} \qquad (4.55a)$$

The solutions are as follows:

$$\left.\begin{aligned} g_1(s) &= K_1^1 \sin\mu_1(2s-1)\sinh\mu_1(2s-1)+K_2^1\cos\mu_1(2s-1)\cosh\mu_1(2s-1) \\ \bar{g}_1(s) &= \frac{r^2}{k^2} g_1''(s) \end{aligned}\right\} \quad (4.55b)$$

where μ_1, K_1^1 and K_2^1 are constants. The detailed solution procedure and these constants may be found in Appendix D.

$$\left.\begin{aligned} &\frac{r^2}{k^4} g_2'''' - 4\lambda_o g_2 - \frac{1}{k^2}\bar{g}_2'' = 0 \\ &\frac{1}{1-\nu^2}\ \frac{1}{k^4}\bar{g}_2'''' + \frac{1}{k^2} g_2'' = 0 \end{aligned}\right\} \quad (4.56)$$

The boundary conditions at $s = 0, 1$ are:

$$\left.\begin{aligned} g_2(s=0,1) &= -(c_2+c_6) \\ g_2''(s=0,1) &= (2m\pi)^2 c_2 \end{aligned}\right\} \quad (4.56a)$$

The solutions are:

$$g_2(s)=K_1^2\sin\mu_2(2s-1)\sinh\mu_2(2s-1)+K_2^2\cos\mu_2(2s-1)\cosh\mu_2(2s-1) \quad (4.56b)$$

$$\bar{g}_2''(s) = -k^2(1-\nu^2)g_2(s)$$

where μ_2, K_1^2 and K_2^2 are constants. The detailed solution procedure and these constants may be found in Appendix E.

$$\left.\begin{aligned} r^2\left[\frac{1}{k^4}\,g_3''' - 2\left(\frac{2n}{k}\right)^2 g_3'' + (2n)^4 g_3\right] - \frac{1}{k^2}\,\bar{g}_3'' = 0 \\ \frac{1}{1-\nu^2}\left[\frac{1}{k^4}\,\bar{g}_3'''' - 2\left(\frac{2n}{k}\right)^2 \bar{g}_3'' + (2n)^4 \bar{g}_3\right] + \frac{1}{k^2}\,g_3'' = 0 \end{aligned}\right\} \qquad (4.57)$$

The boundary conditions at s = 0, 1 are:

$$\left.\begin{aligned} g_3(s=0,1) &= -c_3(a^2-b^2) \\ g_3''(s=0,1) &= 0 \\ \bar{g}_3(s=0,1) &= -\bar{c}_3(a^2-b^2) \\ \bar{g}_3''(s=0,1) &= 0 \end{aligned}\right\} \qquad (4.57a)$$

The solutions are:

$$\begin{aligned} g_3(s) &= K_1^3\cos\Lambda_3(2s-1)\cosh\Lambda_1(2s-1) + K_2^3\sin\Lambda_3(2s-1)\sinh\Lambda_1(2s-1) \\ &\quad + K_3^3\cos\Lambda_4(2s-1)\cosh\Lambda_2(2s-1) + K_4^3\sin\Lambda_4(2s-1)\sinh\Lambda_2(2s-1) \\ \bar{g}_3(s) &= 2\mu_3^2 r^2\left[K_2^3\cos\Lambda_3(2s-1)\cosh\Lambda_1(2s-1) - K_1^3\sin\Lambda_3(2s-1)\sinh\Lambda_1(2s-1)\right. \\ &\quad \left. + K_4^3\cos\Lambda_4(2s-1)\cosh\Lambda_2(2s-1) - K_3^3\sin\Lambda_4(2s-1)\sinh\Lambda_2(2s-1)\right] \end{aligned} \qquad (4.57b)$$

where K_1^3, K_2^3, K_3^3, K_4^3, Λ_1, Λ_2, Λ_3, Λ_4 and μ_3 are constant. The detailed solution procedure and these constants may be found in Appendix F.

$$\left.\begin{aligned} r^2\left[\frac{1}{k^4}\,g_4'''' - 2\left(\frac{2n}{k}\right)^2 g_4'' + (2n)^4 g_4\right] - 4\lambda_o g_4 - \frac{1}{k^2}\bar{g}_4'' = 0 \\ \frac{1}{1-\nu^2}\left[\frac{1}{k^4}\,\bar{g}_4'''' - 2\left(\frac{2n}{k}\right)^2 \bar{g}_4'' + (2n)^4 \bar{g}_4\right] + \frac{1}{k^2}\,g_4'' = 0 \end{aligned}\right\} \qquad (4.58)$$

The boundary conditions at s = 0, 1 are

$$\left.\begin{aligned} g_4(s=0,1) &= -c_4 \\ g_4''(s=0,1) &= 0 \\ \bar{g}_4(s=0,1) &= -\bar{c}_4 \\ \bar{g}_4''(s=0,1) &= 0 \end{aligned}\right\} \qquad (4.58a)$$

The solutions are:

$$\begin{aligned} g_4(s) &= K_1^4 \cos\bar{\Lambda}_3(2s-1)\cosh\bar{\Lambda}_1(2s-1) + K_2^4 \sin\bar{\Lambda}_3(2s-1)\sinh\bar{\Lambda}_1(2s-1) \\ &\quad + K_3^4 \cos\bar{\Lambda}_4(2s-1)\cosh\bar{\Lambda}_2(2s-1) + K_4^4 \sin\bar{\Lambda}_4(2s-1)\sinh\bar{\Lambda}_2(2s-1) \\ \bar{g}_4(s) &= \bar{K}_1^4 \cos\bar{\Lambda}_3(2s-1)\cosh\bar{\Lambda}_1(2s-1) + \bar{K}_2^4 \sin\bar{\Lambda}_3(2s-1)\sinh\bar{\Lambda}_1(2s-1) \\ &\quad + \bar{K}_3^4 \cos\bar{\Lambda}_4(2s-1)\cosh\bar{\Lambda}_2(2s-1) + K_4^4 \sin\bar{\Lambda}_4(2s-1)\sinh\bar{\Lambda}_2(2s-1) \end{aligned} \qquad (4.58b)$$

The detailed solution procedure and the constants in the solutions may be found in Appendix G.

$$\left.\begin{aligned} r^2\left[\frac{1}{k^4}g_5'''' - 2\left(\frac{2n}{k}\right)^2 g_5'' + (2n)^4 g_5\right] - 4\lambda_o g_5 - \frac{1}{k^2}\bar{g}_5'' = 0 \\ \frac{1}{1-\nu^2}\left[\frac{1}{k^4}\bar{g}_5'''' - 2\left(\frac{2n}{k}\right)^2 \bar{g}_5'' + (2n)^4 \bar{g}_5\right] + \frac{1}{k^2} g_5'' = 0 \end{aligned}\right\} \quad (4.59)$$

The boundary conditions at s = 0, 1 are:

$$\left.\begin{aligned} g_5(s=0,1) &= -c_7 ab \\ g_5''(s=0,1) &= 0 \\ \bar{g}_5(s=0,1) &= -\bar{c}_7 ab \\ \bar{g}_5''(s=0,1) &= 0 \end{aligned}\right\} \quad (4.59a)$$

The solutions are:

$$\begin{aligned} g_5(s) &= K_1^5 \cos\bar{\Lambda}_3(2s-1)\cosh\bar{\Lambda}_1(2s-1) + K_2^5 \sin\bar{\Lambda}_3(2s-1)\sinh\bar{\Lambda}_1(2s-1) \\ &\quad + K_3^5 \cos\bar{\Lambda}_4(2s-1)\cosh\bar{\Lambda}_2(2s-1) + K_4^5 \sin\bar{\Lambda}_4(2s-1)\sinh\bar{\Lambda}_2(2s-1) \\ \bar{g}_5(s) &= \bar{K}_1^5 \cos\bar{\Lambda}_3(2s-1)\cosh\bar{\Lambda}_1(2s-1) + \bar{K}_2^5 \sin\bar{\Lambda}_3(2s-1)\sinh\bar{\Lambda}_1(2s-1) \\ &\quad + \bar{K}_3^5 \cos\bar{\Lambda}_4(2s-1)\cosh\bar{\Lambda}_2(2s-1) + \bar{K}_4^5 \sin\bar{\Lambda}_4(2s-1)\sinh\bar{\Lambda}_2(2s-1) \end{aligned} \quad (4.59b)$$

The detailed solution procedure and the constants in the solutions may be found in Appendix G.

$$\left.\begin{aligned} r^2\left[\frac{1}{k^4}\bar{g}_6'''' - 2\left(\frac{2n}{k}\right)^2 \bar{g}_6'' + (2n)^4 g_6\right] + \frac{1}{k^2} g_6'' = 0 \\ \frac{1}{1-\nu^2}\left[\frac{1}{k^4} g_6'''' - 2\left(\frac{2n}{k}\right)^2 g_6'' + (2n)^4 \bar{g}_6\right] - \frac{1}{k^2} g_6'' = 0 \end{aligned}\right\} \quad (4.60)$$

The boundary conditions at s = 0, 1 are:

$$g_6(s=0,1) = -c_8 ab$$

$$g_6''(s=0,1) = 0$$

$$\bar{g}_6(s=0,1) = -\bar{c}_8 ab \qquad (4.60a)$$

$$\bar{g}_6''(s=0,1) = 0$$

The solutions are:

$$g_6(s)=K_1^6\cos\Lambda_3(2s-1)\cosh\Lambda_1(2s-1)+K_2^6\sin\Lambda_3(2s-1)\sinh\Lambda_1(2s-1)$$
$$+K_3^6\cos\Lambda_4(2s-1)\cosh\Lambda_2(2s-1)+K_4^6\sin\Lambda_4(2s-1)\sinh\Lambda_2(2s-1)$$

$$\bar{g}_6(s)=2\mu_3^2 r^2[K_2^6\cos\Lambda_3(2s-1)\cosh\Lambda_1(2s-1)-K_1^6\sin\Lambda_3(2s-1)\sinh\Lambda_1(2s-1)$$
$$+K_4^6\cos\Lambda_4(2s-1)\cosh\Lambda_2(2s-1)-K_3^6\sin\Lambda_4(2s-1)\sinh\Lambda_2(2s-1)] \qquad (4.60b)$$

The detailed solution procedure and the constants in the solution may be found in Appendix F.

Now the solutions for the first order(ϵ) perturbation equations have been solved. The specified circumferential periodicity condition and boundary conditions are all satisfied. Combining the zero order solutions and the first order solutions the response of the large amplitude vibration of a cylindrical shell can be obtained to the accuracy of the order of $\epsilon = \frac{w_m}{R}$. If the maximum radial displacement w_m is of the order of shell thickness h, in view of

the shell theory used in which $\frac{h}{R} << 1$ is applied, the solution up to the order of ϵ should be considered adequate in consistency with the shell theory. However the response-frequency relationship has yet to be determined. The second order perturbation equation will be used to obtain this relationship.

4.4 Response-Frequency Relationship from Second Order Equations

The second order perturbation equations, (4.22) and (4.23), are of inhomogeneous type as are the first order equations. The right-hand side of equations (4.22) and (4.23) are functions of zero order solution and first order solution. Since only the response-frequency relationship is sought from the second order equation, the so-called "secular terms" are of particular interest; in other words, the terms with the spatial dependents $\cos n\theta \sin m\pi s$ and $\sin n\theta \sin m\pi s$. However, as the complementary solution of the first order equation is not expressed in the form of a trigonometric function in s, it is necessary to expand these solutions in terms of trigonometric functions. A careful examination of the complementary solution of the first order equation indicates that it is finite and integrable in the interval s = 0 to s = 1 and has a finite number of maxima and minima. Therefore a convergent Fourier series exists for the complementary solution, such as

$$\left.\begin{aligned} g_1(s) &= \xi_o^1 + \sum_{j=1}^{\infty} \xi_j^1 \cos 2j\pi s \\ \bar{g}_1''(s) &= -k^2(1-\nu^2)\left[\xi_o^1 + \sum_{j=1}^{\infty} \xi_j^1 \cos 2j\pi s\right] \end{aligned}\right\} \qquad (4.61)$$

$$\left.\begin{aligned} g_2(s) &= \xi_o^2 + \sum_{j=1}^{\infty} \xi_j^2 \cos 2j\pi s \\ \bar{g}_2''(s) &= -k^2(1-\nu^2)\left[\xi_o^2 + \sum_{j=1}^{\infty} \xi_j^2 \cos 2j\pi s\right] \end{aligned}\right\} \quad (4.62)$$

$$\left.\begin{aligned} g_3(s) &= \xi_o^3 + \sum_{j=1}^{\infty} \xi_j^3 \cos 2j\pi s \\ \bar{g}_3(s) &= \bar{\xi}_o^3 + \sum_{j=1}^{\infty} \bar{\xi}_j^3 \cos 2j\pi s \end{aligned}\right\} \quad (4.63)$$

$$\left.\begin{aligned} g_4(s) &= \xi_o^4 + \sum_{j=1}^{\infty} \xi_j^4 \cos j\pi s \\ \bar{g}_4(s) &= \bar{\xi}_o^4 + \sum_{j=1}^{\infty} \bar{\xi}_j^4 \cos 2j\pi s \end{aligned}\right\} \quad (4.64)$$

$$\left.\begin{aligned} g_5(s) &= \xi_o^5 + \sum_{j=1}^{\infty} \xi_j^5 \cos 2j\pi s \\ \bar{g}_5(s) &= \bar{\xi}_o^5 + \sum_{j=1}^{\infty} \bar{\xi}_j^5 \cos 2j\pi s \end{aligned}\right\} \quad (4.65)$$

$$\left.\begin{aligned} g_6(s) &= \xi_o^6 + \sum_{j=1}^{\infty} \xi_j^6 \cos 2j\pi s \\ \bar{g}_6(s) &= \bar{\xi}_o^6 + \sum_{j=1}^{\infty} \bar{\xi}_j^6 \cos 2j\pi s \end{aligned}\right\} \quad (4.66)$$

The detailed Fourier series expansion and their coefficients are discussed in Appendix H.

With these Fourier series expansions for the first order complementary solution, eqs. (4.22) and (4.23) can be written as

$$\left.\begin{aligned} &r^2\left[\frac{1}{k^4}\frac{\partial^4 W_2}{\partial s^4} + \frac{2}{k^2}\frac{\partial^4 W_2}{\partial \theta^2 \partial s^2} + \frac{\partial^4 W_2}{\partial \theta^4}\right] + \lambda_o \frac{\partial^2 W_2}{\partial \tau^2} - \frac{1}{k^2}\frac{\partial^2 \phi_2}{\partial s^2} \\ &= f' \cos\tau \cos(n\theta) \sin(m\pi s) - \lambda_2 \frac{\partial^2 W_o}{\partial \tau^2} - \sqrt{\lambda}_o \sqrt{\lambda}\bar{\gamma}\frac{\partial W_o}{\partial \tau} + \left[(G_1+G_3)\cos(n\theta) + \right. \\ &\left. +(G_2+G_4)\sin(n\theta)\right] \sin(m\pi s) + G_o(s,\theta,\tau) \end{aligned}\right\} \quad (4.67)$$

$$\left.\begin{aligned}&\frac{1}{1-\nu^2}\left[\frac{1}{k^4}\frac{\partial^4\phi_2}{\partial s^4}+\frac{2}{k^2}\frac{\partial^4\phi_2}{\partial\theta^2\partial s^2}+\frac{\partial^4\phi_2}{\partial\theta^4}\right]+\frac{1}{k^2}\frac{\partial^2 W_2}{\partial s^2}\\&=\left[(\overline{G}_1+\overline{G}_3)\cos(n\theta)+(\overline{G}_2+\overline{G}_4)\sin(n\theta)\right]\sin(m\pi s)+\overline{G}_o(s,\theta,\tau)\end{aligned}\right\}\quad(4.68)$$

The right-hand side of eqs. (4.67) and (4.68) are the results of the right-hand side of eqs. (4.22) and (4.23). The expressions of G_1, G_2, G_3, G_4, $\overline{G}_1$, $\overline{G}_2$, $\overline{G}_3$ and $\overline{G}_4$ can be found in Appendix. I. $G_o(s,\theta,\tau)$ and $\overline{G}_o(s,\theta,\tau)$ are functions with the spatial dependents other than $\cos(i\theta)\sin(j\pi s)$ and $\sin(i\theta)\sin(j\pi s)$ where $i \neq n$, $j \neq m$.

Now let the solutions of second order equations be:

$$\left.\begin{aligned}W_2(s,\theta,\tau)&=\left[A_2(\tau)\cos n\theta+B_2(\tau)\sin n\theta\right]\sin m\pi s+\overline{W}_2(s,\theta,\tau)\\\phi_2(s,\theta,\tau)&=\left[\overline{A}_2(\tau)\cos n\theta+B_2(\tau)\sin n\theta\right]\sin m\pi s+\Phi_2(s,\theta,\tau)\end{aligned}\right\}\quad(4.69)$$

Substituting eqs. (4.69) into eqs. (4.67) and (4.68) and equating the coefficients of $\cos(n\theta)\sin(m\pi s)$ and $\sin(n\theta)\sin(m\pi s)$, the following ordinary differential equations may be obtained:

$$\left\{\begin{aligned}&\ddot{A}_2+A_2=\frac{1}{\lambda_o}\left\{f'\cos\delta_a+\alpha a^3+\left[\beta+\sigma\cos 2(\delta_b-\delta_a)\right]ab^2+\lambda_2 a\right\}\cos(\tau+\delta_a)\\&+\frac{1}{\lambda_o}\left\{f'\sin\delta_a+\eta ab^2\sin 2(\delta_b-\delta_a)+\sqrt{\lambda}\sqrt{\lambda_o}\,\overline{\gamma}a\right\}\sin(\tau+\delta_a)\end{aligned}\right.\quad(4.70)$$

$$\left.\begin{aligned}&\ddot{B}_2+B_2=\frac{1}{\lambda_o}\left\{\alpha b^3+\left[\beta+\sigma\cos 2(\delta_b-\delta_a)\right]a^2b+\lambda_2 b\right\}\sin(\tau+\delta_b)\\&+\frac{1}{\lambda_o}\left\{\eta a^2 b\sin 2(\delta_b-\delta_a)-\sqrt{\lambda}\sqrt{\lambda_o}\,\overline{\gamma}b\right\}\cos(\tau+\delta_b)\end{aligned}\right\}\quad(4.71)$$

where α, β, σ, and η are functions of circumferential wave number n, half axial wave number m, Poisson's ratio ν, length to radius k and nondimensional bending rigidity r. Their expressions can also be found in Appendix I.

It should be remembered that, a, is the amplitude of driven mode and, b, is the amplitude of companion mode.

Equations (4.70) and (4.71) are similar to eq. (4.48). Therefore the solution A_2 and B_2 are the secular terms which grow indefinitely as $\tau \to \infty$. Consequently for a steady state solution the following must be true:

$$\lambda_2 a + \alpha a^3 + [\beta + \sigma \cos\Delta]\, ab^2 + f' \cos\delta = 0 \tag{4.72}$$

$$\sqrt{\lambda}\sqrt{\lambda_o}\,\bar{\gamma} a + \eta ab^2 \sin\Delta + f' \sin\delta = 0 \tag{4.73}$$

$$\lambda_2 b + \alpha b^3 + [\beta + \sigma \cos\Delta]\, a^2 b = 0 \tag{4.74}$$

$$\sqrt{\lambda}\sqrt{\lambda_o}\,\bar{\gamma} b - \eta a^2 b \sin\Delta = 0 \tag{4.75}$$

$$\text{where } \delta = \delta_a \text{ and } \Delta = 2(\delta_b - \delta_a) \tag{4.76}$$

Eqs. (4.72), (4.73), (4.74) and (4.75) are four algebraic equations for four unknowns, namely a, b, δ and Δ. These unknowns can be solved in terms of α, β, σ, η, which are functions of wave numbers and shell configurations, and γ, the damping in the shell and f, the magnitude of the external forcing function. λ_2 the second order frequency parameter, is also an unknown but it appears in the solutions of the driven mode, a, which provides the

response-frequency relationship.

Single mode (driven mode only) response

$b \equiv 0$ is one of the solutions for eqs. (4.72) to (4.75). In this case the companion mode is not participating in the vibration. The response involves the single mode, namely the driven mode only. The equations governing the driven mode response can be reduced to as follows:

$$\lambda_2 a + \alpha a^3 + f' \cos\delta = 0$$
$$\sqrt{\lambda}\sqrt{\lambda_o}\,\bar{\gamma} a + f' \sin\delta = 0 \qquad (4.77)$$

Eliminating δ from eq. (4.77), one obtains:

$$(\lambda_2 + \alpha a^2)^2 + \sqrt{\lambda}\sqrt{\lambda_o}\,\bar{\gamma}^2 = \frac{f'^2}{a^2} \qquad (4.78)$$

Now defining

$$\Omega = \frac{\omega}{\omega_o}, \quad \Omega^2 = \frac{\lambda}{\lambda_o} = 1 + \epsilon^2 \frac{\lambda_2}{\lambda_o} \qquad (4.79)$$

equation (4.78) can be reduced to

$$\left[\Omega^2 - 1) + \epsilon^2 \frac{\lambda}{\lambda_o} a^2\right]^2 + \gamma^2\Omega^2 = \frac{f}{a^2} \qquad (4.80)$$

Here the relations $\gamma = \epsilon^2\bar{\gamma}$ and $f = \epsilon^2 f'$, which have been defined before, are used.

Equation (4.80) can be rewritten as:

$$\left[(\Omega^2 - 1) + \frac{1}{R^2}\frac{\alpha}{\lambda_o} w_m^2 a^2\right]^2 + \gamma^2\Omega^2 = \frac{h^2 G^2}{\lambda_o^2 w_m^2 a^2} \qquad (4.80a)$$

Here eqs. (4.6) and (4.12) are used. The physical deformation of

the shell can be expressed as

$$w(x, y, t) = w_m[\, W_o + \epsilon W_1 + \epsilon^2 W_2 + \ldots \,]$$

$$= w_m\{[a\cos(\omega t+\delta_a)\cos\frac{ny}{R} + b\sin(\omega t+\delta_b)\sin\frac{ny}{R}] + O(\epsilon)\ldots\}$$

where a and b are nondimensionalized amplitudes of the driven mode and the companion mode respectively. Obviously the quantities $w_m a$ and $w_m b$ are the physical amplitude of the driven mode and the companion mode respectively. Since the deflection is of the order of shell thickness for the convenience of comparison, the following nondimensionalized quantities will be defined

$$w_a = \frac{w_m a}{h} \quad , \qquad w_b = \frac{w_m b}{h} \tag{4.80b}$$

Then eq. (4.80a) can be written as

$$[\Omega^2 - 1 + (\frac{h}{R})^2 \frac{\alpha}{\lambda_o} w_a^2]^2 + \gamma^2\Omega^2 = \frac{G^2}{\lambda_o^2 w_a} \tag{4.80c}$$

Throughout this study, the driven mode and the companion mode are plotted in terms of w_a and w_b respectively.

Eq. (4.80) is the so-called response-frequency relationship. Fig. 4 is a typical plot of eq. (4.80) for m = 1, n = 6, R = 4'', L = 8'', h = 0.010'' and $\frac{h}{R}$ = 0.0025, f = 0.0012, γ = 0.001. As can be seen, the nonlinearity is of the softening type, i.e., the frequency decreases with increasing response amplitude. This curve is similar to the response-frequency relationship of a simple spring-mass system with a nonlinear softening type spring as described in Ref. 1. Physically, when the frequency is increasing the response will follow

the curve a-b-c and then jump to d. Further increasing the frequency, the response will follow the curve from d to f. When the frequency is decreasing the response will follow the curve f-d-e and then jump to b. Further decreasing the frequency, the response will follow the curve from b to a. The discontinuous responses at c, d and e, b are called "jump phenomena" which have been observed in various nonlinear vibration systems. Figs. 5, 6, and 7 are the similar plots for different wave numbers, damping and amplitude of external forcing functions.

In the case of free vibration, the response-frequency relationship can be obtained by letting $f = \gamma = 0$ in eq. (4.80), namely,

$$\Omega^2 = 1 - \epsilon^2 \frac{\alpha}{\lambda_o} a^2 \tag{4.81}$$

which are plotted by dashed lines in Figs. 4, 5, 6 and 7 and referred to as "backbone curves."

The backbone curves can be used to determine the type of nonlinearities (softening or hardening) and the degree of nonlinearity. If the backbone curve bends toward the left, the nonlinearity is softening, if to the right the nonlinearity is hardening.

Although a softening type nonlinearity is indicated in Figs. 4 to 7, not all the modes (combination of m and n) are of the softening type. Fig. 8 shows the backbone curves for different modes. It is clear that the nonlinearity in the vibration of a circular cylindrical shell with finite length is of both the softening and hardening type.

An examination of eq. (4.81) shows that the type of nonlinearity depends on the sign of the quantity α. Positive α implies a

softening type nonlinearity and negative α implies a hardening type nonlinearity. Also the degree of nonlinearity is dependent on the magnitude of α. The larger α implies the larger nonlinearity. Figs. 9 and 10 show the quantity $(\frac{h}{R})^2 \frac{\alpha}{\lambda_o}$ (note λ_o is always positive) as a function of half axial wave number m and circumferential wave number n for $\frac{L}{R} = 2$ and $\frac{h}{R} = 0.0025$. For m = 1 the nonlinearity is of the softening type only. For $m \geq 2$ the nonlinearity is either of the softening or hardening type depending on the circumferential wave number n.

The forced response-frequency relationship is given by the solution of eq. (4.80). At a given frequency the response can be expressed as a function of the external forcing function. Figs. 4 to 7 show that the response at certain frequencies is not single-valued. For instance in Fig. 4 the response is triple-valued for $0.9965 < \Omega < 0.9984$ and double-valued for $\Omega = 0.9965$ and $\Omega = 0.9984$. In the multiple-valued response region, a stability analysis must be performed to determine the stable response. This stability analysis will not be included in this investigation. However, it can be observed from the response-frequency relationship that the multiple response region is confined between the two frequencies where the tangent of eq. (4.80) is vertical, i.e., $\frac{d\Omega}{da} = 0$. In other words, the locus of these vertical tangents is the stability boundary (Ref. 1). Fig. 11 shows the locus of vertical tangents for $\gamma = 0.001$ and $\gamma = 0.003$ respectively of a shell having $\frac{L}{R} = 2$, $\frac{h}{R} = 0.0025$. The shaded area indicates that the jump phenomenon will occur. The amount of damping in shell vibration plays an important role in the

jump phenomenon. Larger damping will make the jump phenomenon occur at a higher amplitude of response.

Companion Mode Participation

In the case of the companion mode participating in the vibration, i.e., $b \neq 0$, eqs. (4.72) to (4.75) can be reduced as follows by eliminating δ and Δ:

$$[(\Omega^2-1)(a^2-b^2)+\epsilon^2\frac{\alpha}{\lambda_o}(a^4-b^4)]^2+\Omega^2\gamma^2(a^2+b^2)^2=(\frac{f}{\lambda_o})^2a^2 \quad (4.82)$$

$$\frac{1}{\sigma^2}[\Omega^2-1+\frac{\epsilon^2}{\lambda_o}(\alpha b^2+\beta a^2)]^2+\frac{1}{\eta^2}\Omega^2\gamma^2=\epsilon^4\frac{a^4}{\lambda_o^2} \quad (4.83)$$

Eqs. (4.82) and (4.83) are nonlinear algebraic equations for two unknowns, namely a and b. A direct solution for a and b as functions of f, Ω and γ is difficult. Therefore a small computer program was developed to calculate b and $\frac{f}{\lambda_o}$ for given a and Ω. By cross-plotting the results, it is possible to obtain curves of a vs. Ω and b vs. Ω for constant $\frac{f}{\lambda_o}$ and γ. Figs. 12 and 13 show the amplitude of the driven mode a with and without the companion mode participation for constant $\frac{f}{\lambda_o}$ and γ. Since $b \equiv 0$ is a solution of eqs. (4.72) to (4.75), both curves in the figure represent the possible response of the shell. The actual response in the multi-valued region has to be determined by a stability analysis. Fig. 14 shows the corresponding amplitude of the companion mode as a function of Ω for constant $\frac{f}{\lambda_o}$ and γ. As can be observed, the response of the driven mode is affected by the companion mode only in a narrow region in the vicinity of $\Omega = 1$. Its amplitude, a, is always greater than a certain value in this region. This minimum value can be

derived from eq. (4.83) as follows. In order for the companion mode b to be a real value, it is necessary that the following is true.

$$\epsilon^4 \frac{a^4}{\lambda_o^2} \geq \frac{1}{\eta^2} \Omega^2 \gamma^2 \tag{4.84}$$

which in turn can be written as

$$|w_a|^2 \geq \frac{\lambda_o R^2}{\eta} \Omega\gamma \tag{4.85}$$

This indicates that larger damping γ will make the companion mode occur at larger amplitude.

After establishing the minimum amplitude for the driven mode, a minimum magnitude of forcing function f can be established by using eq. (4.82). The existence of a minimum forcing function implies that in order to make the companion mode participate, the external forcing function must be greater than a certain minimum value. This explains the fact that the companion mode can be observed experimentally only for the large external excitation.

It may be concluded that the participation of the companion mode is a phenomenon of large amplitude and large external forcing function. (Note that the large forcing function only does not necessarily imply large amplitude, the large amplitude can also be obtained for small damping at the right frequency for small forcing function.) As mentioned before, the occurrence of the companion mode must be determined by a stability analysis. Nevertheless the region in which the companion mode may exist can be established. Fig. 15 shows the region (the shaded area) in which the companion mode may be

participating for $\frac{L}{R} = 2$, $\frac{h}{R} = 0.0025$, $m = 1$, $n = 6$, $\gamma = 0.001$.

4.5 Discussion of Results and Comparison with Previous Investigation

The radial response of nonlinear vibration of a cylindrical shell simply supported at both ends can be written as

$$W(s, \delta, \tau) = [a\cos(\tau+\delta a)\cos n\theta + b\sin(\tau+\delta_b)\sin n\theta]\sin m\pi s$$

$$\epsilon\Big\{g_o(\tau)+\alpha_1(\tau)\cos 2m\pi s+\alpha_2(\tau)\cos 2n\theta+\alpha_3(\tau)\sin 2n\theta$$

$$+g_1(s)+g_2(s)[a^2\cos 2(\tau+\delta_a)-b^2\cos 2(\tau+\delta_b)]$$

$$+g_3(s)\cos 2n\theta+g_4(s)\cos 2n\theta[a^2\cos 2(\tau+\delta_a)+b^2\cos 2(\tau+\delta_b)]$$

$$+g_5(s)\sin 2n\theta\sin(2\tau+\delta_a+\delta_b)+g_6(s)\sin 2n\theta\sin(\delta_b-\delta_a)\Big\}$$

$$+O(\epsilon^2)+\ldots\ldots \qquad (4.86)$$

where the amplitude of the driven mode, a, and the companion mode b, are functions of the frequency, external forcing function and damping. The terms multiplied by the small parameter ϵ are due to the nonlinearities of the problem. These terms represent the difference of the deflection shape and harmonic content between the linear and nonlinear response of the shell. Therefore, it is of interest to discuss these terms. The functions $g_o(\tau)$, $\alpha_1(\tau)$, $\alpha_2(\tau)$ and $\alpha_3(\tau)$ involve a constant term and a term with coefficient $\cos 2\tau$ or $\sin 2\tau$. The functions $g_1(s)$ to $g_6(s)$ are of the "boundary layer" type, i.e., they possess large magnitude near both ends ($s = 0$ and $s = 1$) and vanishingly small magnitude elsewhere. A typical plot of $g_2(s)$ for $m = 1$, $n = 6$ and $m = 2$, $n = 7$ is shown in Fig. 16. There-

fore, as far as the deflection shape away from the immediate vicinity of the boundary is concerned, terms like $g_o(\tau)$, $\alpha_1(\tau)\cos 2m\pi s$, $\alpha_2(\tau)\cos 2n\theta$ and $\alpha_3(\tau)\sin 2n\theta$ are dominant.

In Section II, previous investigations of nonlinear vibration of cylindrical shells have been discussed. The deflection shape assumed in those previous investigations for applying the Galerkin method will now be compared with the present calculated deflection shape. Since the fundamental deflection shapes are all identical to the linear mode shape, only the "added" terms in the deflection shape will be compared; Chu (Ref. 8) has no added terms for the deflection shape. Nowinski (Ref. 10) has a constant as the added term. Evensen (Ref. 12) has $(1-\cos 2m\pi s)$ as the added terms. Dowell has $\sin m\pi S$ as the added term. All the added terms are axisymmetric. In the present analysis, non-axisymmetric terms such as $\alpha_2(\tau)\cos 2n\theta$ and $\alpha_3(\tau)\sin 2n\theta$ are found. A comparison of the axisymmetric mode of the present solution and Evensen's assumed deflection is shown in Fig. 17 . (Note the axisymmetric modes in the present solution are $g_o(\tau)+\alpha_1(\tau)\cos 2m\pi s+g_1(s)+g_2(s)[\, a^2\cos(\tau+\delta_a)-b^2\cos 2(\tau+\delta_b)]$). For small "aspect ratio," favorable agreement is indicated. However increasing the aspect ratio makes the deviation between the two mode shapes larger. For the m = 3, n = 7 mode the deviation is quite pronounced. One possible explanation of the large deviation at large aspect ratio is that the amplitude of Evensen's axisymmetric mode is independent of the axial half wave number m but the present analysis indicates otherwise.

As mentioned before, the type of nonlinearity of cylindrical shells depends on the shell geometry as well as the mode shape (combination of m and n). In order to compare the nonlinearity in the present results and those in Evensen's results, the response-frequency relationship in Evensen's report (Ref. 12) is modified as

$$\Omega^2 \cong 1-[\frac{3}{4}(n^2\frac{h}{R})^2\gamma+\frac{3}{16}(n^2\frac{h}{R})^2]\,a^2+O[(n^2\frac{h}{R})^4 a^4] \qquad (4.87)$$

where

$$\gamma = \frac{\zeta^4\left[\frac{1}{(\zeta^2+1)^2}-\frac{1}{16}-\frac{(n^2\frac{h}{R})^2}{12(1-\nu^2)}\right]}{\frac{\zeta^4}{(\zeta^2+1)^2}+(n^2\frac{h}{R})^2\frac{(\zeta^2+1)^2}{12(1-\nu^2)}} \qquad (4.88)$$

The quantity in the bracket in eq. (4.87) corresponds to the quantity $(\frac{h}{k})^2\frac{\alpha}{\lambda_o}$ in the present analysis (eq. (4.81)). Fig. 18 shows the comparison of these two quantities. In general, the type of nonlinearity and the degree of nonlinearity are different for the present analysis and that of Evensen's except for m = 1, n> 10. Fig. 19 shows a similar comparison for large circumferential wave number n. The percentage difference is defined as follows:

$$\% = \frac{|(\text{Present})-(\text{Evensen's})|}{(\text{Present})} \times 100 \qquad (4.89)$$

Large percentage differences are observed for 10 > n > 20. The explanation for this difference is as follows. For n < 10, the inplane boundary conditions have greater influence in the results of the linear vibration of cylindrical shells (Ref. 19) and Evensen's solution does not satisfy specified inplane boundary conditions which cause the

large difference. For $n > 20$, Evensen's solution breaks down since it is based on the assumption that $(n^2 \frac{h}{R})^2 << 1$. It appears that more inplane constraints at the boundary makes the degree of nonlinearity greater.

Olson (Ref. 22) performed a vibration experiment on a cylindrical shell flutter model where two rings were rigidly attached to both ends of the shell. The measured frequency for $m = 1$, $n = 10$ mode was 131 cps. The calculated frequencies are 80 cps and 140 cps for the simply-supported case ($w = M_x = N_x = \nu = 0$) and clamped case ($w = \frac{\partial w}{\partial x} = u = v = 0$) respectively. It is obvious that Olson's experimental model is closer to clamped than simply supported. Fig. 20 shows Olson's nonlinear vibration experimental results compared with the backbone curve obtained by the present analysis, Evensen's analysis (Ref. 12) and Matsuzaki and Kobayashi's (Ref. 16) analysis. Here the present analysis has a simply-supported inplane boundary condition. Evensen's analysis has a somewhat more constrained inplane boundary condition due to the violation of simply-supported inplane boundary bondition. Matsuzaki and Kobayashi's analysis was intended for a clamped boundary condition, namely, $w = \frac{\partial w}{\partial x} = N_{xy} = u = 0$ at $s = 0, 1$; however the $u = 0$ condition was violated, which imposes a further inplane constraint to the shell. Clearly Olson's experimental model has a boundary condition somewhere in between the partially unconstrained inplane boundary condition and "super" total constrained inplane boundary condition. Again this confirms that more inplane constraints make larger degrees of nonlinearity.

The presence of the companion mode is a very interesting phenomenon. The appearance of traveling wave response due to the companion mode can be explained as follows:

$$W(\theta, \tau) = a\cos\tau\cos(n\theta) + b\sin\tau\sin(n\theta)$$

The axial dependence is omitted for convenience. If a = b then the following is true.

$$W(y, t) = a\left[\cos\omega t\cos\frac{ny}{R} + \sin\omega t\sin\frac{ny}{R}\right]$$

$$= a\cos\left(\frac{ny}{R} - \omega t\right)$$

Defining the circumferential wave length as:

$$\lambda_c = \frac{2\pi R}{n} \qquad \text{then}$$

$$W(y, t) = \cos\frac{2\pi}{\lambda_c}\left(y - \frac{R\omega}{n}t\right)$$

This is a traveling wave form with wave length λ_c and phase velocity $\frac{R\omega}{n}$ in/sec. Now the period T required for this wave to travel a complete circumference (1 cycle) is:

$$T = \frac{2\pi R}{\frac{R\omega}{n}} = \frac{2n\pi}{\omega} \text{ sec.}$$

hence the frequency of the traveling wave ω_T

$$\omega_T = \frac{\omega}{2n\pi} \text{ cycle/sec} = \frac{\omega}{n} \text{ rad/sec.}$$

Now if $a \neq b$, the total response can be decomposed into a standing wave superimposed on a traveling wave. Fig. 21 shows the difference between a standing wave and a traveling wave by looking

at the shell cross-section and the signal from a displacement pick-up at a fixed point on the shell.

V. EXPERIMENTAL ANALYSIS

An experimental investigation was performed in order to observe qualitatively the phenomena predicted by the analysis and wherever possible to make detail comparison of experiment and theory. Very few experimental studies have been devoted to nonlinear vibration of cylindrical shells. Olson (Ref. 22) studied an electro-plated shell flutter model in which a softening type nonlinearity was observed. However in his experimental study no attempt was made to investigate the companion mode. Kobayashi (Ref. 16) tested another flutter model which was constructed of super-invar sheet bonded into a seamed cylinder. He also found that the nonlinearity was of the softening type and observed the participation of a companion mode over a range of frequency and amplitude.

In the present experimental investigation, it is hoped that the following aspects can be achieved, namely:

1) To observe the type of nonlinearity
2) To measure the response quantitatively and to compare with the theoretical results
3) To determine the range of companion mode participation and the characteristics of the companion mode
4) To make a general comparison between the theoretical and experimental results and to determine the region of validity of the theory
5) To observe the characteristics of nonlinear response which were not predicted by the theoretical analysis and to suggest the modifications to the theory.

5.1 Test Specimen

5.1.1 Description of Test Shell

In the theoretical analysis, a so-called simply-supported shell (SS1/SS1) was studied because of the simplicity of its boundary conditions. The simply-supported boundary condition requires that radial displacement w, bending moment M_x, axial force N_x and circumferential displacement v vanished at both ends. It is almost impossible to simulate these conditions experimentally. Therefore, it was decided to choose a shell with rings at both ends that will approximate the simply-supported condition. The rings were chosen so that the shell's natural frequencies and mode shapes were close to those of a simply-supported shell. Using the program developed by El Raheb (Ref. 19), a preliminary analysis was performed to determine the size of the end rings. It is obvious the ring should be stiff in the radial direction to provide w = 0, torsionally weak to provide $M_x = 0$, and tangentially stiff to provide v = 0. The vanishing axial force N_x is achieved by the low bending stiffness of the ring in the axial direction. The material chosen for the shell-ring system was aluminum alloy 7075-T6. The shell was machined from a seamless tube to its desired inner radius, then placed on a steel mandrel by thermally expanding the aluminum tube. The outside machining process was carried out on the mandrel to the design thickness and ring dimensions. The final shell was removed from the mandrel by thermal heating again. The end rings are an integral part of the shell. The final dimensions are shown in Fig. 22.

5.1.2 Determination of Shell Wall Thickness

It is reasonable to assume that the test shell would not have uniform wall thickness since the machine tool used to manufacture the shell has its own tolerances. Although the tolerances would be of small magnitude, the percentage error might be high since the average shell wall thickness was also very small. Therefore the variation of wall thickness of the test shell was measured to insure the errors were within an acceptable range. It is especially important to minimize the variation in shell thickness not only to obtain the uniform wave pattern for the vibrational mode shape but also to prevent any undesired response during the vibration. A deep throat micrometer was used to take 5 measurements at each of the 36 locations over the entire shell wall. The micrometer and shell were connected to a light bulb and a battery. The contact between the micrometer and shell closes the circuit and turns on the light bulb. This is used as an indicator for contact made to assure the uniform measurement. The maximum deviation of the shell wall thickness among these measurements was found to be 4% which was considered to be acceptable.

However, the average shell thickness was determined in the following manner. The diameter and the length of the shell together with the dimensions of two end rings were measured. The total weight of the shell-ring system was obtained. Then the shell wall thickness is calculated using the density of the material. The density was checked for a piece of material cut from the same stock as the shell and was very close to that reported by the manufacturer.

5.1.3 Support Plate for Shell-Ring System

The support conditions desired for the test were a free support for the shell-ring system. However, it was necessary to constrain the rigid body motion of the shell in order that the mode shapes could be readily measured. This was accomplished by mounting one end of the shell on the base plate but making only a flexible line contact with the end ring. For this purpose, the plate was fitted with two O rings, one to support the axial motion and the other to support the radial motion. The O ring for the radial support is mounted so as to allow a few thousandths of an inch clearance. It was felt that this provided sufficient play so as not to restrict the radial motion and at the same time sufficiently restrain the rigid body motion. Fig. 23 shows a photograph of the test shell and its supporting end plate.

5.1.4 Comparison Between the Shell-Ring System and the Simply-Supported Shell

After the dimensions of the shell ring system and its support end plate were determined, it was necessary to perform an analysis to see how close the shell-ring system could approximate the simply-supported shell. The natural frequencies and mode shapes were chosen for the comparison.

Table I lists the calculated natural frequencies of the shell-ring system based on El Raheb's solution (Ref. 19) and of the simply-supported shell (SS1/SS1) based on the Donnell approximation (eq. (4.32)) which is used in the present investigation. Also the experimentally measured natural frequencies are listed. The

percentage difference of the calculated frequencies between the shell-ring system and the simply-supported shell are less than 8.62% for $n \geq 5$ and decrease with increasing circumferential wave number n. The experimentally measured natural frequencies are generally in good agreement with the calculated frequencies based on the shell-ring system. Fig. 24 shows the frequency spectrum of the shell specimen as a function of half axial wave number m and circumferential wave number n.

The mode shapes of radial displacement w, bending moment M_x, axial compression N_x and circumferential displacement v for m = 1, n = 6 mode are plotted in Fig. 25 for the shell-ring system and the simply-supported shell. They are in good agreement except for the bending moment M_x in the vicinity of the boundary where large deviations are indicated. Since the high bending moment is concentrated in the very narrow region close to the boundary and rapidly approaches the values for the simply-supported shell, it was felt that this shell-ring system is acceptable in approximating the simply-supported shell for the nonlinear vibration problem to be studied.

5.2 Description of the Experimental Set-Up

Vibrations of the shell-ring system are excited by an acoustic driver whose acoustic output is focused through a conical nozzle with a 0.25 inch diameter exit hole. The driver is positioned either midway between the ends of the shell to excite m = 1 modes or a quarter length of the shell from the top end ring to excite m = 2 modes. The nozzle of the acoustic driver was a small distance d away from the

shell skin and the distance d could be adjusted since the acoustic driver was mounted on a traversing mechanism. Previous experiments (Ref. 22) indicated that as long as the distance d is less than 0.03 inch, the pressure output from the driver will be essentially sinusoidal.

Motion of the shell skin is measured with a non-contact reluctance-type pickup which was mounted on a fixture with a large bearing that could be traversed circumferentially. The pickup could be stationed at any position along the axis of the shell. The reluctance pickup-amplifier system was calibrated by varying the distance between the reluctance pickup and shell skin and recording the voltage output from the amplifier. The distance-voltage calibration relationship is shown in Fig. 26. The arrangement of the acoustic driver and reluctance pickup is shown in Fig. 27.

Since the calibration curve of the reluctance pickup is not a linear one, higher harmonics may be generated by the pickup. An examination was carried out as follows. During the vibration test, the distance between the pickup and shell wall was preset at 0.0215 inch in order to have optimum usage of the linear part of the calibration curve. The coordinates of the calibration curve may be rearranged as shown in Fig. 26 by output V and displacement δ. Then the calibration curve can be represented by a power series,

$$V(t) = a_1 \delta(t) + a_2 \delta^2(t) + a_3 \delta^3(t) + \ldots \qquad (5.1)$$

here $a_1 = 23.7$, $a_2 = 220.0$, ...

If the displacement δ is sinusoidal in time, the output voltage V will

contain higher harmonics, due to the nonlinearity of the calibration curve. For instance for $\delta = a\sin\omega t$ (5.2)

$$V(t) = a_1 a\sin\omega t + \tfrac{1}{2}a_2 a^2(1-\cos 2\omega t) + \ldots \quad (5.3)$$

Here the ratio of amplitudes of the second harmonic and the fundamental harmonic is

$$\text{Amplitude Ratio} = \frac{\frac{1}{2}a_2 a^2}{a_1 a} = \frac{1}{2}\frac{a_2}{a_1}\cdot a \quad (5.4)$$

In the present experiment, the maximum amplitude of the fundamental harmonics is about 0.010 inch, hence the amplitude ratio is

$$\text{Amplitude Ratio} = 0.5 \times \frac{220}{23.7} = 0.046 \quad (5.5)$$

If one attempts to measure a nonlinear displacement containing higher harmonics such as

$$\delta(t) = \delta_1\cos\omega t + \delta_2\cos 2\omega t + \delta_3\cos 3\omega t + \ldots. \quad (5.6)$$

one will find that it is difficult to determine the magnitude of δ_2 and δ_3 unless the ratio of $\frac{\delta_2}{\delta_1}$ and $\frac{\delta_3}{\delta_1}$ are much greater than the amplitude ratio found in the calibration curve. Unfortunately in the present experiment, the amplitude ratio of the higher harmonics is of the same order as that of the calibration curve.

The magnitude and frequency output of the acoustic driver were controlled by a standard oscillator-power amplifier system. The response signal from the pickup was fed into a cathode ray oscilloscope and a Ballantine true RMS (Root-mean-square) voltmeter.

The frequency of the oscillator and response is monitored by a digital counter. The circumferential mode shape was plotted by connecting the y-axis of an x-y plotter to the RMS response signal and the x-axis to a potentiometer which indicated the position of the reluctance pickup. Thus the circumferential mode shape could be plotted in forms of RMS value. A schematic diagram of the instrumentation arrangement is shown in Fig. 28, and a photograph of the experimental set-up is shown in Fig. 29.

5.3 Driven Mode Response

The m = 1 modes were used for frequency-response relation study because these modes are the easiest to excite into a nonlinear region. The acoustic driver was placed midway between the end rings. The reluctance pickup was also pointed at the midsection of the shell and fixed at an antinode of cosnθ about 180° from the acoustic driver. The magnitude of the force output of the acoustic driver was kept constant by applying a constant voltage across the driver (driver voltage). At each data point the frequency measured by an electronic counter was normalized by the linear frequency ω_o which is known prior to the test and the response measurement was converted into physical value (i. e., displacement) and then normalized by the shell thickness.

Fig. 30 shows the frequency-response relation for m = 1, n = 6 mode. When the external force is small, no jump phenomena is detected. But the "jump" is detected when the external force becomes larger.

Similar results are observed in Fig. 31 and Fig. 32 for

m = 1, n = 10 mode and m = 1, n = 12 mode respectively. All three modes tested possessed the softening-type nonlinearity as the theoretical analysis indicated. Equivalent theoretical results are also plotted which show good agreement with the experimental results. Fig. 33 shows the RMS circumferential mode shape. Clearly it was a single driven mode response since no response was measured at the nodes.

5.4 Response with Companion Mode Participation

Since the m = 1, n = 6 mode was the easiest to excite, it was chosen for further investigation. With the magnitude of the acoustic input increased further, a different frequency-response relation was obtained which is shown in Fig. 34. The response measurement is taken at the antinode of $\cos n\theta$. This result indicates that in the vicinity of the resonance frequency the response became "non-stationary" in the sense that the response would not remain at one amplitude, rather it drifted slowly from one amplitude to another. In some cases as many as 4 different amplitudes were observable at a given frequency. These are shown in Fig. 34. No regularity was observed in the drifting rate. It was obvious that at these frequencies the driven mode response became multi-valued. Outside of this frequency range, the response was single-valued. For this particular test, the region of multi-response was at $\Omega < 1$. A RMS circumferential mode plotted at constant external force for different frequencies is shown in Fig. 35. As the mode shape indicates, for larger amplitude the response was no longer a single driven mode $\cos n\theta$. These are shown in Fig. 34. At the node point of $\cos n\theta$ which is the antinode of $\sin n\theta$,

the deflection did not vanish. This was the first indication that the companion mode was participating in the vibration.

The presence of the companion mode can also be detected by the use of Lissajous figures. The voltage proportional to the radial deflection of the shell was fed into the vertical axis of the cathode ray oscilloscope, with the horizontal axis being driven from the oscillator which controlled the acoustic driver. The resulting Lissajous figure indicates the amplitude and the phase (relative to the input force) of the vibration at that point of the shell. By moving the reluctance pickup along the circumferential direction of the shell and noting the Lissajous figure, it is possible to detect which modes are present. The Lissajous figure at antinode of $\cos n\theta$ is shown in Fig. 36. The open ellipse indicated a response that is $\pm 90°$ out of phase with the input forcing function. The Lissajous figure at the adjacent node of $\cos n\theta$ which is the antinode of $\sin n\theta$ is shown in Fig. 37. The diagonal line demonstrated that the response is in phase with the input forcing function. This shows that the responses of the driven mode $\cos n\theta$ and the companion mode $\sin n\theta$ are $\pm 90°$ different in phase which indicates the deflection form of the shell at the midsection is of the form

$$w(\theta, t) = a\cos\omega t\cos n\theta + b\sin\omega t\sin n\theta \qquad (5.7)$$

The response-frequency relation of the companion mode was also measured for the driver voltage equal to the 8.0 v case and is shown in Fig. 38. The experimental results compared with the theoretical results show some discrepancies for $\Omega > 1$. This may be due to the

following facts. The amplitude of the companion mode was measured at a predetermined node of the driven mode cosnθ. However the shifting of the node as shown in Fig. 35 made the companion mode measurement "contaminated" by some amount of the amplitude of the driven mode.

The participation of the companion mode has changed the characteristics of nonlinear vibration of the cylindrical shell as compared to the case of driven mode response only. The "jump phenomenon" has been eliminated and instead a "non-stationary" response is observed in which the amplitude drifts from one value to another.

An attempt was made to constrain the companion mode by lightly placing a sharp point at the antinode of the companion mode sinnθ and then taking measurements at the antinode of the driven mode cosnθ. The result is shown in Fig. 39. The classical "jump phenomena" was recovered and the shell vibrated in the driven mode only.

With the voltage of the acoustic driver increased further to 15 v., another test was conducted and the response-frequency relation was obtained as shown in Fig. 40. Again there was a narrow region in the vicinity of $\Omega = 1$ in which the response drifted between several values. In this case, the drifting rate was somewhat faster than the previous case but still no regularity was detected in the drifting rate. The companion mode was participating in the vibration although no attempt was made to measure it. Within the narrow frequency region where the drifting response was found, a few points

very close to $\Omega = 1$ seemed to be "stationary" or the drifting range was too small to detect. The high amplitude response found outside of the drifting region ($\Omega < 1$) was extremely difficult to obtain, since the amplitude had a tendency to drop to the lower value. Only with extreme caution and patience were these amplitudes measured. Also an attempt was made to constrain the companion mode by an external constraint but no significant difference was found.

Another test was performed with the driver voltage increased further to 21 v. Similar results were obtained with a few differences as shown in Fig. 41. A larger drifting response region was found and the drifting rate became faster. Fig. 42 was taken from the cathode ray oscilloscope; the voltage from the response measurement was fed into the vertical axis with the horizontal axis being the time scale. The time scale was adjusted in such a way that the regular wave pattern was crowded together such that the photograph could not distinguish them. Therefore a white belt was shown in the picture instead of a wave form. The top straight belt represents the input signal from the oscillator. The lower wavy belt was the signal from the reluctance pickup measuring at the antinode of the driven mode $\cos n\theta$. As can be observed in Fig. 42, the amplitude is drifting from one value to another in a much faster rate than the other cases with smaller external force. Also the drifting rate follows a certain pattern which is repeated over a period of time.

Another interesting result found was that the response in the immediate vicinity of $\Omega = 1$ is much lower than that resulting from smaller external force as shown in Fig. 34 and Fig. 40.

5.5 Other Results of Interest

5.5.1 Observation of the Traveling Wave

As mentioned in the theoretical analysis, the response of a nonlinear vibration of cylindrical shells takes the form of a traveling wave in the circumferential direction superimposed on a standing wave. This is due to the participation of the companion mode such as

$$w(x, y, t) = [a\cos\omega_c t\cos\frac{ny}{R} + b\sin\omega_c t\sin\frac{ny}{R}]\sin\frac{m\pi x}{L} \qquad (5.8)$$

This can be rearranged as

$$w(x, y, t) = [c\cos\omega_c t\cos\frac{ny}{R} + b\cos(\omega_c t - \frac{ny}{R})]\sin\frac{m\pi x}{L} \qquad (5.9)$$

where $c = a-b$.

The second term $\cos(\omega_c t - \frac{ny}{R})$ is a traveling wave. The phase velocity of this traveling wave is $\frac{\omega_c}{n}$ rad/sec. In other words, it takes $T = \frac{2n\pi}{\omega_c}$ seconds for this wave to travel 360° or a complete circumference of the shell. Therefore, what the pickup will measure at a fixed station is the standing wave $c\cos\omega_c t$ plus a wave with amplitude b, coming every $\frac{2n\pi}{\omega_c}$ seconds. From the pickup's point of view this appears to be another standing wave with a frequency $\frac{\omega_c}{n}$. This was observed by the cathode ray oscilloscope as shown in Fig. 43. In both pictures, the upper signal was taken from the oscillator and the lower signal was taken from the pickup. A similar figure was shown for the theoretical results in Fig. 21.

5.5.2 Regions of Multiple Responses

For the driven mode response only, it was observed that jumps

occurred at certain amplitudes and frequencies for each level of the forcing function. The boundaries of the jump are plotted in Fig. 44 and compared to the analysis. The comparison shows qualitative agreement between the analysis and experiment. The difference may be caused by the choice of damping in the analysis.

A similar plot was made for the response with companion mode participation. The boundaries of this region are shown in Fig. 45. Similar qualitative agreement between the analysis and experiment is indicated.

5.5.3 Rotating of the Shell at Large Amplitude

One of the most surprising results discovered in this experimental study was that the shell rotated at certain amplitudes and frequencies. As mentioned before, the shell-ring system was supported by an end plate with two O-rings. Although it was designed to freely support the shell-ring system, due to friction between the ring and rubber O-ring, it required a certain amount of torque to rotate the shell with respect to the end plate. However, the large amplitude vibration somehow introduced a net torque to the shell and the shell rotated with respect to its end plate. This would occur only at a certain discrete frequency for a constant driver voltage. Depending on the amplitude and frequency, the shell rotated either in one direction or back and forth. At the present time no reasonable explanation can be offered. However two possibilities can be eliminated, namely

1) It was not a spontaneous occurrence, since all of the rotating shell phenomena were repeatable.

2) It was not due to the resonance of the table where the experimental apparatus was placed, since adding heavy weights on the table, thus changing its resonance, did not eliminate the rotating phenomena.

VI. CONCLUDING REMARKS

The experimental results of the driven mode response show good agreement both quantitatively and qualitatively with that of the analytical results. This indicates that Donnell's nonlinear equations for a cylindrical shell can be used in the large amplitude vibration problem. When the response amplitude exceeds a certain "critical value," its companion mode becomes excited. Here the analyses are qualitatively in agreement with the experimental results. The regions of the companion mode participation and resulting traveling wave phenomena have been demonstrated by the experiment as the analysis indicated. However the drifting of the amplitude at a certain frequency range was not predicted by the analysis. It appears that a transient analysis should be performed to study these phenomena.

It has also been demonstrated that the perturbation technique used in the present investigation has a few advantages over the methods used in previous investigations such as without predetermining the deflection shape. The comparison between the present study and the previous investigation indicates the importance of the assumed deflection shape with respect to the type of nonlinearity and the degree of nonlinearities. The ability to satisfy the specified boundary conditions asymptotically in the present analysis is another advantage.

In conclusion, it seems that the basic approach presented here is applicable to the problem of large amplitude vibration of cylindrical shells, as well as many other axisymmetric systems.

REFERENCES

1. Stoker, J. J., "Nonlinear Vibrations in Mechanical and Electrical Systems," Interscience Publication, Inc., 1950.

2. Olson, M. D. and Fung, Y. C., "Supersonic Flutter of Circular Cylindrical Shells Subjected to Internal Pressure and Axial Compression." AIAA J., vol. 4, no. 5, May 1966, pp. 858-864.

3. Evensen, D. A., "A Theoretical and Experimental Study of the Nonlinear Flexural Vibrations of Thin Circular Rings," NASA TR R-227, 1965.

4. Tobias, S. A., "Non-Linear Forced Vibrations of Circular Discs," Engineering, vol. 186, no. 4818, July 11, 1958, pp. 51-56.

5. Mixon, J. S. and Herr, R. W., "An Investigation of Vibration Characteristics of Pressurized Thin-Walled Circular Cylinders Partly Filled with Liquid." NASA TR R-145, 1962.

6. von Kármán, T. and Tsien, H. S., "The Buckling of Thin Cylindrical Shells under Axial Compression," J. Aeronautical Sci., 8, June 1941, pp. 303-312.

7. Reissner, Eric, "Nonlinear Effects in the Vibrations of Cylindrical Shells," Report No. AM5-6, Guided Missile Res. Dir., Ramo-Wooldridge Corp., Sept. 30, 1955.

8. Chu, Hu-Nan, "Influence of Large Amplitudes on Flexural Vibrations of a Thin Circular Cylindrical Shell," J. Aerospace Sci., vol. 28, no. 8, Aug. 1961, pp. 602-609.

9. Cummings, B. E., "Some Nonlinear Vibration and Response Problems of Cylindrical Panels and Shells." SM 62-32 (AFOSR 3123) Graduate Aero. Labs., Calif. Inst. Tech., June 1962.

10. Nowinski, J. L., "Nonlinear Transverse Vibrations of Orthotropic Cylindrical Shells," AIAA J. vol. 1, no. 3, Mar. 1963, pp. 617-620.

11. Mayers, J. and Wrenn, B. G., "On the Nonlinear Free Vibrations of Thin Circular Cylindrical Shells," SUDAAR 269, June 1966, Dept. of Aeronautics and Astronautics, Stanford Univ.

12. Evensen, D. A., "Nonlinear Flexural Vibrations of Thin-Walled Circular Cylinders," NASA TN D-4090, Aug. 1967.

13. Dowell, E. H. and Ventres, C. S., "Modal Equations for the Nonlinear Flexural Vibrations of a Cylindrical Shell," International Journal of Solids and Structures, vol. 4, no. 6, June 1968, pp. 975-991.

14. Evensen, D. A., "Nonlinear Vibrations of an Infinitely Long Cylindrical Shell," AIAA J., vol. 6, no. 7, July 1968, pp. 1401-1403.

15. Matsuzaki, Y. and Kobayashi, S., "An Analytical Study of Nonlinear Flexural Vibration of Thin Circular Shells," J. of Japan Society for Aeronautical and Space Sciences, vol. 17, no. 187, pp. 308-315, 1969.

16. Matsuzaki, Y. and Kobayashi, S., "A Theoretical and Experimental Study of the Nonlinear Flexural Vibration of Thin Circular Cylindrical Shells with Clamped Ends," Japan Society for Aeronautical and Space Sciences, vol. 12, no. 21, 1970.

17. Bleich, H. H. and Ginsberg, J. H., "Nonlinear Forced Vibrations of Infinitely Long Cylindrical Shells," Technical Report No. 46, Contract Nonr-266(86), Dept. of Civil Engineering and Engineering Mechanics, Columbia University, Nov. 1970.

18. Evensen, D. A., private communication, Sept. 1971.

19. El Raheb, M., "Some Approximations in the Dynamic Shell Equations," Ph. D. Thesis, California Institute of Technology, Dec. 1, 1969.

20. Koiter, W., "A Consistent First Approximation in the General Theory of Thin Elastic Shells," I. U. T. A. M., North Holland Publishing Co., Amsterdam, 1960.

21. Evensen, D. A., "The Influence of Initial Stresses and Boundary Restraints on the Nonlinear Vibrations of Cylindrical Shells," unpublished paper, private communication, Oct. 1971.

22. Olson, M. D., "Some Experimental Observations on the Nonlinear Vibration of Cylindrical Shells," AIAA J., vol. 3, No. 9, Sept. 1965, pp. 1775-1777.

APPENDIX A

LINEAR FORCED VIBRATION OF CYLINDRICAL SHELLS

The governing equations for the linear vibration of cylindrical shells are:

$$D\nabla^4 w + \rho h \frac{\partial^2 w}{\partial t^2} = q(x,y,t) + \frac{1}{R}\frac{\partial^2 F}{\partial x^2} \tag{A. 1}$$

$$\frac{1}{Eh}\nabla^4 F = -\frac{1}{R}\frac{\partial^2 w}{\partial x^2} \tag{A. 2}$$

where q(x, y, t) is the external forcing function applied in the radial direction.

It can be shown that the solutions for the homogeneous equations of (A. 1) and (A. 2) are:

$$w(x,y,t) = e^{i\omega_{mn}t}\left[a_{mn}\cos\frac{ny}{R} + b_{mn}\sin\frac{ny}{R}\right]\sin\frac{m\pi x}{L} \tag{A. 3}$$

$$F(x,y,t) = \frac{\frac{Eh}{R}\left(\frac{m\pi}{L}\right)^2}{\left[\left(\frac{m\pi}{L}\right)^2 + \left(\frac{n}{R}\right)^2\right]^2} e^{i\omega_{mn}t}\left[a_{mn}\cos\frac{ny}{R} + b_{mn}\sin\frac{ny}{R}\right]\sin\frac{m\pi x}{L} \tag{A. 4}$$

The solutions expressed by (A. 3) and (A. 4) satisfy the simply-supported boundary condition, namely

$$w = \frac{\partial^2 w}{\partial x^2} = N_x = v = 0 \tag{A. 5}$$

The eigenvalues of the homogeneous equations can be written as

$$\omega_{mn}^2 = \frac{1}{\rho h}\left\{D\left[\left(\frac{m\pi}{L}\right)^2 + \left(\frac{n}{R}\right)^2\right]^2 - \frac{Eh}{R^2}\frac{\left(\frac{m\pi}{L}\right)^4}{\left[\left(\frac{m\pi}{L}\right)^2 + \left(\frac{n}{R}\right)^2\right]^2}\right\} \tag{A. 6}$$

The solutions given by (A. 3) and (A. 4) are the eigenfunctions (normal modes) of the cylindrical shell since they satisfy the governing equations and the specified boundary conditions.

For the forced response problem, the solution can be written in terms of the eigenfunctions with undetermined coefficients as follows:

$$W(x,y,t) = \sum_{i=1}^{\infty}\sum_{j=1}^{\infty}\left[A_{ij}(t)\cos\frac{jy}{R} + B_{ij}(t)\sin\frac{jy}{R}\right]\sin\frac{i\pi x}{L} \qquad (A.7)$$

Upon substituting (A. 7) into eqs. (A. 1) and (A. 2) and eliminating the stress function F, the following equations governing A_{ij} and B_{ij} are obtained after multiplying the equation by $\cos\frac{ky}{R}\sin\frac{m\pi x}{L}$ and $\sin\frac{ky}{R}\sin\frac{m\pi x}{L}$ and integrating over the shell surface.

$$\ddot{A}_{ij}(t) + \omega_{ij}^2 A_{ij}(t) = Q_{ij} \qquad (A.8)$$

$$\ddot{B}_{ij}(t) + \omega_{ij}^2 B_{ij}(t) = P_{ij} \qquad (A.9)$$

where

$$Q_{ij} = \frac{2}{(\pi RL)\rho h}\int_0^L\int_0^{2\pi R} q(x,y,t)\cos\frac{jy}{R}\sin\frac{i\pi x}{L}\,dy\,dx \qquad (A.10)$$

$$P_{ij} = \frac{2}{(\pi RL)\rho h}\int_0^L\int_0^{2\pi R} q(x,y,t)\sin\frac{jy}{R}\sin\frac{i\pi x}{L}\,dy\,dx \qquad (A.11)$$

Distributed External Excitation

Now assuming the external forcing function is given as

$$q(x,y,t) = f\cos\omega t\cos\frac{ky}{R}\sin\frac{m\pi x}{L} \qquad (A.12)$$

then from eqs. (A. 10) and (A. 11),

$$Q_{ij} = \frac{f}{\rho h} \cos \omega t \qquad \text{for} \quad i=m \,,\; j=n$$

$$Q_{ij} = 0 \qquad \text{for} \quad i \neq m \,,\; j \neq n \qquad \text{(A. 13)}$$

$$P_{ij} = 0 \qquad \text{for} \quad \text{all} \;\; i \,,\; j$$

Substituting eq. (A. 13) into eqs. (A. 8) and (A. 9) the undetermined coefficient can be calculated as

$$A_{ij}(t) = \frac{f}{\rho h (\omega_{ij}^2 - \omega^2)} \cos \omega t \qquad \text{for} \quad i=m \,,\; j=n$$

$$A_{ij}(t) \equiv 0 \qquad \text{for} \quad i \neq m \,,\; j \neq n \qquad \text{(A. 14)}$$

$$B_{ij}(t) \equiv 0 \qquad \text{for all} \;\; i \,,\; j$$

Now the response of the shell under the given external excitation (A. 12) may be written as

$$W(x,y,t) = \frac{f}{\rho h (\omega_{mn}^2 - \omega^2)} \cos \omega t \cos \frac{ny}{R} \sin \frac{m\pi x}{L} \qquad \text{(A. 15)}$$

Concentrated External Excitation

Now assuming a concentrated external forcing function given as follows

$$q(x,y,t) = f \cos \omega t \qquad \text{for} \quad \left(\frac{L}{2} - \frac{c}{2}\right) \leq x \leq \left(\frac{L}{2} + \frac{c}{2}\right)$$
$$-\frac{c}{2} \leq y \leq \frac{c}{2}$$

$$q(x,y,t) = 0 \qquad \text{otherwise} \qquad \text{(A. 16)}$$

From eqs. (A. 10) and (A. 11) the generalized force can be obtained as follows:

$$Q_{mn} = \frac{8}{\pi^2 mn\rho h} \sin\frac{n\pi c}{2R} \sin\frac{m\pi c}{2L} \sin\frac{m\pi}{2} f \cos\omega t$$

$$P_{mn} = 0 \qquad \text{(A. 17)}$$

From eqs. (A. 8) and (A. 9) the undetermined coefficients $A_{mn}(t)$ and $B_{mn}(t)$ can be obtained as follows:

$$A_{mn}(t) = \frac{8f}{\pi^2 mn\rho h(\omega_{mn}^2 - \omega^2)} \sin\frac{n\pi c}{2R} \sin\frac{m\pi c}{2L} \sin\frac{m\pi}{2} \cos\omega t$$

$$B_{mn}(t) = 0 \qquad \text{(A. 18)}$$

The response of the shell can be written as

$$w(x,y,t) = \frac{8f}{\pi^2\rho h} \sum_{m=1}^{\infty} \sum_{n=1}^{\infty} a_{mn} \cos\omega t \cos\frac{ny}{R} \sin\frac{m\pi x}{L} \qquad \text{(A. 19)}$$

where

$$a_{mn} = \frac{\sin\frac{n\pi c}{2R} \sin\frac{m\pi c}{2L} \sin\frac{m\pi}{2}}{mn(\omega_{mn}^2 - \omega^2)} \qquad \text{(A. 20)}$$

For a cylindrical shell with viscous structural damping, the response can be obtained as follows:

$$w(x,y,t) = \frac{8f}{\pi^2\rho h} \sum_{m=1}^{\infty} \sum_{n=1}^{\infty} a'_{mn} \cos(\omega t - \delta_{mn}) \cos\frac{ny}{R} \sin\frac{m\pi x}{L}$$

where (A. 21)

$$a'_{mn} = \frac{\sin\frac{nc}{2R}\sin\frac{m\pi c}{2L}\sin\frac{m\pi}{1}}{mn\,\omega^2_{mn}\left[\left(1-\frac{\omega^2}{\omega^2_{mn}}\right)^2 + 4\gamma^2_{mn}\frac{\omega^2}{\omega^2_{mn}}\right]^{1/2}} \qquad \text{(A. 22)}$$

and phase angle δ_{mn} is given as

$$\delta_{mn} = \frac{2\gamma_{mn}\omega_{mn}\omega}{\omega^2_{mn} - \omega^2} \qquad \text{(A. 23)}$$

and γ_{mn} is the percentage of the critical damping. Now assuming the percentage of critical damping γ_{mn} is 0. 001 for every mode and the finite area C^2, where the external forcing function is applied, is $(0.25 \text{ inch})^2$. The magnitude of a_{mn} will be calculated for the shell specimen used in the experiment.

1. At resonance of m = 1, n = 6, ω = 558. 07 cps

$$\frac{a'_{mn}}{a'_{1,6}} = \frac{6}{mn}\,\frac{\sin\frac{nc}{2R}\sin\frac{m\pi c}{2L}\sin\frac{m\pi}{2}}{\sin\frac{6c}{2R}\sin\frac{\pi c}{2L}\sin\frac{\pi}{2}}\,\frac{(558.07)^2}{\omega^2_{mn}}\,\frac{2\gamma\frac{558.07}{\omega_{mn}}}{\left[\left(1-\frac{558.07^2}{\omega^2_{mn}}\right)^2+4\gamma\frac{558.07^2}{\omega^2_{mn}}\right]^{1/2}} \qquad \text{(A. 24)}$$

The values of $\frac{a'_{mn}}{a'_{1,6}}$ are tabulated in the following for m = 1, $4 \leq n \leq 13$

n	4	5	6	7	8	9
$\frac{a'_{mn}}{a'_{1,6}}$	0. 00075	0. 00276	1. 000	0. 00827	0. 00806	0. 03414

10	11	12	13
0. 00734	0. 002617	0. 001392	0. 000863

From this tabulation, it is clear that the response is dominated by the m = 1, n = 6 mode. Therefore it may be concluded that at the resonance frequency for a lightly damped shell under concentrated external excitation the response can be approximated as

$$w(x,y,t) = a'_{mn} \cos(\omega t - \delta_{mn}) \cos\frac{ny}{R} \sin\frac{m\pi x}{L} \qquad \text{(A. 25)}$$

2. At the vicinity of a resonance, m = 1, n = 6

In the analysis and the experiment, the frequency of the concentrated external forcing function is varied in the vicinity of the resonance. In the following, it will be shown as long as the frequency variation is small the approximation expressed by eq. (A. 25) still holds.

Let the frequency of the external forcing function be 0. 4% more than the resonant frequency for m = 1, n = 6. In other words let ω = 560. 30 cps, then

$$\frac{a'_{mn}}{a'_{1,6}} = \frac{6}{mn} \frac{\sin\frac{nc}{2R} \sin\frac{m\pi c}{2L} \sin\frac{m\pi}{2}}{\sin\frac{6c}{2R} \sin\frac{\pi c}{2L} \sin\frac{\pi}{2}} \frac{558.07^2}{\omega_{mn}^2} \frac{\left[\left(1-\frac{560.3^2}{558.07^2}\right)^2 + 4\gamma^2 \frac{560.3^2}{558.07^2}\right]^{1/2}}{\left[\left(1-\frac{560.3^2}{\omega_{mn}^2}\right)^2 + 4\gamma^2 \frac{560.3^2}{558.07^2}\right]^{1/2}} \qquad \text{(A. 26)}$$

The values of $\frac{a'_{mn}}{a'_{1,6}}$ are tabulation in the following for m = 1, $4 \leq n \leq 13$

n	4	5	6	7	8
$\frac{a'_{mn}}{a'_{1,6}}$	0. 00311	0. 0115	1. 000	0. 033	0. 0351
	9	10	11	12	13
	0. 071	0. 0312	0. 0109	0. 00578	0. 00357

Again the response is dominated by the m = 1, n = 6 mode. However the magnitude of other modes is significantly larger than the previous case. For instance the m = 1, n = 9 mode has an amplitude of 7.1% of the m = 1, n = 6 mode compared to 3.4% in the previous case. Using the approximation response as shown by eq. (A.25) for this case is neglecting the terms with magnitude up to 7.1% of the m = 1, n = 6 mode.

APPENDIX B

CIRCUMFERENTIAL PERIODICITY CONDITION

The solutions for the zero order equations satisfy the circumferential periodicity condition identically due to the linear relationship between the stress function and the radial displacement and tangential displacements. The circumferential periodicity condition for the first order equations will be derived in the following.

From eqs. (4. 21) and (4. 35), one obtains

$$\begin{aligned}\frac{\partial V_1}{\partial \theta} &= \frac{1}{1-\nu^2}\left[\frac{1}{R^2}\frac{\partial^2 \phi_1}{\partial s^2} - \nu\frac{\partial^2 \phi_1}{\partial \theta^2}\right] + W_1 - \frac{1}{2}\left(\frac{\partial W_0}{\partial \theta}\right)^2 \\ &= \frac{1}{1-\nu^2}\left[\frac{1}{R^2}\frac{\partial^2 \phi_1^p}{\partial s^2} - \nu\frac{\partial^2 \phi_1^p}{\partial \theta^2}\right] + W_1^p - \frac{1}{2}\left(\frac{\partial W_0}{\partial \theta}\right)^2 \\ &\quad + \frac{1}{1-\nu^2}\left[\frac{1}{R^2}\frac{\partial^2 \phi_1^c}{\partial s^2} - \nu\frac{\partial^2 \phi_1^c}{\partial \theta^2}\right] + W_1^c \end{aligned} \tag{B. 1}$$

upon substitution of eqs. (4. 38), (4. 52) and (4. 53) into eq. (B. 1). The following may be obtained:

$$\begin{aligned}\frac{\partial V_1}{\partial \theta} &= q_0(\tau) + \frac{1}{1-\nu^2}\frac{2}{R^2}\bar{q}_0(\tau) - \frac{n^2}{8}\left[A^2(\tau) + B^2(\tau)\right] + q_1(s) + \frac{1}{1-\nu^2}\frac{1}{R^2}\bar{q}_1''(s) \\ &\quad + \left[q_2(s) + \frac{1}{1-\nu^2}\frac{1}{R^2}\bar{q}_2''(s)\right]\left[a^2\cos 2(\tau+\delta_a) - b^2\cos 2(\tau+\delta_b)\right] \\ &\quad + \left[\alpha_1 - \frac{1}{1-\nu^2}\left(\frac{2m\pi}{R}\right)^2\bar{\alpha}_1 + \frac{n^2}{8}(A^2+B^2)\right]\cos 2m\pi s \\ &\quad + Q_1(s,\tau)\cos 2n\theta + Q_2(s,\tau)\sin 2n\theta \end{aligned} \tag{B. 2}$$

where

$$Q_1(s,\tau) = \alpha_2(\tau) + g_3(s) + g_4(s)[a^2\cos 2(\tau+\delta_a) + b^2\cos 2(\tau+\delta_b)]$$
$$+ \frac{4\kappa^2\nu}{1-\nu^2}\left\{\bar{\alpha}_2(\tau) + \bar{g}_3(s) + \bar{g}_4(s)[a^2\cos 2(\tau+\delta_a) + b^2\cos 2(\tau+\delta_b)]\right\}$$
$$+ \frac{1}{1-\nu^2}\frac{1}{R^2}\left\{\bar{g}_3''(s) + \bar{g}_4''(s)[a^2\cos 2(\tau+\delta_a) + b^2\cos 2(\tau+\delta_b)]\right\}$$
$$+ \frac{\kappa^2}{8}(B^2 - A^2)(\cos 2m\pi s - 1) \qquad \text{(B. 3)}$$

$$Q_2(s,\tau) = \alpha_3(\tau) + g_5(s)\sin(2\tau+\delta_a+\delta_b) + g_6\sin(\delta_b-\delta_a)$$
$$+ \frac{4\kappa^2\nu}{1-\nu^2}\left[\bar{\alpha}_3(\tau) + \bar{g}_5(s)\sin(2\tau+\delta_a+\delta_b) + \bar{g}_6\sin(\delta_b-\delta_a)\right]$$
$$+ \frac{1}{1-\nu^2}\frac{1}{R^2}\left[\bar{g}_5''(s)\sin(2\tau+\delta_a+\delta_b) + \bar{g}_6''(s)\sin(\delta_b-\delta_a)\right]$$
$$+ \frac{\kappa^2}{4}AB(1-\cos 2m\pi s) \qquad \text{(B. 4)}$$

Now from eq. (4. 39), it may be concluded that

$$\alpha_1(\tau) - \frac{1}{1-\nu^2}\left(\frac{2m\pi}{R}\right)^2 + \frac{\kappa^2}{8}(A^2+B^2) = 0 \quad .$$

From eqs. (4. 55) and (4. 56) by integration twice and setting the integration constants equal to zero, it may be concluded that

$$q_1(s) + \frac{1}{1+\nu^2}\frac{1}{k^2}\bar{q}_1''(s) = 0 \quad \text{and} \quad q_2(s) + \frac{1}{1+\nu^2}\frac{1}{k^2}\bar{q}_2''(s) = 0 \ .$$

Therefore the circumferential periodicity conditions can be written as

$$\int_0^{2\pi} \frac{\partial v_1}{\partial \theta}\, d\theta = \int_0^{2\pi} \Big\{ \Big[q_0(\tau) + \frac{1}{1+\nu^2}\frac{2}{k^2}\bar{q}_0(\tau) - \frac{h^2}{8}(A^2+B^2) \Big] + Q_1(s,\tau)\cos 2n\theta + Q_2(s,\tau)\sin 2n\theta \Big\}\, d\theta$$

$$= 2\pi \Big[q_0(\tau) + \frac{1}{1+\nu^2}\frac{2}{k^2}\bar{q}_0(\tau) - \frac{h^2}{8}(A^2+B^2) \Big] = 0 \qquad \text{(B. 5)}$$

It is obvious now that

$$q_0(\tau) + \frac{1}{1+\nu^2}\frac{2}{k^2}\bar{q}_0(\tau) = \frac{h^2}{8}\left[A^2(\tau) + B^2(\tau)\right] \qquad \text{(B. 6)}$$

is the equation which assures that the first order solution satisfies the circumferential periodicity condition. Eq. (B. 6) appears as the second equation of eq. (4. 54) which determines the function $q_0(\tau)$ and $\bar{q}_0(\tau)$.

APPENDIX C

BOUNDARY CONDITIONS FOR THE FIRST ORDER COMPLEMENTARY SOLUTION

The boundary conditions for the first order complementary solution are obtained such that the sum of the first order particular solution and complementary solution satisfy the specified boundary conditions as expressed by eq. (4.20).

The radial displacement W_1 can be expressed as

$$
\begin{aligned}
W_1(S,\theta,\tau) &= W_1^P(S,\theta,\tau) + W_1^C(S,\theta,\tau) \\
&= \Big\{C_1(a^2+b^2) + C_2\left[a^2\cos 2(\tau+\delta_a) - b^2\cos 2(\tau+\delta_b)\right]\Big\}\cos 2m\pi S + C_3(a^2-b^2)\cos 2n\theta \\
&+ C_4\left[a^2\cos 2(\tau+\delta_a) + b^2\cos 2(\tau+\delta_b)\right]\cos 2n\theta + C_7 ab\sin(2\tau+\delta_a+\delta_b)\sin 2n\theta \\
&+ C_8 ab\sin(\delta_b-\delta_a)\sin 2n\theta + g_1(S) + g_2(S)\left[a^2\cos 2(\tau+\delta_a) - b^2\cos 2(\tau+\delta_b)\right] \\
&+ g_3(S)\cos 2n\theta + g_4(S)\left[a^2\cos 2(\tau+\delta_a) + b^2\cos 2(\tau+\delta_b)\right]\cos 2n\theta \\
&+ g_5(S)\sin(2\tau+\delta_a+\delta_b)\sin 2n\theta + g_6(S)\sin(\delta_b-\delta_a)\sin 2n\theta \\
&+ C_5(a^2+b^2) + C_6\left[a^2\cos 2(\tau+\delta_a) - b^2\cos 2(\tau+\delta_b)\right] \qquad \text{(C. 1)}
\end{aligned}
$$

At $s = 0$ and $s = 1$, the radial displacement vanishes, $W(s = 0,1) = 0$. From eq. (C. 1) this condition can only be satisfied

if the following is true.

$$\left.\begin{aligned} g_1(S=0,1) &= -(C_1+C_5)(a^2+b^2) \\ g_2(S=0,1) &= -(C_2+C_6) \\ g_3(S=0,1) &= -C_3(a^2-b^2) \\ g_4(S=0,1) &= -C_4 \\ g_5(S=0,1) &= -C_7 ab \\ g_6(S=0,1) &= -C_8 ab \end{aligned}\right\} \qquad (C.2)$$

The axial bending moment at s = 0, 1 can be expressed as

$$M_x \sim \frac{1}{k^2}\frac{\partial^2 W_1}{\partial S^2} + \nu\frac{\partial^2 W_1}{\partial \theta^2} = \frac{1}{k^2}\left(\frac{\partial^2 W_1^P}{\partial S^2} + \frac{\partial^2 W_1^C}{\partial S^2}\right) + \nu\left(\frac{\partial^2 W_1^P}{\partial \theta^2} + \frac{\partial^2 W_1^C}{\partial \theta^2}\right) = 0 \qquad (C.3)$$

From eqs. (C. 1) and (C. 2), it can be shown that

$$\frac{\partial^2 W_1}{\partial \theta^2}(S=0,1) = \left[\frac{\partial^2 W_1^P}{\partial \theta^2} + \frac{\partial^2 W_1^C}{\partial \theta^2}\right]_{\text{at } s=0,1} \equiv 0 \qquad (C.4)$$

Therefore,

$$\frac{\partial^2 W_1}{\partial S^2} = \frac{\partial^2 W_1^P}{\partial S^2} + \frac{\partial^2 W_1^C}{\partial S^2} = 0 \qquad \text{at } S=0,1$$

represents the boundary condition that the bending moment vanishes at s = 0, and s = 1. Now $\frac{\partial^2 W_1}{\partial S^2}$ can be expressed as,

$$\frac{\partial^2 W_1}{\partial s^2} = \frac{\partial^2 W_1^P}{\partial s^2} + \frac{\partial^2 W_1^C}{\partial s^2}$$

$$= -(2m\pi)^2 \left\{ C_1 (a^2+b^2) + C_2 \left[a^2 \cos 2(\tau+\delta_a) - b^2 \cos 2(\tau+\delta_b) \right] \right\} + g_1''(s)$$

$$+ g_2''(s) \left[a^2 \cos 2(\tau+\delta_a) - b^2 \cos 2(\tau+\delta_b) \right] + g_3''(s) \cos 2n\theta$$

$$+ g_4''(s) \left[a^2 \cos 2(\tau+\delta_a) + b^2 \cos 2(\tau+\delta_b) \right] \cos 2n\theta$$

$$+ g_5''(s) \sin(2\tau+\delta_a+\delta_b) \sin 2n\theta + g_6''(s) \sin(\delta_b-\delta_a) \sin 2n\theta$$

(C. 5)

At s = 0 and s = 1, $\frac{\partial^2 W_1}{\partial s^2} = 0$ gives the following conditions,

$$\left.\begin{aligned}
&g_1''(s=0,1) = (2m\pi)^2 C_1 (a^2+b^2) \\
&g_2''(s=0,1) = (2m\pi)^2 C_2 \\
&g_3''(s=0,1) = 0 \\
&g_4''(s=0,1) = 0 \\
&g_5''(s=0,1) = 0 \\
&g_6''(s=0,1) = 0
\end{aligned}\right\} \qquad \text{(C. 6)}$$

The axial stress vanishing at s = 0, 1 implies that

$$\frac{\partial^2 \Phi_1}{\partial \theta^2} = \frac{\partial^2 \Phi_1^P}{\partial \theta^2} + \frac{\partial^2 \Phi_1^C}{\partial \theta^2} = 0 \qquad \text{(C. 7}$$

Using eqs. (4.38) and (4.53) the expression for $\frac{\partial^2 \Phi_1}{\partial \theta^2}$ can be written as

$$\begin{aligned}\frac{\partial^2 \Phi_1}{\partial \theta^2} = -(2n)^2 \Big\{ & \bar{C}_3 (a^2 - b^2) \cos 2n\theta + \bar{C}_4 \left[a^2 \cos 2(\tau + \delta_a) + b^2 \cos 2(\tau + \delta_b) \right] \cos 2n\theta \\ & + \bar{C}_8 ab \sin(\delta_b - \delta_a) \sin 2n\theta + \bar{C}_9 ab \sin(2\tau + \delta_a + \delta_b) \sin 2n\theta \\ & + \bar{q}_3(s) \cos 2n\theta + \bar{q}_4(s) \left[a^2 \cos 2(\tau + \delta_a) + b^2 \cos 2(\tau + \delta_b) \right] \cos 2n\theta \\ & + \bar{q}_5(s) \sin(2\tau + \delta_a + \delta_b) \sin 2n\theta \\ & + \bar{q}_6(s) \sin(\delta_b - \delta_a) \sin 2n\theta \Big\} \end{aligned} \tag{C.8}$$

At $s = 0$ and $s = 1$, $\frac{\partial^2 \Phi_1}{\partial \theta^2} = 0$ gives the following conditions,

$$\left.\begin{aligned} \bar{q}_3(s=0,1) &= -\bar{C}_3 (a^2 - b^2) \\ \bar{q}_4(s=0,1) &= -\bar{C}_4 \\ \bar{q}_5(s=0,1) &= -\bar{C}_9 ab \\ \bar{q}_6(s=0,1) &= -\bar{C}_8 ab \end{aligned}\right\} \tag{C.9}$$

The last boundary condition is the vanishing circumferential displacement at $s = 0$ and $s = 1$. From eqs. (B.2), (4.39), (4.55) and (4.56), the circumferential displacement $V_1(s, \theta, \tau)$ can be

expressed as

$$\frac{\partial V_1}{\partial \theta} = Q_1(s,\tau)\cos 2n\theta + Q_2(s,\tau)\sin 2n\theta \qquad \text{(C. 10)}$$

where $Q_1(s,\tau)$ and $Q_2(s,\tau)$ are defined by eqs. (B. 5) and (B. 6).

Upon integration, the following equation may be obtained.

$$V_1(s,\theta,\tau) = \frac{1}{2n}\left[Q_1(s,\tau)\sin 2n\theta - Q_2(s,\tau)\cos 2n\theta\right] + K(s,\tau) \qquad \text{(C. 11)}$$

where $K(s,\tau)$ is an integration constant.

At s = 0 and s = 1, using previous boundary conditions, it can be shown that

$$Q_1(s=0,1) = \frac{1}{1-\nu^2}\frac{1}{R^2}\left\{\bar{q}_3''(s=0,1) + \bar{q}_4''(s=0,1)\left[a^2\cos 2(\tau+\delta_a) + b^2\cos 2(\tau+\delta_b)\right]\right\} \qquad \text{(C. 12)}$$

$$Q_2(s=0,1) = \frac{1}{1-\nu^2}\frac{1}{R^2}\left\{\bar{q}_5''(s=0,1)\sin(2\tau+\delta_a+\delta_b) + \bar{q}_6''(s=0,1)\sin(\delta_b-\delta_a)\right\}$$

Setting the integration constant $K(s,\tau) \equiv 0$, the vanishing circumferential displacement at s = 0 and s = 1 can be satisfied if the following condition is satisfied.

$$Q_1(s=0,1) = Q_2(s=0,1) = 0 \qquad \text{(C. 13)}$$

which in turn gives the following conditions,

$$\left.\begin{aligned} \bar{q}_3''(s=0,1) &= 0 \\ \bar{q}_4''(s=0,1) &= 0 \\ \bar{q}_5''(s=0,1) &= 0 \\ \bar{q}_6''(s=0,1) &= 0 \end{aligned}\right\} \qquad \text{(C. 14)}$$

In summary, the following boundary conditions are obtained at s = 0 and s = 1

$$\left.\begin{aligned} g_1(S=0,1) &= -(C_1+C_5)(a^2+b^2) \\ g_1''(S=0,1) &= (2m\pi)^2 C_1 (a^2+b^2) \end{aligned}\right\} \qquad (4.55a)$$

$$\left.\begin{aligned} g_2(S=0,1) &= -(C_2+C_6) \\ g_2''(S=0,1) &= (2m\pi)^2 C_2 \end{aligned}\right\} \qquad (4.56a)$$

$$\left.\begin{aligned} g_3(S=0,1) &= -C_3(a^2-b^2) \\ \bar{g}_3(S=0,1) &= -\bar{C}_3(a^2-b^2) \\ g_3''(S=0,1) &= 0 \\ \bar{g}_3''(S=0,1) &= 0 \end{aligned}\right\} \qquad (4.57a)$$

$$\left.\begin{aligned} g_4(S=0,1) &= -C_4 \\ \bar{g}_4(S=0,1) &= -\bar{C}_4 \\ g_4''(S=0,1) &= 0 \\ \bar{g}_4''(S=0,1) &= 0 \end{aligned}\right\} \qquad (4.58a)$$

$$
\left.
\begin{aligned}
&g_5(s=0,1) = -c_7 ab \\
&\bar{g}_5(s=0,1) = -\bar{c}_7 ab \\
&g_5''(s=0,1) = 0 \\
&\bar{g}_5''(s=0,1) = 0
\end{aligned}
\right\} \qquad (4.59a)
$$

$$
\left.
\begin{aligned}
&g_6(s=0,1) = -c_8 ab \\
&\bar{g}_6(s=0,1) = -\bar{c}_8 ab \\
&g_6''(s=0,1) = 0 \\
&\bar{g}_6''(s=0,1) = 0
\end{aligned}
\right\} \qquad (4.60a)
$$

APPENDIX D

SOLUTIONS FOR $g_1(s)$ AND $\bar{g}_1(s)$ OF THE COMPLEMENTARY EQUATIONS

The governing equations for $g_1(s)$ and $\bar{g}_1(s)$ and its boundary conditions [eqs. (4.55) and (4.55a)] are as follows:

$$\left.\begin{aligned} \frac{r^2}{k^2} g_1''(s) - \bar{g}_1(s) = 0 \\ \frac{1}{1-\nu^2}\frac{1}{k^2}\bar{g}_1''(s) + g_1(s) = 0 \end{aligned}\right\} \qquad (D.1)$$

$$\left.\begin{aligned} g_1(s=0,1) = -(C_4+C_5)(a^2+b^2) \\ g_1''(s=0,1) = (2m\pi)^2 C_4 (a^2+b^2) \end{aligned}\right\} \qquad (D.2)$$

Here eq. (D.1) is obtained by integration of eq. (4.55) and the integration constants are set to be equal to zero due to the requirement of circumferential periodicity condition (see Appendix B).

Let $$\mu_1 = \sqrt[4]{\frac{k^4(1-\nu^2)}{64\, r^2}} \qquad (D.3)$$

Then eq. (D.1) can be reduced to

$$g_1''''(s) + 64\,\mu_1^4 g_1(s) = 0 \qquad (D.4)$$

The solution for eq. (D. 4) can be written as

$$g_1(s) = K_1' \sin\mu_1(2s-1)\sinh\mu_1(2s-1) + K_2' \cos\mu_1(2s-1)\cosh\mu_1(2s-1) \quad \text{(D. 5)}$$

Using the boundary conditions in eq. (D. 2), the constants K_1^1 and K_2^1 can be obtained as

$$\left.\begin{aligned} K_1' &= \left[\frac{H_1 \sin\mu_1 \sinh\mu_1 + \bar{H}_1 \cos\mu_1 \cosh\mu_1}{\cos^2\mu_1 + \sinh^2\mu_1}\right] \\ K_2' &= \left[\frac{H_1 \cos\mu_1 \cosh\mu_1 - \bar{H}_1 \sin\mu_1 \sinh\mu_1}{\cos^2\mu_1 + \sinh^2\mu_1}\right] \end{aligned}\right\} \quad \text{(D. 6)}$$

$$\left.\begin{aligned} H_1 &= g_1(s=0,1) = -(C_4 + C_5)(a^2+b^2) \\ \bar{H}_1 &= \frac{1}{8\mu_1^2} g_1''(s=0,1) = \frac{(2m\pi)^2}{8\mu_1^2} C_1 (a^2+b^2) \end{aligned}\right\} \quad \text{(D. 7)}$$

APPENDIX E

SOLUTIONS FOR $g_2(s)$ AND $\bar{g}_2(s)$ OF THE COMPLEMENTARY EQUATIONS

The governing equations for $g_2(s)$ and $\bar{g}_2(s)$ are given by eq. (4.56) and the boundary conditions are given by eq. (4.56a).

Let $$\mu_2 = \sqrt[4]{\frac{R^4[(1-\nu^2)-4\lambda_0]}{64h^2}} \tag{E.1}$$

Then eq. (4.56) can be reduced to

$$g_2''''(s) + 64\mu^4 g_2 = 0 \tag{E.2}$$

The solution of eq. (E.2) can be written as

$$g_2(s) = K_1^2 \sin\mu_2(2s-1)\sinh\mu_2(2s-1) + K_2^2 \cos\mu_2(2s-1)\cosh\mu_2(2s-1)$$

Using the boundary conditions expressed by eq. (4.56a), the constants K_1^2 and K_2^2 can be found as

$$\left.\begin{aligned} K_1^2 &= \frac{H_2 \sin\mu_2 \sinh\mu_2 + \bar{H}_2 \cos\mu_2 \cosh\mu_2}{\cos^2\mu_2 + \sinh^2\mu_2} \\ K_2^2 &= \frac{H_2 \cos\mu_2 \cosh\mu_2 - \bar{H}_2 \sin\mu_2 \sinh\mu_2}{\cos^2\mu_2 + \sinh^2\mu_2} \end{aligned}\right\} \tag{E.3}$$

$$\left.\begin{aligned} H_2 &= g_2(s=0,1) = -(C_2 + C_6) \\ \bar{H}_2 &= \frac{1}{8\mu_2^2} g_2''(s=0,1) = \frac{(2m\pi)^2}{8\mu_2^2} C_2 \end{aligned}\right\} \tag{E.4}$$

APPENDIX F

SOLUTIONS FOR $g_3(s)$, $\bar{g}_3(s)$ and $g_6(s)$, $\bar{g}_6(s)$ OF THE COMPLEMENTARY EQUATIONS

The governing equations and boundary conditions for $g_3(s)$ and $\bar{g}_3(s)$ are given by eqs. (4.57) and (4.57a) respectively.

Let

$$\mu_3 = \sqrt[4]{\frac{1-\nu^2}{4\pi^2}} \quad , \quad I = \frac{4\pi}{\sqrt{2}}\sqrt{\sqrt{1+\frac{\mu_3^4}{64\pi^4}}+1} \quad , \quad J = \frac{4\pi}{\sqrt{2}}\sqrt{\sqrt{1+\frac{\mu_3^4}{64\pi^4}}-1} \tag{F.1}$$

$$\left.\begin{aligned} \Lambda_1 &= \frac{k}{4}(\mu_3 + I) \quad , \quad & \Lambda_2 &= \frac{k}{4}(\mu_3 - I) \\ \Lambda_3 &= \frac{k}{4}(\mu_3 + J) \quad , \quad & \Lambda_4 &= \frac{k}{4}(\mu_3 - J) \end{aligned}\right\} \tag{F.2}$$

The solutions for eq. (4.57) can be written as

$$\left.\begin{aligned} g_3(s) &= K_1^3 \cos\Lambda_3(2s-1)\cosh\Lambda_1(2s-1) + K_2^3 \sin\Lambda_3(2s-1)\sinh\Lambda_1(2s-1) \\ &\quad + K_3^3 \cos\Lambda_4(2s-1)\cosh\Lambda_2(2s-1) + K_4^3 \sin\Lambda_4(2s-1)\sinh\Lambda_2(2s-1) \\ \bar{g}_3(s) &= 2\mu_3^2\pi^2\left[K_2^3\cos\Lambda_3(2s-1)\cosh\Lambda_1(2s-1) - K_1^3\sin\Lambda_3(2s-1)\sinh\Lambda_1(2s-1)\right. \\ &\quad \left. + K_4^3\cos\Lambda_4(2s-1)\cosh\Lambda_1(2s-1) - K_3^3\sin\Lambda_4(2s-1)\sinh\Lambda_2(2s-1)\right] \end{aligned}\right\} \tag{F.3}$$

Using the boundary conditions [eq. (4.57a)], the constants in eq. (F.3) can be found as

$$
\left.
\begin{aligned}
K_1^3 &= \frac{\bar{X}_1 \cos\Lambda_3 \cosh\Lambda_1 - \bar{X}_2 \sin\Lambda_3 \sinh\Lambda_1}{\cos^2\Lambda_3 \cosh^2\Lambda_1 + \sin^2\Lambda_3 \sinh^2\Lambda_1} \\
K_2^3 &= \frac{\bar{X}_1 \sin\Lambda_3 \sinh\Lambda_1 + \bar{X}_2 \cos\Lambda_3 \cosh\Lambda_1}{\cos^2\Lambda_3 \cosh^2\Lambda_1 + \sin^2\Lambda_3 \sinh^2\Lambda_1} \\
K_3^3 &= \frac{\bar{X}_3 \cos\Lambda_4 \cosh\Lambda_2 - \bar{X}_4 \sin\Lambda_4 \sinh\Lambda_2}{\cos^2\Lambda_4 \cosh^2\Lambda_2 + \sin^2\Lambda_4 \sinh^2\Lambda_2} \\
K_4^3 &= \frac{\bar{X}_3 \sin\Lambda_4 \sinh\Lambda_2 + \bar{X}_4 \cos\Lambda_4 \cosh\Lambda_2}{\cos^2\Lambda_4 \cosh^2\Lambda_2 + \sin^2\Lambda_4 \sinh^2\Lambda_2}
\end{aligned}
\right\} \qquad \text{(F. 4)}
$$

where

$$
\left.
\begin{aligned}
\bar{X}_1 &= \tfrac{1}{2} H_3 + \frac{[(4n^2-\mu_3^2)J - (4n^2+\mu_3^2)I]H_3 + [(4n^2-\mu_3^2)I + (4n^2+\mu_3^2)J]\bar{H}_3}{2\mu_3(I^2+J^2)} \\
\bar{X}_2 &= \tfrac{1}{2} \bar{H}_3 + \frac{-[(4n^2-\mu_3^2)I + (4n^2+\mu_3^2)J]H_3 + [(4n^2-\mu_3^2)J - (4n^2+\mu_3^2)I]\bar{H}_3}{2\mu_3(I^2+J^2)} \\
\bar{X}_3 &= \tfrac{1}{2} H_3 - \frac{[(4n^2-\mu_3^2)J - (4n^2+\mu_3^2)I]H_3 + [(4n^2-\mu_3^2)I + (4n^2+\mu_3^2)J]\bar{H}_3}{2\mu_3(I^2+J^2)} \\
\bar{X}_4 &= \tfrac{1}{2} \bar{H}_3 + \frac{-[(4n^2-\mu_3^2)I + (4n^2+\mu_3^2)J]H_3 + [(4n^2-\mu_3^2)J + (4n^2+\mu_3^2)I]\bar{H}_3}{2\mu_3(I^2+J^2)} \\
H_3 &= q_3(s=0,1) = -C_3(a^2-b^2), \quad \bar{H}_3 = \frac{1}{2\mu_3^2 r^2}\bar{q}_3(s=0,1) = \frac{-1}{2\mu_3^2 r^2}\bar{C}_3(a^2-b^2)
\end{aligned}
\right\}
$$

(F. 5)

The governing equations for $g_6(s)$ and $\bar{g}_6(s)$ [eq. (4.60)] are identical to those of $g_3(s)$ and $\bar{g}_3(s)$ with the similar boundary conditions [eq. (4.60a)]. Therefore, the solutions for $g_6(s)$ and $\bar{g}_6(s)$ will be the same as $g_3(s)$ and $\bar{g}_3(s)$ respectively with H_6 and $\bar{H}_6$ replacing H_3 and $\bar{H}_3$ respectively, where

$$H_6 = g_6(s=0,1) = -C_8 ab \,, \quad \bar{H}_6 = \frac{1}{2\mu_3^2 r^2}\bar{g}_6(s=0,1) = \frac{-\bar{C}_8}{2\mu_3^2 r^2} ab \qquad \text{(F.6)}$$

APPENDIX G

SOLUTIONS FOR $g_4(s)$, $\bar{g}_4(s)$ AND $g_5(s)$, $\bar{g}_5(s)$ OF THE COMPLEMENTARY EQUATIONS

The governing equations for $g_4(s)$ and $\bar{g}_4(s)$ are given by eq. (4.58) and its boundary conditions are given by eq. (4.58a). The solutions of eq. (4.58) can be written as

$$\left.\begin{aligned} g_4(s) &= K_1^4 \cos\bar{\Lambda}_3(2s-1)\cosh\bar{\Lambda}_1(2s-1) + K_2^4 \sin\bar{\Lambda}_3(2s-1)\sinh\bar{\Lambda}_1(2s-1) \\ &\quad + K_3^4 \cos\bar{\Lambda}_4(2s-1)\cosh\bar{\Lambda}_2(2s-1) + K_4^4 \sin\bar{\Lambda}_4(2s-1)\sinh\bar{\Lambda}_2(2s-1) \\ \bar{g}_4(s) &= \bar{K}_1^4 \cos\bar{\Lambda}_3(2s-1)\cosh\bar{\Lambda}_1(2s-1) + \bar{K}_2^4 \sin\bar{\Lambda}_3(2s-1)\sinh\bar{\Lambda}_1(2s-1) \\ &\quad + \bar{K}_3^4 \cos\bar{\Lambda}_4(2s-1)\cosh\bar{\Lambda}_2(2s-1) + \bar{K}_4^4 \sin\bar{\Lambda}_4(2s-1)\sinh\bar{\Lambda}_2(2s-1) \end{aligned}\right\} \quad \text{(G. 1)}$$

where

$$\left.\begin{aligned} \bar{\Lambda}_1 &= \frac{k}{2\sqrt{2}}\sqrt{\sqrt{(4n^2+P_1)^2+(P_2-P_3)^2}+(4n^2+P_1)} \\ \bar{\Lambda}_2 &= \frac{k}{2\sqrt{2}}\sqrt{\sqrt{(4n^2-P_1)^2+(P_2+P_3)^2}+(4n^2-P_1)} \\ \bar{\Lambda}_3 &= \frac{k}{2\sqrt{2}}\sqrt{\sqrt{(4n^2+P_1)^2+(P_2-P_3)^2}-(4n^2+P_1)} \\ \bar{\Lambda}_4 &= \frac{k}{2\sqrt{2}}\sqrt{\sqrt{(4n^2-P_1)^2+(P_2+P_3)^2}-(4n^2-P_1)} \end{aligned}\right\} \quad \text{(G. 2)}$$

$$
\left.
\begin{aligned}
P_1^2 &= \sqrt{C^2+\frac{e}{3}}\cos\frac{\bar\theta}{3} - C \\
P_2^2 &= \tfrac{1}{2}\sqrt{C^2+\frac{e}{3}}\left(\cos\frac{\bar\theta}{3}+\sqrt{3}\sin\frac{\bar\theta}{3}\right)+C \\
P_3^2 &= \tfrac{1}{2}\sqrt{C^2+\frac{e}{3}}\left(\cos\frac{\bar\theta}{3}-\sqrt{3}\sin\frac{\bar\theta}{3}\right)+C \\
C &= \frac{1}{6}\left(\frac{1-\nu^2}{r^2}-\frac{4\lambda_0}{r^2}\right), \quad e = 16\pi^4\frac{H^2}{r^2}, \quad d = 2\pi^2\frac{H^2}{r^2} \\
\sin\bar\theta &= \frac{\bar r}{\sqrt{\frac{\beta^2}{4}+\bar r^2}}, \qquad \cos\bar\theta = \frac{-\frac{\beta}{2}}{\sqrt{\frac{\beta^2}{4}+\bar r^2}} \\
\alpha &= -\tfrac{3}{4}\left(C^2+\frac{e}{3}\right), \quad \beta = \tfrac{1}{4}\left(ce-C^3-d^2\right), \\
\bar r &= -\left(\frac{\beta^2}{4}+\frac{\alpha^3}{27}\right)
\end{aligned}
\right\} \qquad \text{(G. 3)}
$$

The constants in the solutions (G. 1) may be determined by using the boundary conditions [eq. (4. 58a)] which will be written as follows.

$$
\left.
\begin{aligned}
K_1^4 &= \frac{\gamma_1\cos\bar\Lambda_3\cosh\bar\Lambda_1 - \gamma_2\sin\bar\Lambda_3\sinh\bar\Lambda_1}{\cos^2\bar\Lambda_3\cosh^2\bar\Lambda_1+\sin^2\bar\Lambda_3\sinh^2\bar\Lambda_1} \\
K_2^4 &= \frac{\gamma_1\sin\bar\Lambda_3\sinh\bar\Lambda_1 + \gamma_2\cos\bar\Lambda_3\cosh\bar\Lambda_1}{\cos^2\bar\Lambda_3\cosh^2\bar\Lambda_1+\sin^2\bar\Lambda_3\sinh^2\bar\Lambda_1} \\
K_3^4 &= \frac{\gamma_3\cos\bar\Lambda_4\cosh\bar\Lambda_2 - \gamma_4\sin\bar\Lambda_4\sinh\bar\Lambda_2}{\cos^2\bar\Lambda_4\cosh^2\bar\Lambda_2+\sin^2\bar\Lambda_4\sinh^2\bar\Lambda_2} \\
K_4^4 &= \frac{\gamma_3\sin\bar\Lambda_4\sinh\bar\Lambda_2 + \gamma_4\cos\bar\Lambda_4\cosh\bar\Lambda_2}{\cos^2\bar\Lambda_4\cosh^2\bar\Lambda_2+\sin^2\bar\Lambda_4\sinh^2\bar\Lambda_2}
\end{aligned}
\right\} \qquad \text{(G. 4)}
$$

$$\left.\begin{aligned}
\bar{K}_1^4 &= \frac{\bar{\gamma}_1 \cos\bar{\Lambda}_3 \cosh\bar{\Lambda}_1 - \bar{\gamma}_2 \sin\bar{\Lambda}_3 \sinh\bar{\Lambda}_1}{\cos^2\bar{\Lambda}_3 \cosh^2\bar{\Lambda}_1 + \sin^2\bar{\Lambda}_3 \sinh^2\bar{\Lambda}_1} \\
\bar{K}_2^4 &= \frac{\bar{\gamma}_1 \sin\bar{\Lambda}_3 \sinh\bar{\Lambda}_1 + \bar{\gamma}_2 \cos\bar{\Lambda}_3 \cosh\bar{\Lambda}_1}{\cos^2\bar{\Lambda}_3 \cosh^2\bar{\Lambda}_1 + \sin^2\bar{\Lambda}_3 \sinh^2\bar{\Lambda}_1} \\
\bar{K}_3^4 &= \frac{\bar{\gamma}_3 \cos\bar{\Lambda}_4 \cosh\bar{\Lambda}_2 - \bar{\gamma}_4 \sin\bar{\Lambda}_4 \sinh\bar{\Lambda}_2}{\cos^2\bar{\Lambda}_4 \cosh^2\bar{\Lambda}_2 + \sin^2\bar{\Lambda}_4 \sinh^2\bar{\Lambda}_2} \\
\bar{K}_4^4 &= \frac{\bar{\gamma}_3 \sin\bar{\Lambda}_4 \sinh\bar{\Lambda}_2 + \bar{\gamma}_4 \cos\bar{\Lambda}_4 \cosh\bar{\Lambda}_2}{\cos^2\bar{\Lambda}_4 \cosh^2\bar{\Lambda}_2 + \sin^2\bar{\Lambda}_4 \sinh^2\bar{\Lambda}_2}
\end{aligned}\right\} \quad \text{(G. 5)}$$

where

$$\left.\begin{aligned}
\bar{\gamma}_1 &= \frac{H_4}{2} + \frac{\frac{16\kappa^4}{r^2}P_1\bar{H}_4 - \left[8\kappa^2 P_1(P_2^2+P_3^2) - (\frac{4\lambda_0}{r^2}+3C)P_2P_3 + 2\kappa^2\frac{4\lambda_0}{r^2}P_1\right]H_4}{4(P_1^2+P_2^2)(P_1^2+P_3^2)} \\
\bar{\gamma}_2 &= \frac{\left[8\kappa^2 P_2(P_1^2-P_3^2) - (\frac{4\lambda_0}{r^2}+3C)P_1P_3 - 2\kappa^2\frac{4\lambda_0}{r^2}P_2\right]H_4 + \frac{16\kappa^4}{r^2}P_2\bar{H}_4}{4(P_1^2+P_2^2)(P_3^2-P_2^2)} \\
&\quad + \frac{\left[8\kappa^2 P_3(P_1^2-P_2^2) - (\frac{4\lambda_0}{r^2}+3C)P_1P_2 - 2\kappa^2\frac{4\lambda_0}{r^2}P_3\right]H_4 + \frac{16\kappa^4}{r^2}P_3\bar{H}_4}{4(P_1^2+P_3^2)(P_3^2-P_2^2)} \\
\bar{\gamma}_3 &= \frac{H_4}{2} - \frac{\frac{16\kappa^4}{r^2}P_1\bar{H}_4 - \left[8\kappa^2 P_1(P_2^2+P_3^2) - (\frac{4\lambda_0}{r^2}+3C)P_2P_3 + 2\kappa^2\frac{4\lambda_0}{r^2}P_1\right]H_4}{4(P_1^2+P_2^2)(P_1^2+P_3^2)} \\
\bar{\gamma}_4 &= \frac{\left[8\kappa^2 P_2(P_1^2-P_3^2) - (\frac{4\lambda_0}{r^2}+3C)P_1P_3 - 2\kappa^2\frac{4\lambda_0}{r^2}P_2\right]H_4 + \frac{16\kappa^4}{r^2}P_2\bar{H}_4}{4(P_1^2+P_2^2)(P_3^2-P_2^2)} \\
&\quad - \frac{\left[8\kappa^2 P_3(P_1^2-P_2^2) - (\frac{4\lambda_0}{r^2}+3C)P_1P_2 - 2\kappa^2\frac{4\lambda_0}{r^2}P_3\right]H_4 + \frac{16\kappa^4}{r^2}P_3\bar{H}_4}{4(P_1^2+P_3^2)(P_3^2-P_2^2)}
\end{aligned}\right\} \quad \text{(G. 6)}$$

$$
\left.
\begin{aligned}
\bar{\gamma}_1 &= \frac{\bar{H}_4}{2} + \frac{[3C P_2 P_3 - 6\pi^2 \frac{4\lambda_0}{\rho c^2} P_1 - 8\pi^2 P_1 (P_2^2 + P_3^2)]\bar{H}_4 + (1-\nu^2)(\frac{4\lambda_0}{\rho c^2} - 16\pi^4) P_1 H_4}{4(P_1^2 + P_2^2)(P_1^2 + P_3^2)} \\
\bar{\gamma}_2 &= \frac{[8\pi^2 P_2 (P_1^2 - P_3^2) - 6\pi^2 \frac{4\lambda_0}{\rho c^2} P_2 - 3C P_1 P_3]\bar{H}_4 + (1-\nu^2)(\frac{4\lambda_0}{\rho c^2} - 16\pi^4) P_2 H_4}{4(P_3^2 - P_2^2)(P_1^2 + P_2^2)} \\
&\quad + \frac{[8\pi^2 P_3 (P_1^2 - P_2^2) - 6\pi^2 \frac{4\lambda_0}{\rho c^2} P_3 - 3C P_1 P_2]\bar{H}_4 + (1-\nu^2)(\frac{4\lambda_0}{\rho c^2} - 16\pi^4) P_3 H_4}{4(P_3^2 - P_2^2)(P_1^2 + P_3^2)} \\
\bar{\gamma}_3 &= \frac{\bar{H}_4}{2} - \frac{[3C P_2 P_3 - 6\pi^2 \frac{4\lambda_0}{\rho c^2} P_1 - 8\pi^2 P_1 (P_2^2 + P_3^2)]\bar{H}_4 + (1-\nu^2)(\frac{4\lambda_0}{\rho c^2} - 16\pi^4) P_1 H_4}{4(P_1^2 + P_2^2)(P_1^2 + P_3^2)} \\
\bar{\gamma}_4 &= \frac{[8\pi^2 P_2 (P_1^2 - P_3^2) - 6\pi^2 \frac{4\lambda_0}{\rho c^2} P_2 - 3C P_1 P_3]\bar{H}_4 + (1-\nu^2)(\frac{4\lambda_0}{\rho c^2} - 16\pi^4) P_2 H_4}{4(P_3^2 - P_2^2)(P_1^2 + P_2^2)} \\
&\quad - \frac{[8\pi^2 P_3 (P_1^2 - P_2^2) - 6\pi^2 \frac{4\lambda_0}{\rho c^2} P_3 - 3C P_1 P_2]\bar{H}_4 + (1-\nu^2)(\frac{4\lambda_0}{\rho c^2} - 16\pi^4) P_3 H_4}{4(P_3^2 - P_2^2)(P_1^2 + P_3^2)}
\end{aligned}
\right\} \quad \text{(G. 7)}
$$

where

$$
H_4 = g_4(s=0,1) = -C_4 \quad , \quad \bar{H}_4 = \bar{g}_4(s=0,1) = -\overline{C_4} \qquad \text{(G. 8)}
$$

The governing equations and the boundary conditions for $g_5(s)$ and $\bar{g}_5(s)$ are similar to those for $g_4(s)$ and $\bar{g}_4(s)$. The solutions for $g_5(s)$ and $\bar{g}_5(s)$ are the same as eq. (G. 1) with H_4 replaced by H_5 and $\bar{H}_4$ replaced by $\bar{H}_5$, where

$$H_5 = g_5(s=0, 1) = -C_7 ab, \quad \bar{H}_5 = \bar{g}_5(s=0, 1) = -\bar{C}_7 ab \tag{G. 9}$$

APPENDIX H

FOURIER SERIES EXPANSION OF THE COMPLEMTARY SOLUTION

$$g_1(s) = \xi_1^0 - \sum_{j=1}^{\infty} \xi_1^j \cos 2j\pi s \tag{H. 1}$$

$$\xi_1^0 = \frac{1}{4} \frac{\left[(H_1 - \bar{H}_1)\sinh 2\mu_1 + (H_1 + \bar{H}_1)\sin 2\mu_1\right]}{\mu_1(\cosh^2\mu_1 - \sin^2\mu_1)} \tag{H. 2}$$

$$\xi_1^j = \frac{1}{2}\left\{ \frac{H_1 \sinh 2\mu_1 + \bar{H}_1 \sin 2\mu_1}{\cosh^2\mu_1 - \sin^2\mu_1}\left[\frac{\mu_1}{(j\pi+\mu_1)^2+\mu_1^2} + \frac{\mu_1}{(j\pi-\mu_1)^2+\mu_1^2}\right] \right.$$

$$\left. + \frac{H_1 \sin 2\mu_1 - \bar{H}_1 \sinh 2\mu_1}{\cosh^2\mu_1 - \sin^2\mu_1}\left[\frac{j\pi+\mu_1}{(j\pi+\mu_1)^2+\mu_1^2} - \frac{j\pi-\mu_1}{(j\pi-\mu_1)^2+\mu_1^2}\right]\right\} \tag{H. 3}$$

$$\bar{g}_1''(s) = -k^2(1-\nu^2)\left[\xi_1^0 + \sum_{j=1}^{\infty} \xi_1^j \cos 2j\pi s\right] \tag{H.4}$$

$$g_2(s) = \xi_2^0 + \sum_{j=1}^{\infty} \xi_2^j \cos 2j\pi s \tag{H. 5}$$

$$\xi_2^0 = \frac{1}{4} \frac{\left[(H_2 - \bar{H}_2)\sinh 2\mu_2 + (H_2 + \bar{H}_2)\sin 2\mu_2\right]}{\mu_2(\cosh^2\mu_2 - \sin^2\mu_2)} \tag{H. 6}$$

$$\xi_2^j = \frac{1}{2}\left\{ \frac{H_2 \sinh 2\mu_2 + \bar{H}_2 \sin 2\mu_2}{\cosh^2\mu_2 - \sin^2\mu_2}\left[\frac{\mu_2}{(j\pi+\mu_2)^2+\mu_2^2} + \frac{\mu_2}{(j\pi-\mu_2)^2+\mu_2^2}\right] \right.$$

$$\left. + \frac{H_2 \sin 2\mu_2 - \bar{H}_2 \sinh 2\mu_2}{\cosh^2\mu_2 - \sin^2\mu_2}\left[\frac{j\pi+\mu_2}{(j\pi+\mu_2)^2+\mu_2^2} - \frac{j\pi-\mu_2}{(j\pi-\mu_2)^2+\mu_2^2}\right]\right\} \tag{H. 7}$$

$$\bar{g}_2''(s) = -k^2(1-\nu^2)\left[\xi_2^0 + \sum_{j=1}^{\infty} \xi_2^j \cos 2j\pi s\right] \tag{H. 8}$$

$$g_3(s) = \xi_3^0 + \sum_{j=1}^{\infty} \xi_3^j \cos 2j\pi s \tag{H. 9}$$

$$\xi_3^0 = \frac{1}{2}\left\{ \frac{\Lambda_1(\bar{X}_1 \sinh 2\Lambda_1 + \bar{X}_2 \sin 2\Lambda_3) + \Lambda_3(\bar{X}_1 \sin 2\Lambda_3 - \bar{X}_2 \sinh 2\Lambda_1)}{(\Lambda_1^2 + \Lambda_3^2)(\cosh^2\Lambda_1 - \sin^2\Lambda_3)} \right.$$

$$\left. + \frac{\Lambda_2(\bar{X}_3 \sinh 2\Lambda_2 + \bar{X}_4 \sin 2\Lambda_4) + \Lambda_4(\bar{X}_3 \sin 2\Lambda_4 - \bar{X}_4 \sinh 2\Lambda_2)}{(\Lambda_2^2 + \Lambda_4^2)(\cosh^2\Lambda_2 - \sin^2\Lambda_4)} \right\} \tag{H. 10}$$

$$\xi_3^j = \frac{1}{2}\left\{ \frac{\bar{X}_1 \sinh 2\Lambda_1 + \bar{X}_2 \sin 2\Lambda_3}{\cosh^2\Lambda_1 - \sin^2\Lambda_3} \left[\frac{\Lambda_1}{(j\pi + \Lambda_3)^2 + \Lambda_1^2} + \frac{\Lambda_1}{(j\pi - \Lambda_3)^2 + \Lambda_1^2} \right] \right.$$

$$+ \frac{\bar{X}_1 \sin 2\Lambda_3 - \bar{X}_2 \sinh 2\Lambda_1}{\cosh^2\Lambda_1 - \sin^2\Lambda_3} \left[\frac{j\pi + \Lambda_3}{(j\pi + \Lambda_3)^2 + \Lambda_1^2} - \frac{j\pi - \Lambda_3}{(j\pi - \Lambda_3)^2 + \Lambda_1^2} \right]$$

$$+ \frac{\bar{X}_3 \sinh 2\Lambda_2 + \bar{X}_4 \sin 2\Lambda_4}{\cosh^2\Lambda_2 - \sin^2\Lambda_4} \left[\frac{\Lambda_2}{(j\pi + \Lambda_4)^2 + \Lambda_2^2} + \frac{\Lambda_2}{(j\pi - \Lambda_4)^2 + \Lambda_2^2} \right]$$

$$\left. + \frac{\bar{X}_3 \sin 2\Lambda_2 - \bar{X}_4 \sinh 2\Lambda_2}{\cosh^2\Lambda_2 - \sin^2\Lambda_4} \left[\frac{j\pi + \Lambda_4}{(j\pi + \Lambda_4)^2 + \Lambda_2^2} - \frac{j\pi - \Lambda_4}{(j\pi - \Lambda_4)^2 + \Lambda_2^2} \right] \right\} \tag{H. 11}$$

$$g_6(s) = \xi_6^0 + \sum_{j=1}^{\infty} \xi_6^j \cos 2j\pi s \tag{H. 12}$$

$$\bar{q}_3(s) = \bar{\xi}_3^0 + \sum_{j=1}^{\infty} \bar{\xi}_3^j \cos 2j\pi s \tag{H. 13}$$

$$\bar{\xi}_3^0 = \frac{1}{2}\left\{\frac{\Lambda_1(\bar{X}_1 \sinh 2\Lambda_1 + \bar{X}_2 \sin 2\Lambda_3) + \Lambda_3(\bar{X}_1 \sin 2\Lambda_3 - \bar{X}_2 \sinh 2\Lambda_1)}{(\Lambda_1^2 + \Lambda_3^2)(\cosh^2\Lambda_1 - \sin^2\Lambda_3)}\right.$$

$$\left. + \frac{\Lambda_2(\bar{X}_3 \sinh 2\Lambda_2 + \bar{X}_4 \sin 2\Lambda_4) + \Lambda_4(\bar{X}_3 \sin 2\Lambda_4 - \bar{X}_4 \sinh 2\Lambda_2)}{(\Lambda_2^2 + \Lambda_4^2)(\cosh^2\Lambda_2 - \sin^2\Lambda_4)}\right\}$$

(H. 14)

$$\bar{\xi}_3^j = \frac{1}{2}\left\{\frac{\bar{X}_1 \sinh 2\Lambda_1 + \bar{X}_2 \sin 2\Lambda_3}{\cosh^2\Lambda_1 - \sin^2\Lambda_3}\left[\frac{\Lambda_1}{(j\pi + \Lambda_3)^2 + \Lambda_1^2} + \frac{\Lambda_1}{(j\pi - \Lambda_3)^2 + \Lambda_1^2}\right]\right.$$

$$+ \frac{\bar{X}_1 \sin 2\Lambda_3 - \bar{X}_2 \sinh 2\Lambda_1}{\cosh^2\Lambda_1 - \sin^2\Lambda_3}\left[\frac{j\pi + \Lambda_3}{(j\pi + \Lambda_3)^2 + \Lambda_1^2} - \frac{j\pi - \Lambda_3}{(j\pi - \Lambda_3)^2 + \Lambda_1^2}\right]$$

$$+ \frac{\bar{X}_3 \sinh 2\Lambda_2 + \bar{X}_4 \sin 2\Lambda_4}{\cosh^2\Lambda_2 - \sin^2\Lambda_4}\left[\frac{\Lambda_2}{(j\pi + \Lambda_4)^2 + \Lambda_2^2} + \frac{\Lambda_2}{(j\pi - \Lambda_4)^2 + \Lambda_2^2}\right]$$

$$\left. + \frac{\bar{X}_3 \sin 2\Lambda_4 - \bar{X}_4 \sinh 2\Lambda_2}{\cosh^2\Lambda_2 - \sin^2\Lambda_4}\left[\frac{j\pi + \Lambda_4}{(j\pi + \Lambda_4)^2 + \Lambda_2^2} + \frac{j\pi - \Lambda_4}{(j\pi - \Lambda_4)^2 + \Lambda_2^2}\right]\right\}$$

(H. 15)

$$\bar{q}_6(s) = \bar{\xi}_6^0 + \sum_{j=1}^{\infty} \bar{\xi}_6^j \cos 2j\pi s \tag{H. 16}$$

$$\bar{X}_1 = 2\mu_3^2 r^2 X_2\,, \quad \bar{X}_2 = -2\mu_3^2 X_1 r^2\,, \quad \bar{X}_3 = 2\mu_3^2 r^2 X_4\,, \quad \bar{X}_4 = -2\mu_3^2 r^2 X_3 \tag{H. 17}$$

$$g_4(s) = \xi_4^0 + \sum_{j=1}^{\infty} \xi_4^j \cos 2j\pi s \tag{H. 18}$$

$$\xi_4^0 = \frac{1}{2}\left\{ \frac{\bar{\Lambda}_1(\gamma_1 \sinh 2\bar{\Lambda}_1 + \gamma_2 \sin 2\bar{\Lambda}_3) + \bar{\Lambda}_3(\gamma_1 \sin 2\bar{\Lambda}_3 - \gamma_2 \sinh 2\bar{\Lambda}_1)}{(\bar{\Lambda}_1^2 + \bar{\Lambda}_3^2)(\cosh^2\bar{\Lambda}_1 - \sin^2\bar{\Lambda}_3)} \right.$$

$$\left. + \frac{\bar{\Lambda}_2(\gamma_3 \sinh 2\bar{\Lambda}_2 + \gamma_4 \sin 2\bar{\Lambda}_4) + \bar{\Lambda}_4(\gamma_3 \sin 2\bar{\Lambda}_4 - \gamma_4 \sinh 2\bar{\Lambda}_2)}{(\bar{\Lambda}_2^2 + \bar{\Lambda}_4^2)(\cosh^2\Lambda_2 - \sin^2\Lambda_4)} \right\} \tag{H. 19}$$

$$\xi_4^j = \frac{1}{2}\left\{ \frac{\gamma_1 \sinh 2\bar{\Lambda}_1 + \gamma_2 \sin 2\Lambda_3}{\cosh^2\bar{\Lambda}_1 - \sin^2\bar{\Lambda}_3}\left[\frac{\bar{\Lambda}_1}{(j\pi + \bar{\Lambda}_3)^2 + \bar{\Lambda}_1^2} + \frac{\bar{\Lambda}_1}{(j\pi - \bar{\Lambda}_3)^2 + \bar{\Lambda}_1^2} \right] \right.$$

$$+ \frac{\gamma_1 \sin 2\bar{\Lambda}_3 - \gamma_2 \sinh 2\bar{\Lambda}_1}{\cosh^2\bar{\Lambda}_1 - \sin^2\bar{\Lambda}_3}\left[\frac{j\pi + \bar{\Lambda}_3}{(j\pi + \bar{\Lambda}_3)^2 + \bar{\Lambda}_1^2} - \frac{j\pi - \bar{\Lambda}_3}{(j\pi - \bar{\Lambda}_3)^2 + \bar{\Lambda}_1^2} \right]$$

$$+ \frac{\gamma_3 \sinh 2\bar{\Lambda}_2 + \gamma_4 \sin 2\bar{\Lambda}_4}{\cosh^2\bar{\Lambda}_2 - \sin^2\bar{\Lambda}_4}\left[\frac{\bar{\Lambda}_2}{(j\pi + \bar{\Lambda}_4)^2 + \bar{\Lambda}_2^2} + \frac{\bar{\Lambda}_2}{(j\pi - \bar{\Lambda}_4)^2 + \bar{\Lambda}_2^2} \right]$$

$$\left. + \frac{\gamma_3 \sin 2\bar{\Lambda}_4 - \gamma_4 \sinh 2\bar{\Lambda}_2}{\cosh^2\bar{\Lambda}_2 - \sin^2\bar{\Lambda}_4}\left[\frac{j\pi + \bar{\Lambda}_4}{(j\pi + \bar{\Lambda}_4)^2 + \bar{\Lambda}_2^2} - \frac{j\pi - \bar{\Lambda}_4}{(j\pi - \bar{\Lambda}_4)^2 + \bar{\Lambda}_2^2} \right] \right\} \tag{H. 20}$$

$$g_5(s) = \xi_5^0 + \sum_{j=1}^{\infty} \xi_5^j \cos 2j\pi s \tag{H. 21}$$

$$\bar{q}_4(s) = \bar{\xi}_4^0 + \sum_{j=1}^{\infty} \bar{\xi}_4^j \cos 2j\pi s \tag{H. 22}$$

$$\bar{\xi}_4^0 = \frac{1}{2}\left\{ \frac{\bar{\Lambda}_1(\bar{\gamma}_1 \sinh 2\bar{\Lambda}_1 + \bar{\gamma}_2 \sin 2\bar{\Lambda}_3) + \bar{\Lambda}_3(\bar{\gamma}_1 \sin 2\bar{\Lambda}_3 - \bar{\gamma}_2 \sinh 2\bar{\Lambda}_1)}{(\bar{\Lambda}_1^2 + \bar{\Lambda}_3^2)(\cosh^2\bar{\Lambda}_1 - \sin^2\bar{\Lambda}_3)} \right.$$

$$\left. + \frac{\bar{\Lambda}_2(\bar{\gamma}_3 \sinh 2\bar{\Lambda}_2 + \bar{\gamma}_4 \sin 2\bar{\Lambda}_4) + \bar{\Lambda}_4(\bar{\gamma}_3 \sin 2\bar{\Lambda}_4 - \bar{\gamma}_4 \sinh 2\bar{\Lambda}_2)}{(\bar{\Lambda}_2^2 + \bar{\Lambda}_4^2)(\cosh^2\bar{\Lambda}_2 - \sin^2\bar{\Lambda}_4)} \right\} \tag{H. 23}$$

$$\bar{\xi}_4^j = \frac{1}{2}\left\{ \frac{\bar{\gamma}_1 \sinh 2\bar{\Lambda}_1 + \bar{\gamma}_2 \sin 2\bar{\Lambda}_3}{\cosh^2\bar{\Lambda}_1 - \sin^2\bar{\Lambda}_3} \left[\frac{\bar{\Lambda}_1}{(j\pi + \bar{\Lambda}_3)^2 + \bar{\Lambda}_1^2} + \frac{\bar{\Lambda}_1}{(j\pi - \bar{\Lambda}_3)^2 + \bar{\Lambda}_1^2} \right] \right.$$

$$+ \frac{\bar{\gamma}_1 \sin 2\bar{\Lambda}_3 - \bar{\gamma}_2 \sinh 2\bar{\Lambda}_1}{\cosh^2\bar{\Lambda}_1 - \sin^2\bar{\Lambda}_3} \left[\frac{j\pi + \bar{\Lambda}_3}{(j\pi + \bar{\Lambda}_3)^2 + \bar{\Lambda}_1^2} - \frac{j\pi - \bar{\Lambda}_3}{(j\pi - \bar{\Lambda}_3)^2 + \bar{\Lambda}_1^2} \right]$$

$$+ \frac{\bar{\gamma}_3 \sinh 2\bar{\Lambda}_2 + \bar{\gamma}_4 \sin 2\bar{\Lambda}_4}{\cosh^2\bar{\Lambda}_2 - \sin^2\bar{\Lambda}_4} \left[\frac{\bar{\Lambda}_2}{(j\pi + \bar{\Lambda}_4)^2 + \bar{\Lambda}_2^2} + \frac{\bar{\Lambda}_2}{(j\pi - \bar{\Lambda}_4)^2 + \bar{\Lambda}_2^2} \right]$$

$$\left. + \frac{\bar{\gamma}_3 \sin 2\bar{\Lambda}_4 - \bar{\gamma}_4 \sinh 2\bar{\Lambda}_2}{\cosh^2\bar{\Lambda}_2 - \sin^2\bar{\Lambda}_4} \left[\frac{j\pi + \bar{\Lambda}_4}{(j\pi + \bar{\Lambda}_4)^2 + \bar{\Lambda}_2^2} - \frac{j\pi - \Lambda_4}{(j\pi - \bar{\Lambda}_4)^2 + \bar{\Lambda}_2^2} \right] \right\} \tag{H. 24}$$

$$\bar{q}_5(s) = \bar{\xi}_5^0 + \sum_{j=1}^{\infty} \bar{\xi}_5^j \cos 2j\pi s \tag{H. 25}$$

APPENDIX I

THE EXPRESSIONS FOR G_1, G_2, G_3, G_4 AND $\bar{G}_1$, $\bar{G}_2$, $\bar{G}_3$, $\bar{G}_4$ IN THE SECOND ORDER EQUATIONS

$$G_1 = \frac{1}{k^2}\Big\{\Big\{ n^2k^2(1-\nu^2)\Big[(\xi_1^\circ - \tfrac{1}{2}\xi_1^m) + \tfrac{1}{2}(\xi_2^\circ - \tfrac{1}{2}\xi_2^m)\Big] + 2(mn\pi)^2\big(\Gamma\xi_3^\circ + \bar{\xi}_3^\circ + \tfrac{1}{2}\Gamma\xi_4^\circ + \tfrac{1}{2}\bar{\xi}_4^\circ\big)\Big\} a^3$$
$$+\Big\{ n^2k^2(1-\nu^2)\Big[(\xi_1^\circ - \tfrac{1}{2}\xi_1^m) - \tfrac{1}{2}(\xi_2^\circ - \tfrac{1}{2}\xi_2^m)\cos 2(\delta_b-\delta_a)\Big] - (mn\pi)^2\big(\Gamma\xi_6^\circ + \bar{\xi}_6^\circ\big)\cos 2(\delta_b-\delta_a) + 2(mn\pi)^2\Big[-\big(\Gamma\xi_3^\circ + \bar{\xi}_3^\circ\big)$$
$$+\tfrac{1}{2}\big(\Gamma\xi_4^\circ + \bar{\xi}_4^\circ\big)\cos 2(\delta_b-\delta_a) + \tfrac{1}{2}\big(\Gamma\xi_6^\circ + \bar{\xi}_6^\circ + \Gamma\xi_5^\circ + \bar{\xi}_5^\circ\big)\Big]ab^2\Big\}\cos(\tau+\delta_a)$$
$$+\frac{1}{k^2}\Big\{\Big[\tfrac{1}{2}n^2k^2(1-\nu^2)(\xi_2^\circ - \tfrac{1}{2}\xi_2^m) - (mn\pi)\big(\Gamma\xi_4^\circ + \bar{\xi}_4^\circ - \Gamma\xi_6^\circ - \bar{\xi}_6^\circ\big)\Big] x \; x\, ab^2\sin 2(\delta_b-\delta_a)\Big\}\sin(\tau+\delta_a) \qquad (I.1)$$

$$\bar{G}_1 = \frac{2(mn\pi)^2}{k^2}\Big\{\Big\{-\xi_1^m - \tfrac{1}{2}\xi_2^m - \xi_3^\circ - \tfrac{1}{2}\xi_4^\circ\Big\}a^3 + \Big\{-\xi_1^m + \tfrac{1}{2}\xi_2^m\cos 2(\delta_b-\delta_a) + \xi_3^\circ - \tfrac{1}{2}\xi_4^\circ\cos 2(\delta_b-\delta_a) - \tfrac{1}{2}\xi_5^\circ - \tfrac{1}{2}\xi_6^\circ + \tfrac{1}{2}\xi_6^\circ\cos 2(\delta_b-\delta_a)\Big\}ab^2\Big\}\cos(\tau+\delta_a)$$
$$+\frac{(mn\pi)^2}{k^2}\Big\{-\xi_2^m + \xi_4^\circ - \xi_6^\circ\Big\}ab^2\sin 2(\delta_b-\delta_a)\sin(\tau+\delta_a) \qquad (I.2)$$

$$G_2 = \frac{1}{R^2}\Bigg\{\Big\{ n^2k^2(1-\nu^2)\Big[(\xi_1^\circ - \tfrac{1}{2}\xi_1^m) + \tfrac{1}{2}(\xi_2^\circ - \tfrac{1}{2}\xi_2^m)\Big]$$

$$+ 2(mn\pi)^2\big(\Gamma\xi_3^\circ + \bar{\xi}_3^\circ + \tfrac{1}{2}\Gamma\xi_4^\circ + \tfrac{1}{2}\bar{\xi}_4^\circ\big)\Big\} b^3$$

$$+\Big\{ n^2k^2(1-\nu^2)\Big[(\xi_1^\circ - \tfrac{1}{2}\xi_1^m) - \tfrac{1}{2}(\xi_2^\circ - \tfrac{1}{2}\xi_2^m)\cos 2(\delta_b - \delta_a)\Big]$$

$$+ 2(mn\pi)^2\Big[-(\Gamma\xi_3^\circ + \bar{\xi}_3^\circ) + \tfrac{1}{2}(\Gamma\xi_4^\circ + \bar{\xi}_4^\circ)\cos 2(\delta_b - \delta_a)$$

$$+ \tfrac{1}{2}(\Gamma\xi_5^\circ + \bar{\xi}_5^\circ + \Gamma\xi_6^\circ + \bar{\xi}_6^\circ) - \tfrac{1}{2}(\Gamma\xi_6^\circ + \bar{\xi}_6^\circ)\cos 2(\delta_b - \delta_a)\Big]\Big\} a^2 b\Big\}\sin(\tau + \delta_b)$$

$$+ \frac{1}{R^2}\Big\{\tfrac{1}{2}n^2k^2(1-\nu^2)(\xi_2^\circ - \tfrac{1}{2}\xi_2^m) - (mn\pi)^2(\Gamma\xi_4^\circ + \bar{\xi}_4^\circ$$

$$- \Gamma\xi_6^\circ - \bar{\xi}_6^\circ)\Big\} a^2 b \sin 2(\delta_b - \delta_a)\cos(\tau + \delta_b) \qquad \text{(I. 3)}$$

$$\bar{G}_2 = \frac{2(mn\pi)^2}{R^2}\Bigg\{\Big\{-\xi_1^m - \tfrac{1}{2}\xi_2^m - \xi_3^\circ - \tfrac{1}{2}\xi_4^\circ\Big\} b^3 + \Big\{-\xi_1^m + \tfrac{1}{2}\xi_2^m\cos 2(\delta_b - \delta_a)$$

$$+ \xi_3^\circ - \tfrac{1}{2}\xi_4^\circ\cos 2(\delta_b - \delta_a) - \tfrac{1}{2}\xi_5^\circ - \tfrac{1}{2}\xi_6^\circ + \tfrac{1}{2}\xi_6^\circ\cos 2(\delta_b - \delta_a)\Big\} a^2 b\Big\}\sin(\tau + \delta_b)$$

$$+ \frac{(mn\pi)^2}{R^2}(-\xi_2^m + \xi_4^\circ - \xi_6^\circ) a^2 b \sin 2(\delta_b - \delta_a)\cos(\tau + \delta_b) \qquad \text{(I. 4)}$$

$$G_3 = 2\left(\frac{mn\pi}{k}\right)^2 \Big\{ \Big[\Gamma\left(-C_1 - \tfrac{1}{2}C_2 + C_3 + \tfrac{1}{2}C_4\right) + \left(-\bar{C}_1 - \tfrac{1}{2}\bar{C}_2 + \bar{C}_3 + \tfrac{1}{2}\bar{C}_4 - \tfrac{1}{2}\tfrac{1}{m^2\pi^2}\bar{C}_6\right)\Big] a^3 + \Big\{ \Gamma\Big[-C_1 + \tfrac{1}{2}C_2\cos 2(\delta_b - \delta_a) - C_3 + \tfrac{1}{2}C_4\cos 2(\delta_b - \delta_a) + \tfrac{1}{2}C_7 + \tfrac{1}{2}C_8 - \tfrac{1}{2}C_8\cos 2(\delta_b - \delta_a)\Big] + \Big[-\bar{C}_1 + \tfrac{1}{2}\bar{C}_2\cos 2(\delta_b - \delta_a) - \bar{C}_3 + \tfrac{1}{2}\bar{C}_4\cos 2(\delta_b - \delta_a) + \tfrac{1}{2}\tfrac{1}{(m\pi)^2}C_6\cos 2(\delta_b - \delta_a) + \tfrac{1}{2}\bar{C}_7 + \tfrac{1}{2}\bar{C}_8 - \tfrac{1}{2}\bar{C}_8\cos 2(\delta_b - \delta_a)\Big] \Big\} ab^2 \Big\} \cos(\tau + \delta_a)$$

$$+ \left(\frac{mn\pi}{k}\right)^2 \Big\{ \Gamma\left(-C_2 - C_4 + C_8\right) + \Big[-\bar{C}_2 - \bar{C}_4 - \frac{1}{(m\pi)^2}\bar{C}_6 + \bar{C}_8 \Big] \Big\} ab^2 \sin 2(\delta_b - \delta_a) \sin(\tau + \delta_a) \qquad \text{(I. 5)}$$

$$\bar{G}_3 = 2\left(\frac{mn\pi}{k}\right)^2 \Big\{ \left(C_1 + \tfrac{1}{2}C_2 - C_3 - \tfrac{1}{2}C_4\right) a^3 + \Big[C_1 - \tfrac{1}{2}C_2\cos 2(\delta_b - \delta_a) + C_3 - \tfrac{1}{2}C_4\cos 2(\delta_b - \delta_a) - \tfrac{1}{2}C_7 - \tfrac{1}{2}C_8 + \tfrac{1}{2}C_8\cos 2(\delta_b - \delta_a)\Big] ab^2 \cos(\tau + \delta_a) \Big\}$$

$$+ \left(\frac{mn\pi}{k}\right)^2 \left(C_2 + C_8 - C_8\right) ab^2 \sin 2(\delta_b - \delta_a) \sin(\tau + \delta_a) \qquad \text{(I. 6)}$$

$$G_4 = 2\left(\frac{mn\pi}{k}\right)^2 \Big\{\Big[\Big[\Gamma\left(-C_1 - \tfrac{1}{2}C_2 + C_3 + \tfrac{1}{2}C_4\right) + \left(-\bar{C}_1 - \tfrac{1}{2}\bar{C}_2 + \bar{C}_3 + \tfrac{1}{2}\bar{C}_4 - \tfrac{1}{2}\tfrac{1}{(mn\pi)^2}\bar{C}_6\right)\Big] b^3$$

$$+ \Big\{\Big[\Gamma\Big[-C_1 + \tfrac{1}{2}C_2\cos 2(\delta_b - \delta_a) - C_3 + \tfrac{1}{2}C_4\cos 2(\delta_b - \delta_a) + \tfrac{1}{2}C_7$$

$$+ \tfrac{1}{2}C_8 - \tfrac{1}{2}C_8\cos 2(\delta_b - \delta_a)\Big] + \Big[-\bar{C}_1 + \tfrac{1}{2}\bar{C}_2\cos 2(\delta_b - \delta_a) - \bar{C}_3$$

$$+ \tfrac{1}{2}\bar{C}_4\cos 2(\delta_b - \delta_a) + \tfrac{1}{2}\tfrac{1}{(mn\pi)^2}\bar{C}_6\cos 2(\delta_b - \delta_a) + \tfrac{1}{2}\bar{C}_7$$

$$+ \tfrac{1}{2}\bar{C}_8 - \tfrac{1}{2}\bar{C}_8\cos 2(\delta_b - \delta_a)\Big]\Big\} a^2 b\Big\} \sin(\tau + \delta_b)$$

$$+ \left(\frac{mn\pi}{k}\right)^2 \Big\{\Big[\Gamma\left(-C_2 - C_4 + C_8\right) + \Big[-\bar{C}_2 - \bar{C}_4 - \tfrac{1}{2}\tfrac{1}{(mn\pi)^2}\bar{C}_6 + \bar{C}_8\Big]\Big] \times$$

$$\times a^4 b \sin 2(\delta_b - \delta_a)\cos(\tau + \delta_b) \qquad \text{(I. 7)}$$

$$\bar{G}_4 = 2\left(\frac{mn\pi}{k}\right)^2 \Big\{\Big(C_1 + \tfrac{1}{2}C_2 - C_3 - \tfrac{1}{2}C_4\Big) b^3 + \Big[C_1 - \tfrac{1}{2}C_2\cos 2(\delta_b - \delta_a) + C_3$$

$$- \tfrac{1}{2}C_4\cos 2(\delta_b - \delta_a) - \tfrac{1}{2}C_7 - \tfrac{1}{2}C_8 + \tfrac{1}{2}C_8\cos 2(\delta_b - \delta_a)\Big] a^2 b\Big\} \sin(\tau + \delta_b)$$

$$+ \left(\frac{mn\pi}{k}\right)^2 \left(C_2 + C_4 - C_8\right) a^4 b \sin 2(\delta_b - \delta_a)\cos(\tau + \delta_b) \qquad \text{(I. 8)}$$

Table I

Natural Frequencies of Shell Specimen

	m = 1					m = 2				
n	ω_e	ω_R	ω_D	E_e	E_D	ω_e	ω_R	ω_D	E_e	E_D
4	975.5	971.5	1069.43	0.412	9.16	-	3205.6	3041.89	-	5.38
5	736.2	724.3	733.14	1.644	1.205	-	2102.8	2263.17	-	7.08
6	591.0	583.2	558.07	1.34	4.99	1705.6	1683.8	1734.29	1.296	3.00
7	525.1	526.3	486.02	0.228	8.28	1406.3	1379.7	1378.69	1.93	0.0725
8	530.2	530.3	488.12	0.019	8.62	1204.1	1180.2	1148.21	2.025	2.79
9	-	578.2	541.61	-	6.76	1085.2	1085.2	1014.93	1.88	4.96
10	641.0	652.1	628.75	1.70	3.71	1029.1	1018.9	963.23	1.00	6.00
11	738.4	754.6	738.86	2.15	2.15	1035.6	1024.4	972.40	1.09	5.35
12	857.7	876.1	866.38	2.10	1.12	1091.3	1079.4	1034.14	1.10	4.38
13	991.0	1013.7	1008.55	2.24	0.515	1165.4	1170.7	1133.88	0.453	3.06
14	1138.5	1165.9	1164.02	3.21	0.172	1285.2	1290.8	1262.18	0.434	3.06
15	1302.0	1331.5	1332.08	2.21	0.045	-	1434.3	1412.74	-	1.53

where m = half axial wave number

n = circumferential wave number

ω_e = measured natural frequency (cps)

ω_R = calculated natural frequency of shell with end rings (cps)

ω_D = calculated natural frequency of shell based on Donnell's approximation with simply-supported boundary conditions

$$E_e = \frac{|\omega_e - \omega_R|}{\omega_R} \times 100$$

$$E_D = \frac{|\omega_D - \omega_R|}{\omega_R} \times 100$$

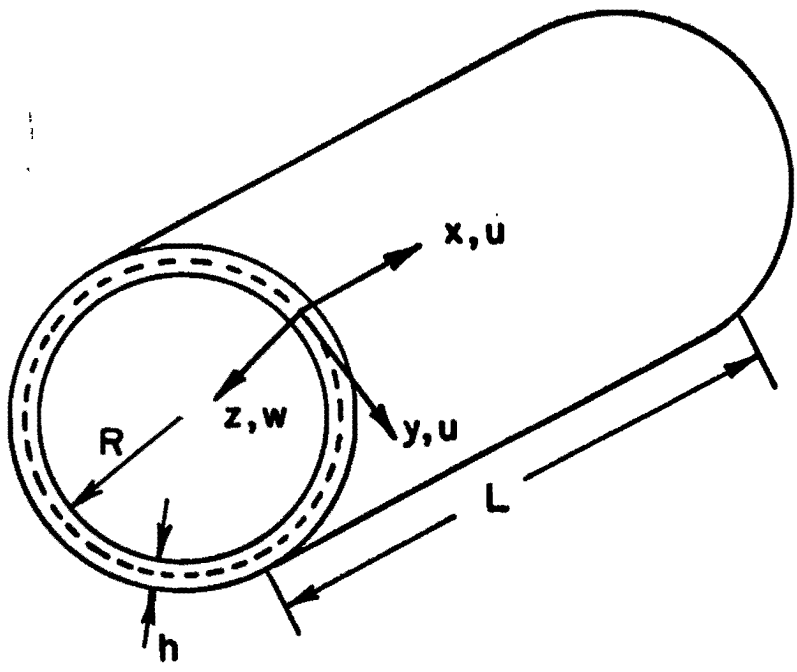

FIG. 1 SHELL GEOMETRY AND COORDINATE SYSTEM

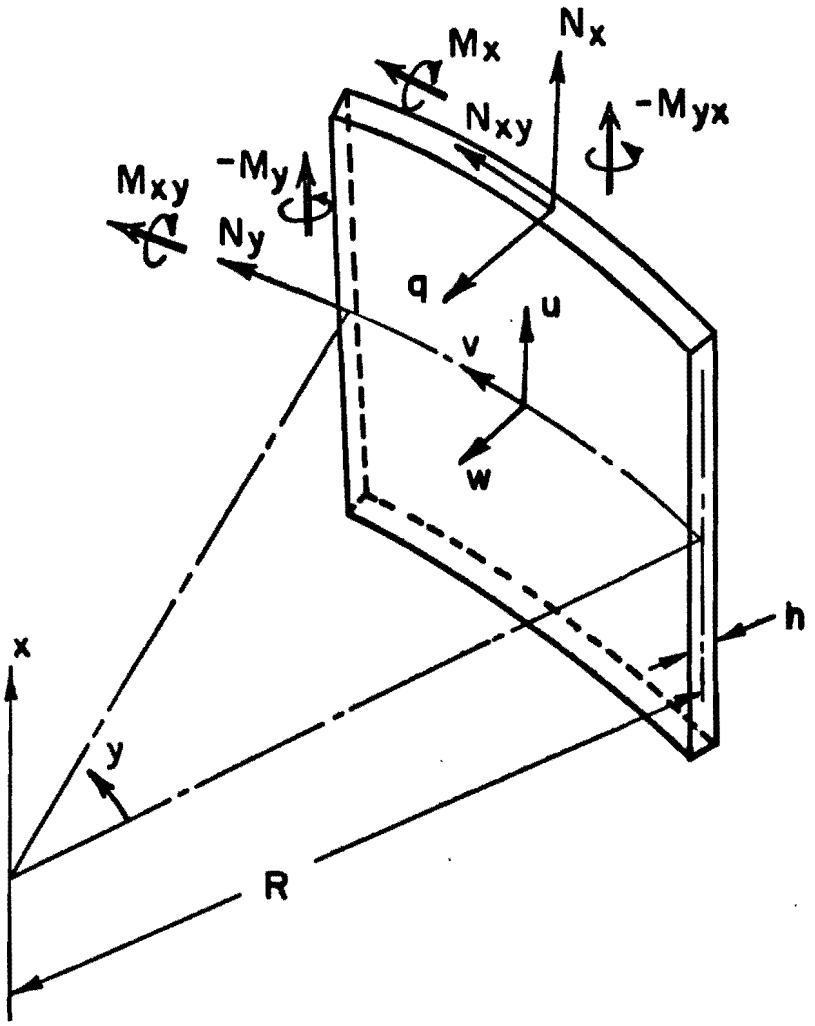

FIG. 2 ELEMENT OF CYLINDRICAL SHELL

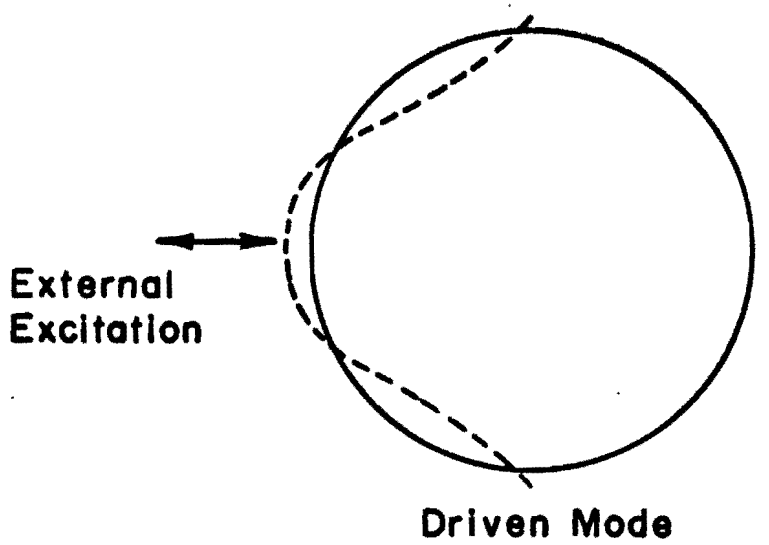

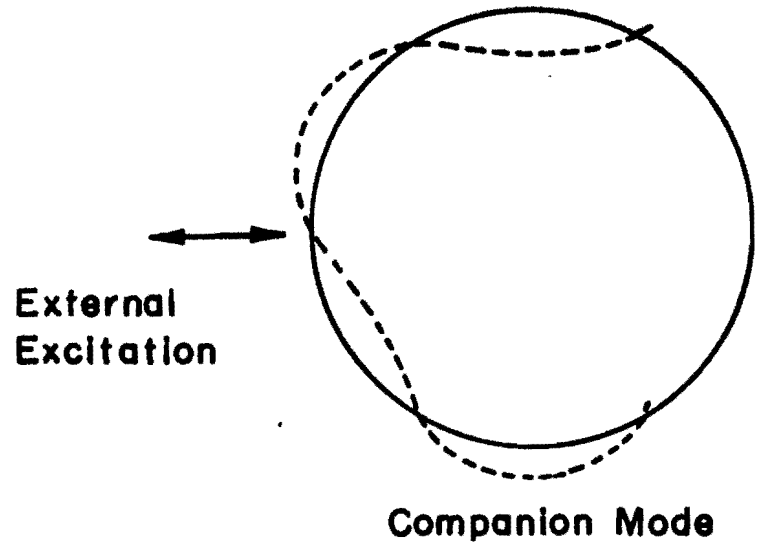

FIG. 3 DRIVEN MODE AND COMPANION MODE

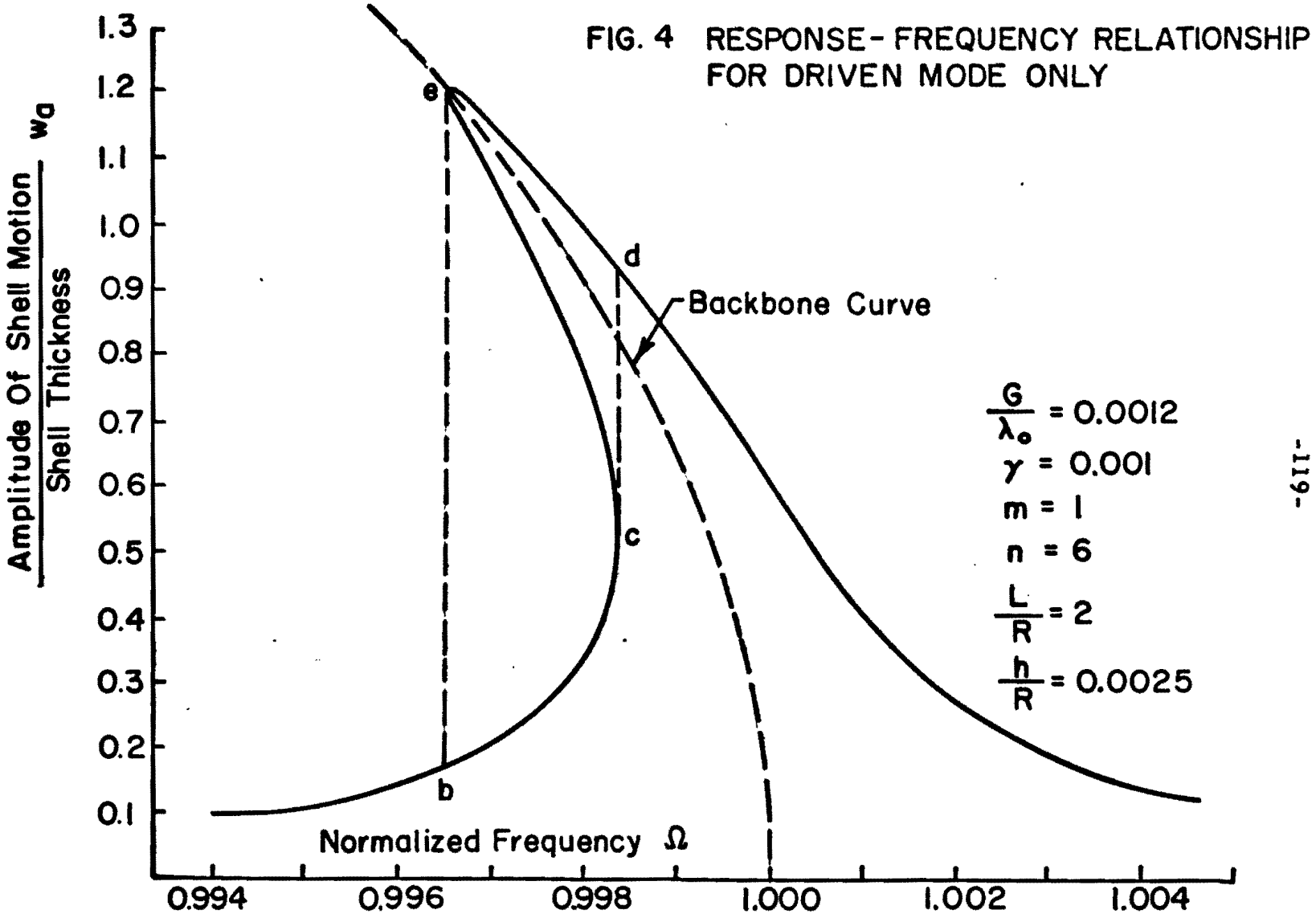

FIG. 4 RESPONSE-FREQUENCY RELATIONSHIP FOR DRIVEN MODE ONLY

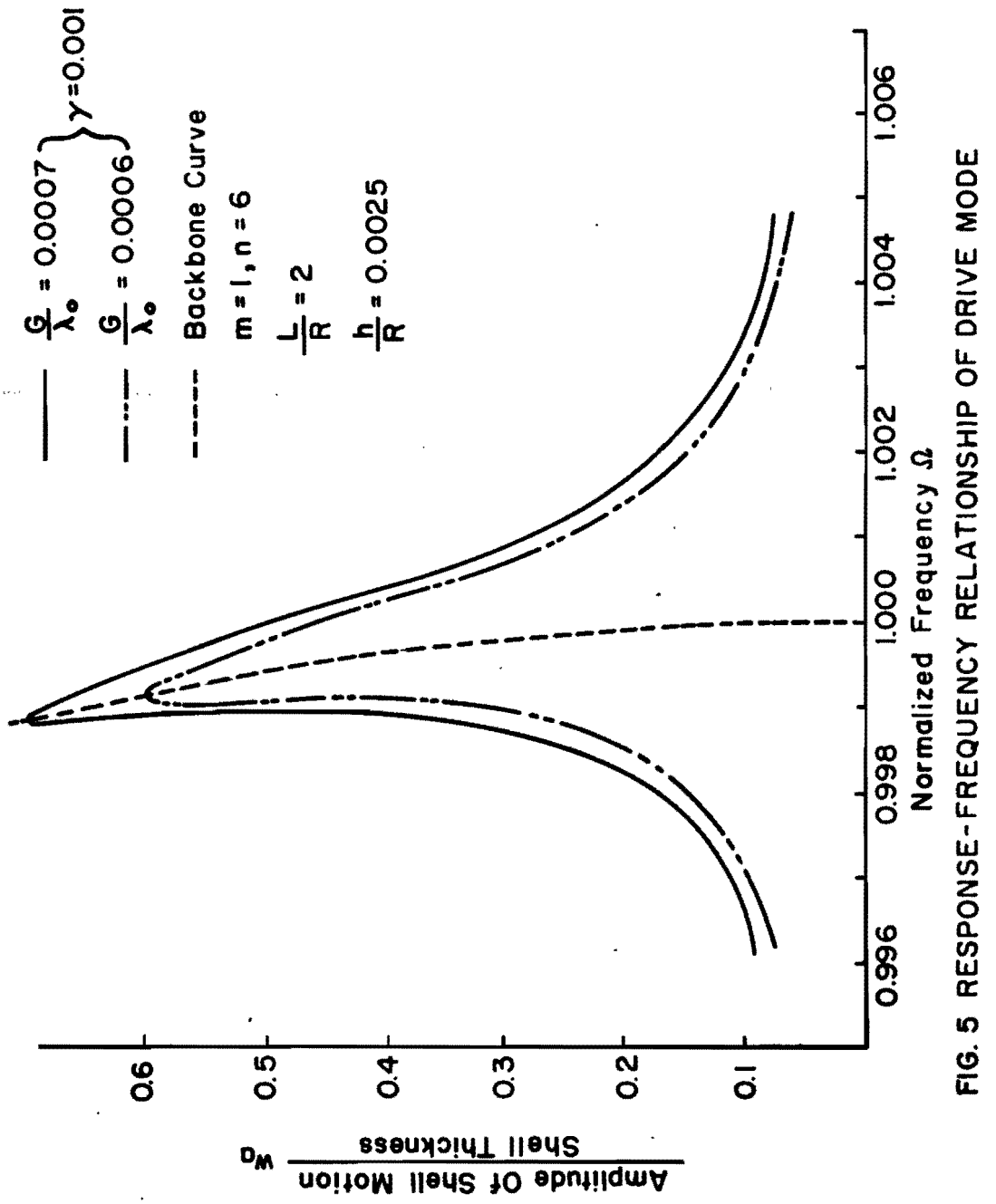

FIG. 5 RESPONSE-FREQUENCY RELATIONSHIP OF DRIVE MODE

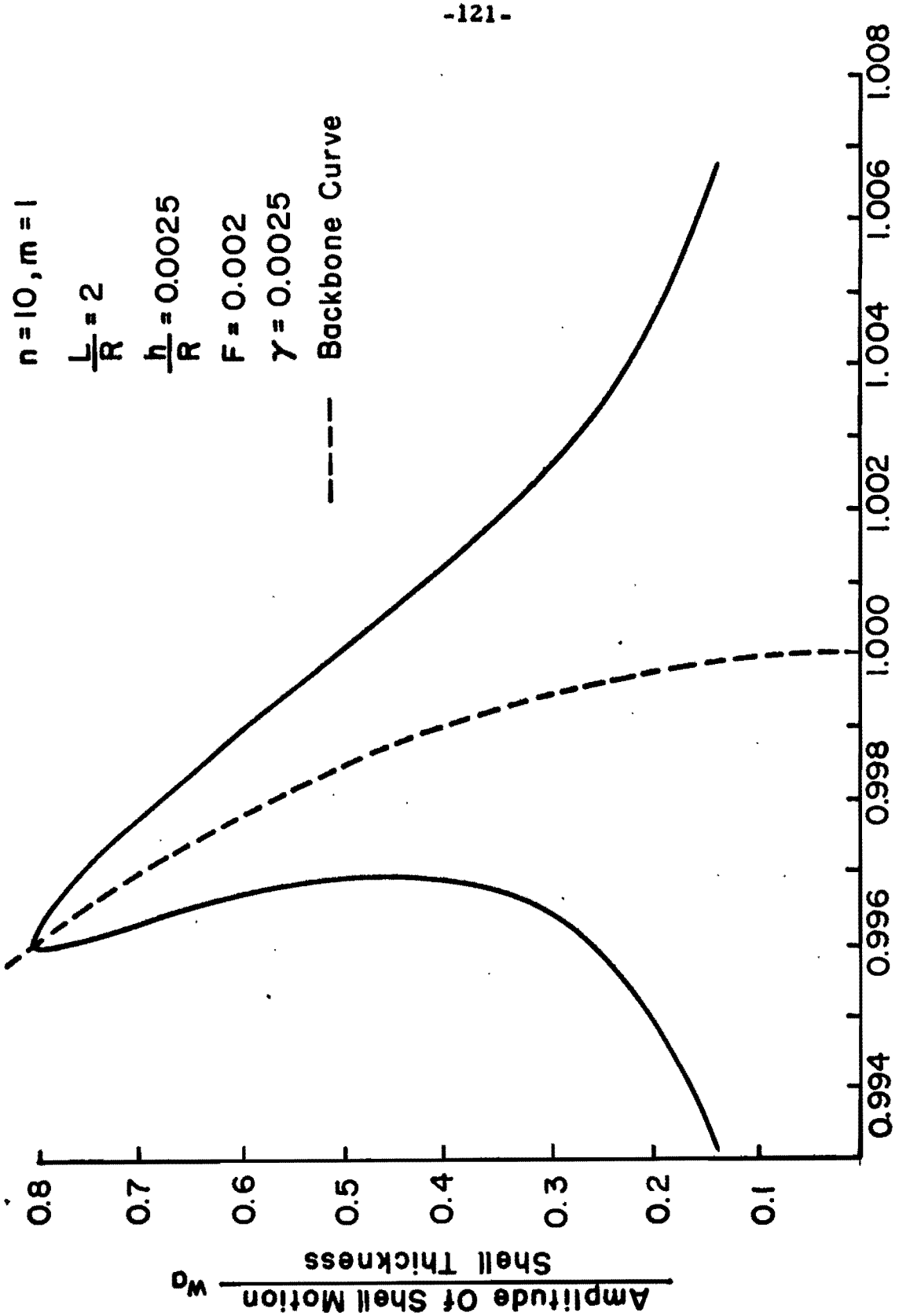

FIG. 6 RESPONSE-FREQUENCY RELATIONSHIP OF DRIVEN MODE

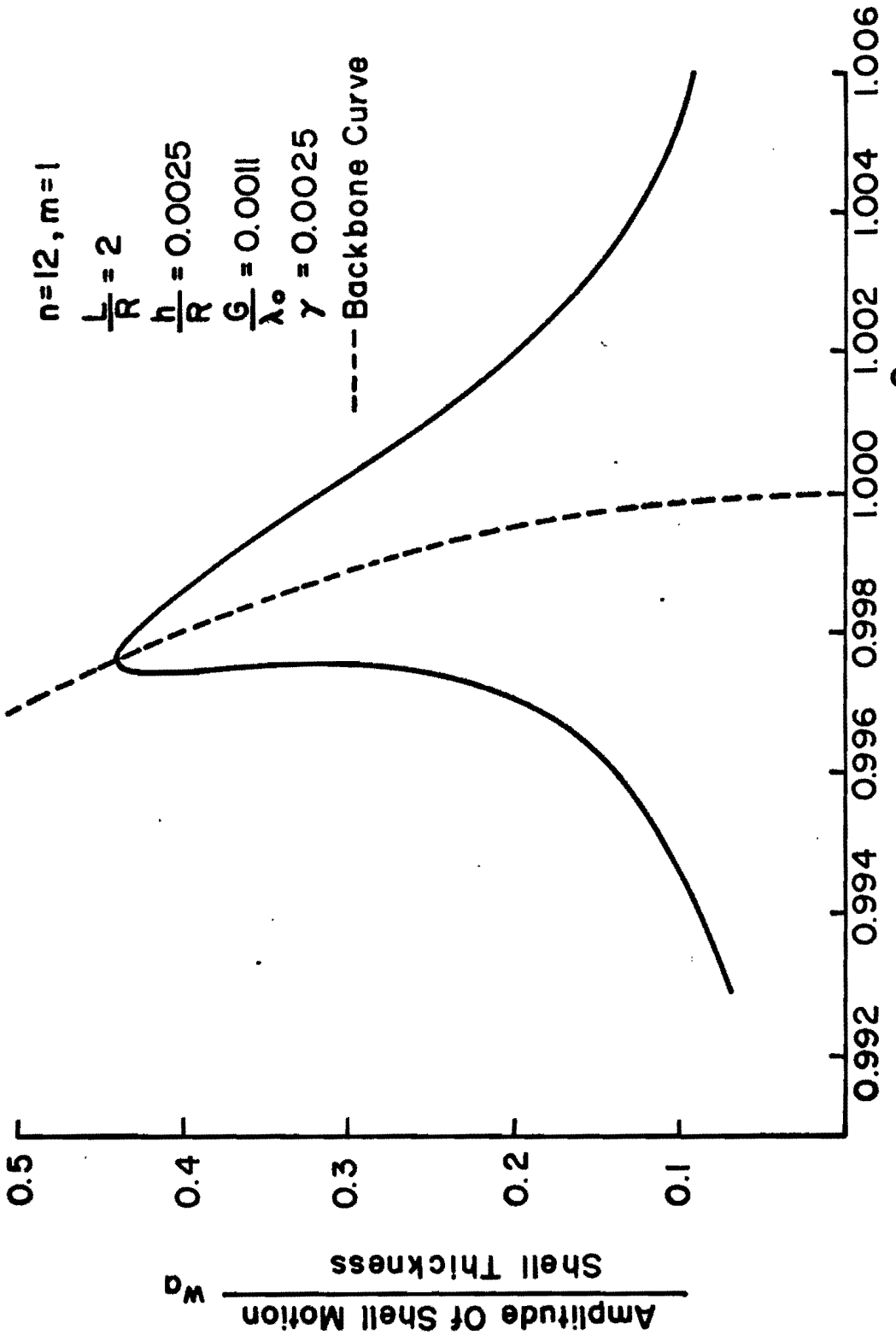

FIG.7 RESPONSE-FREQUENCY RELATIONSHIP OF DRIVEN MODE

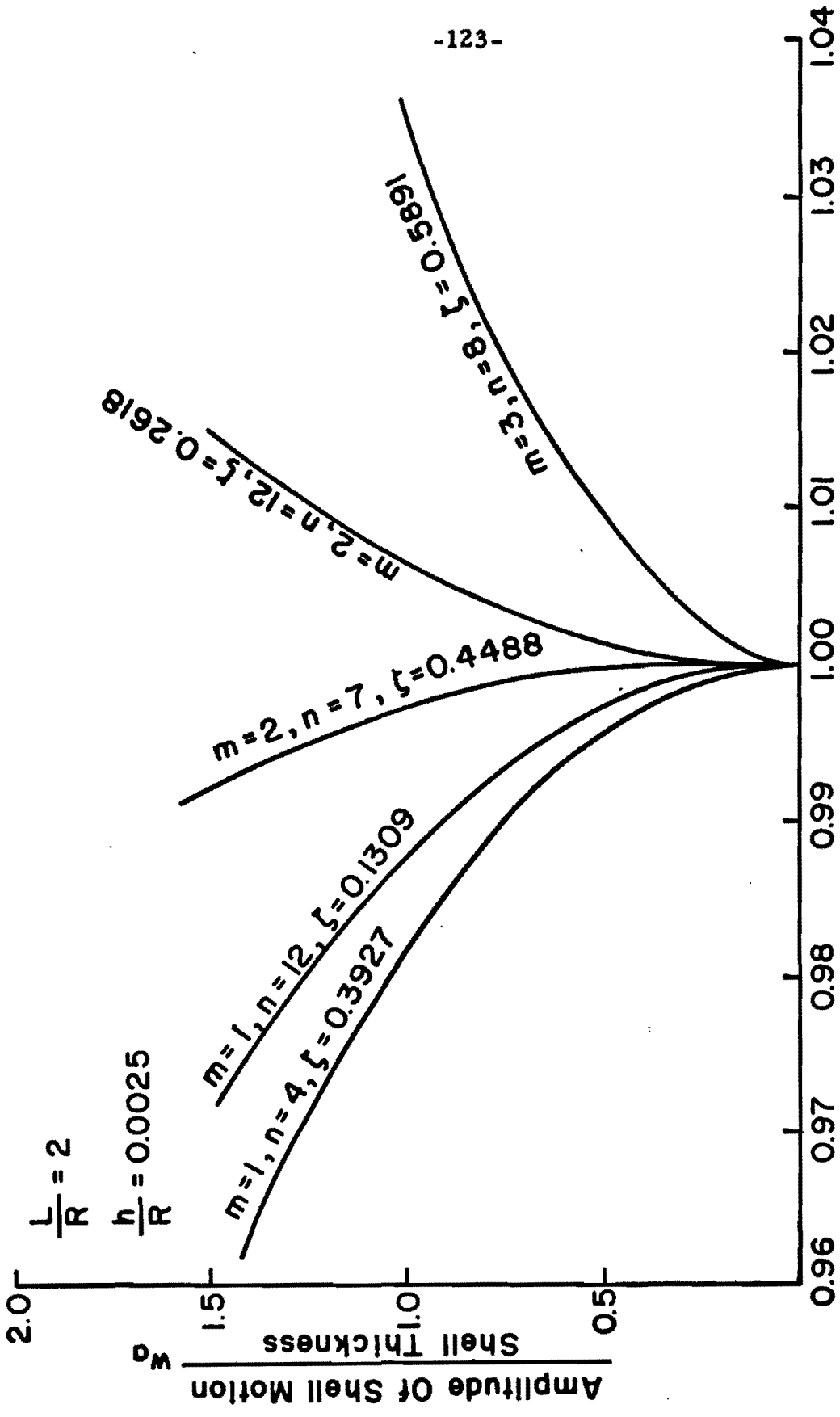

FIG. 8 BACKBONE CURVES FOR VARIOUS DRIVEN MODES

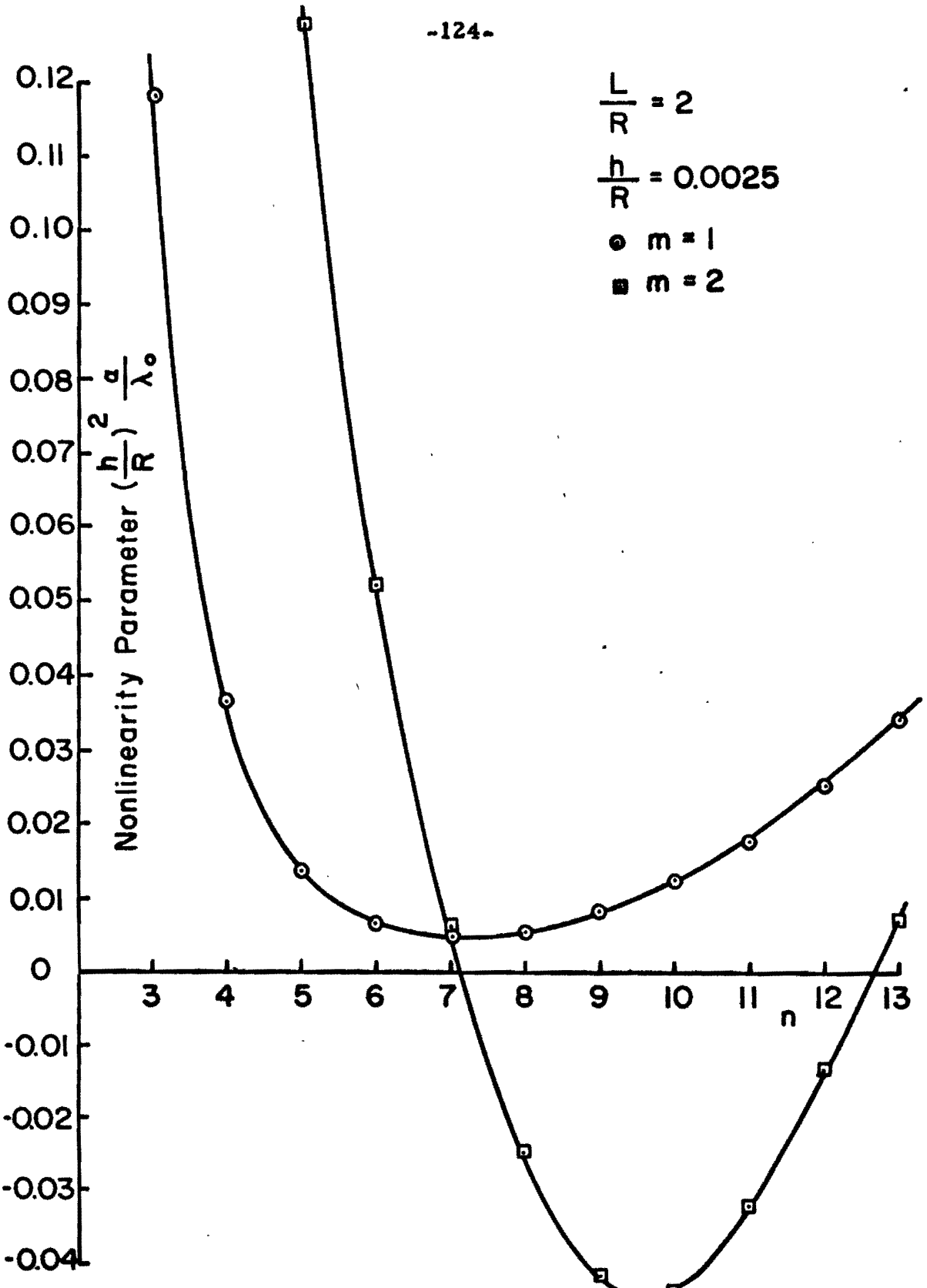

FIG. 9 NONLINEARITY PARAMETER

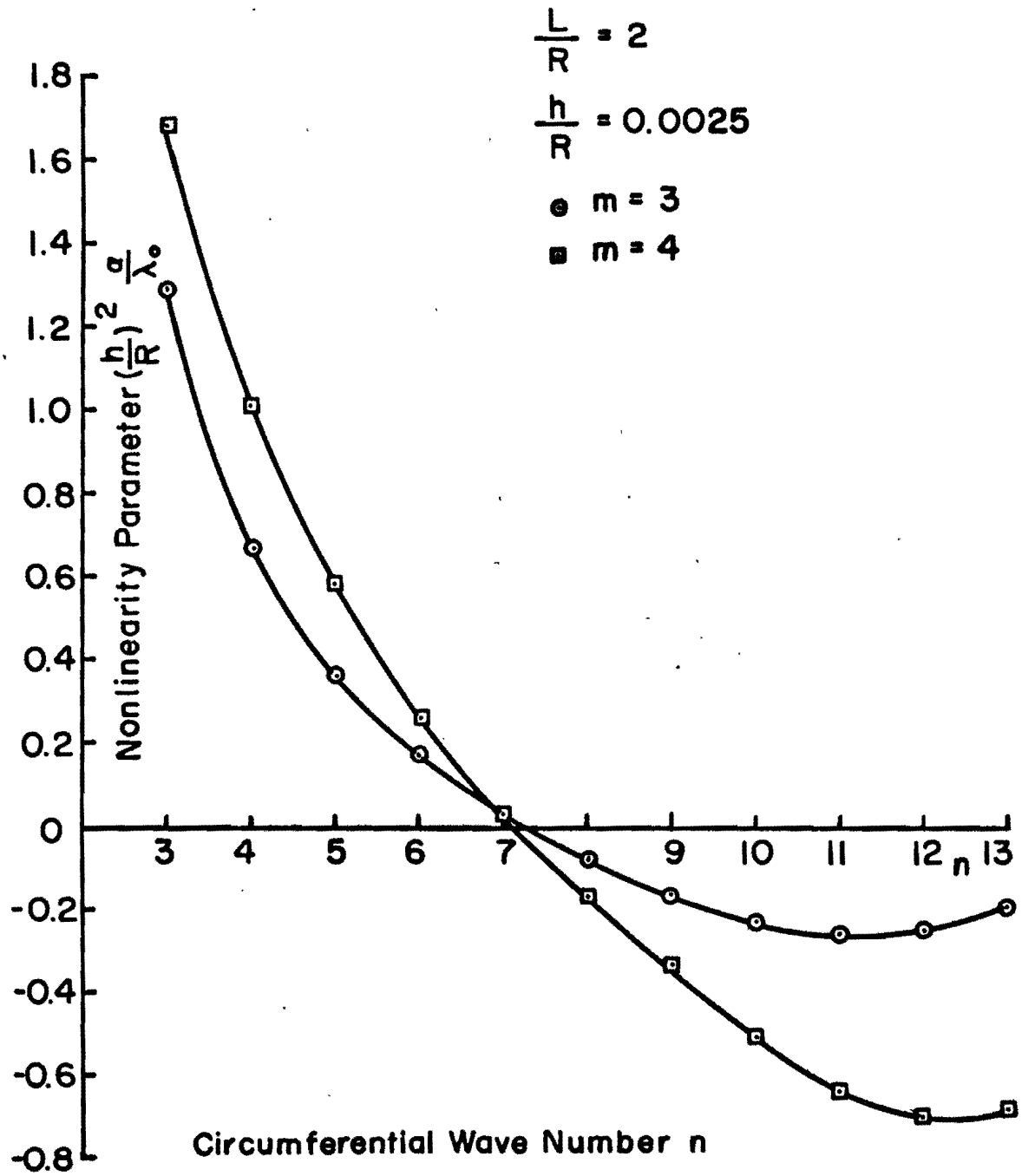

FIG. 10 NONLINEARITY PARAMETER

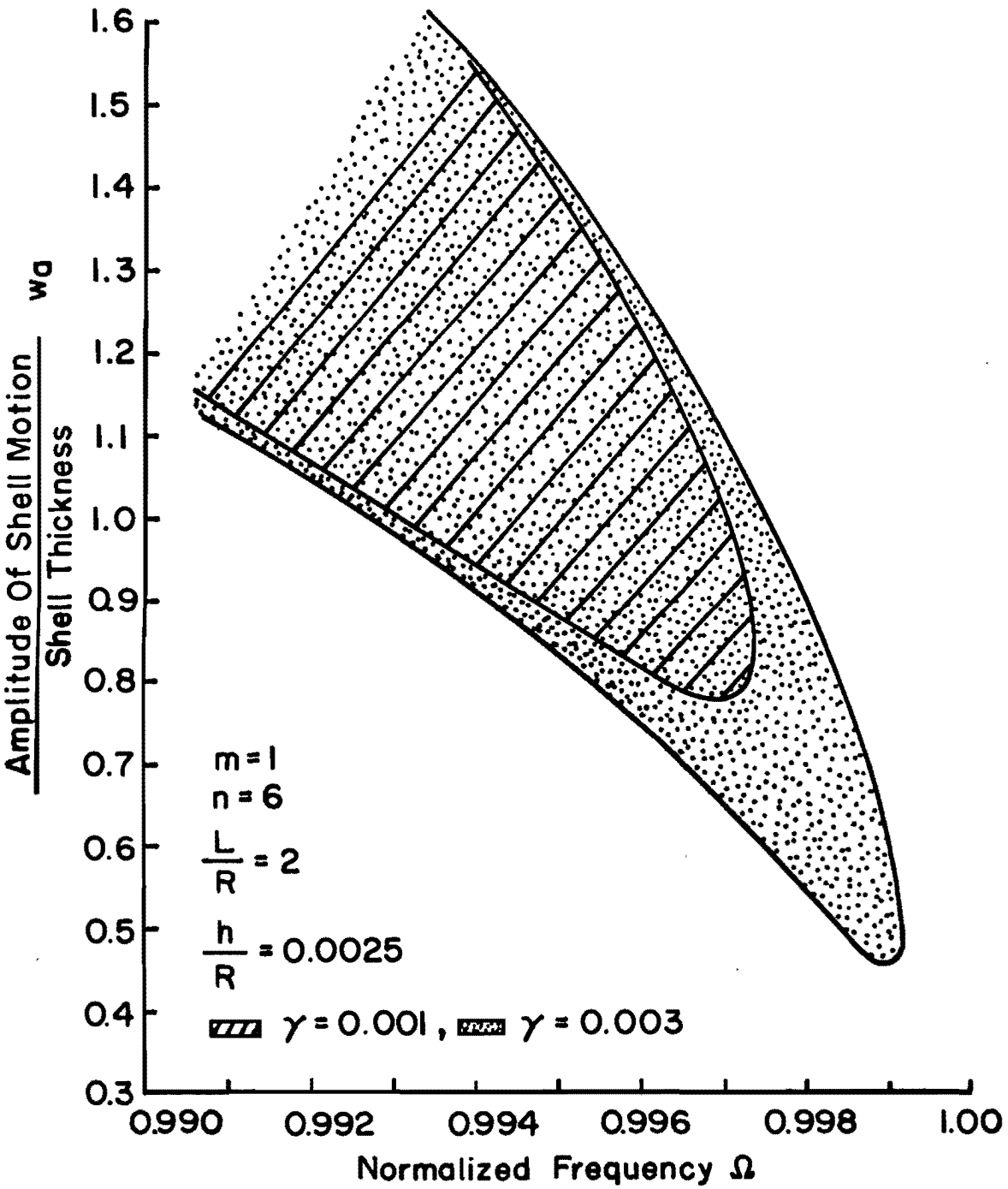

FIG. 11 LOCUS OF VERTICAL TANGENT OF DRIVEN MODE RESPONSE

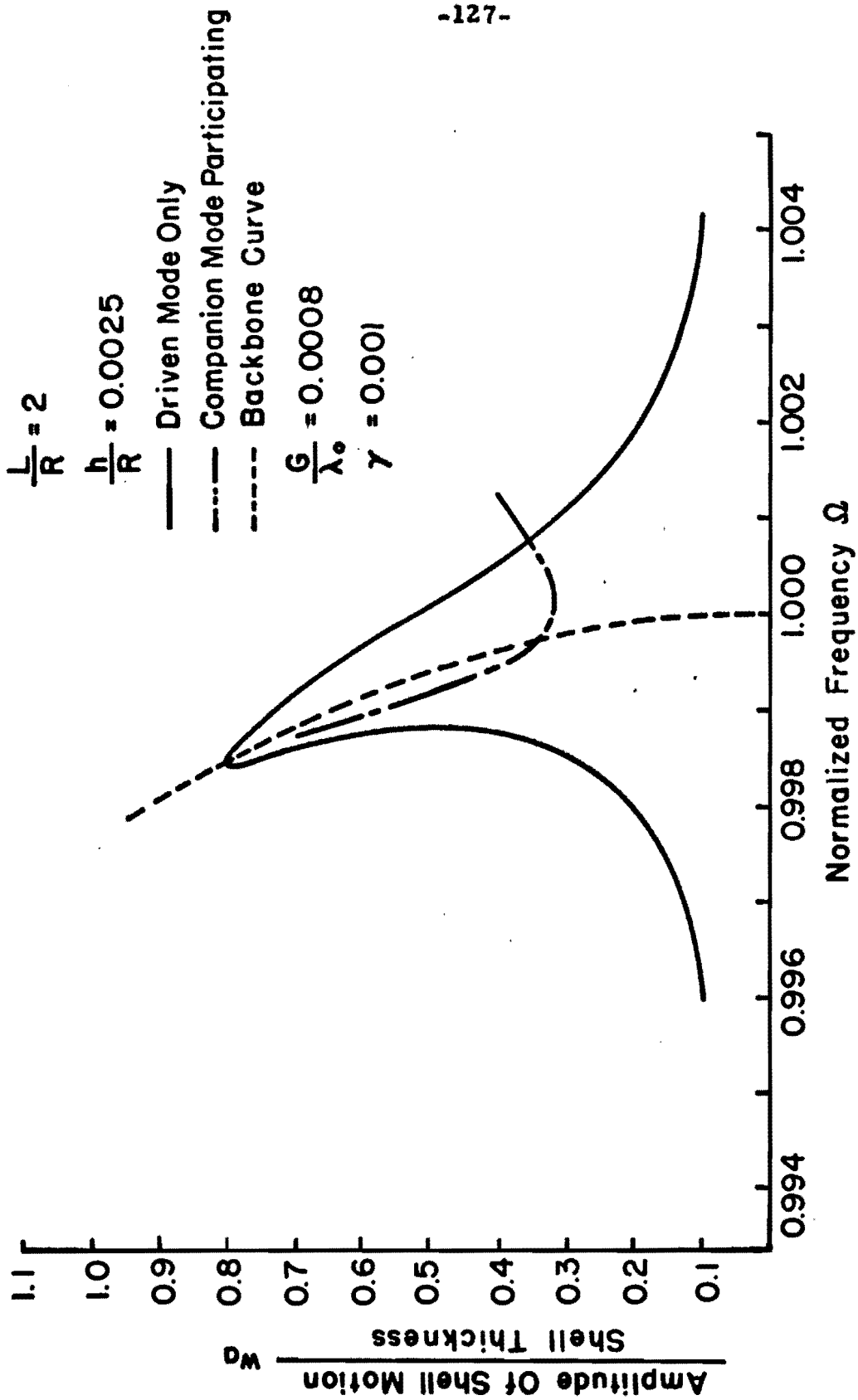

FIG.12 RESPONSE-FREQUENCY RELATIONSHIP OF DRIVEN MODE m=1, n= 6

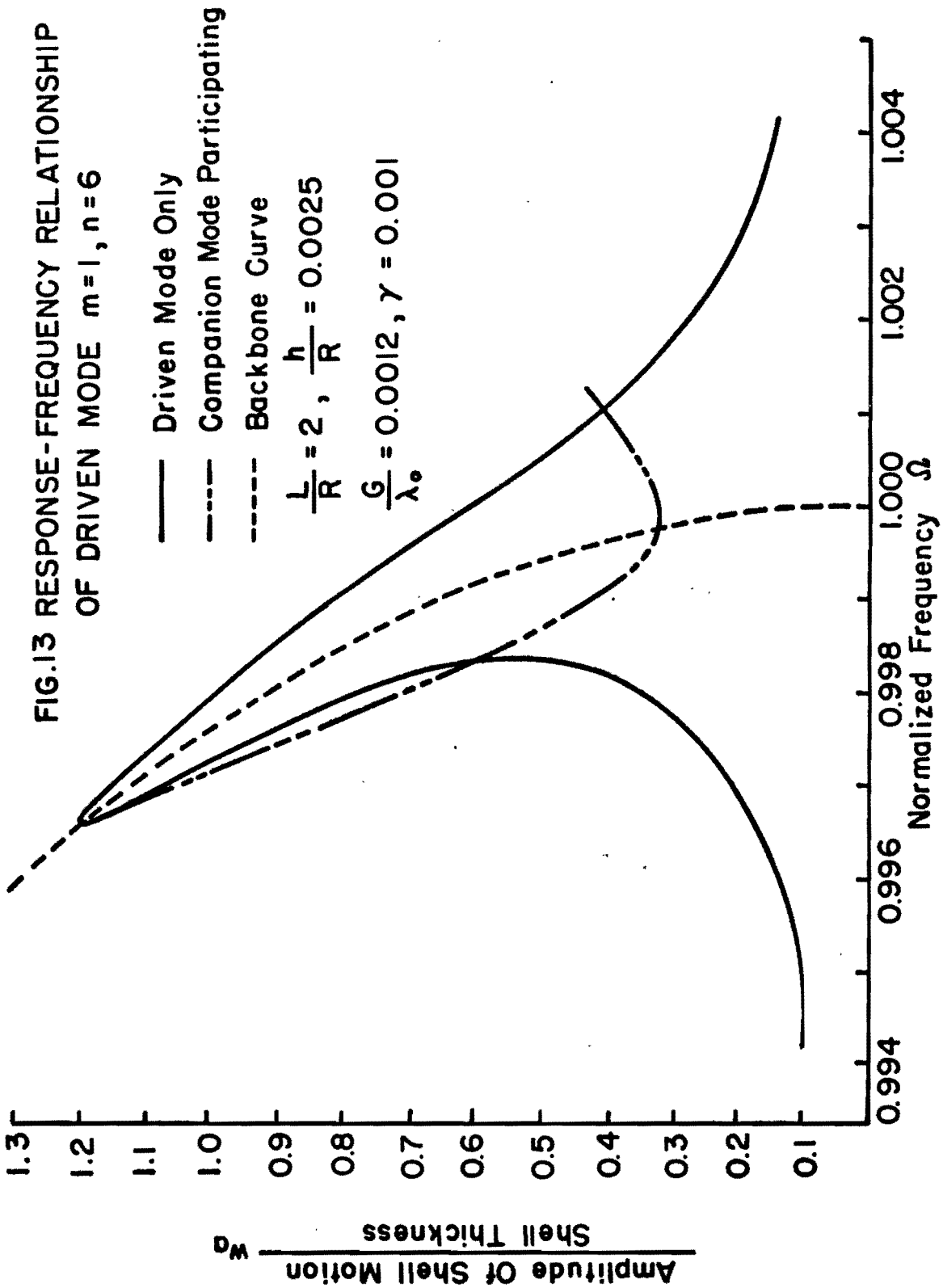

FIG.13 RESPONSE-FREQUENCY RELATIONSHIP OF DRIVEN MODE $m=1, n=6$

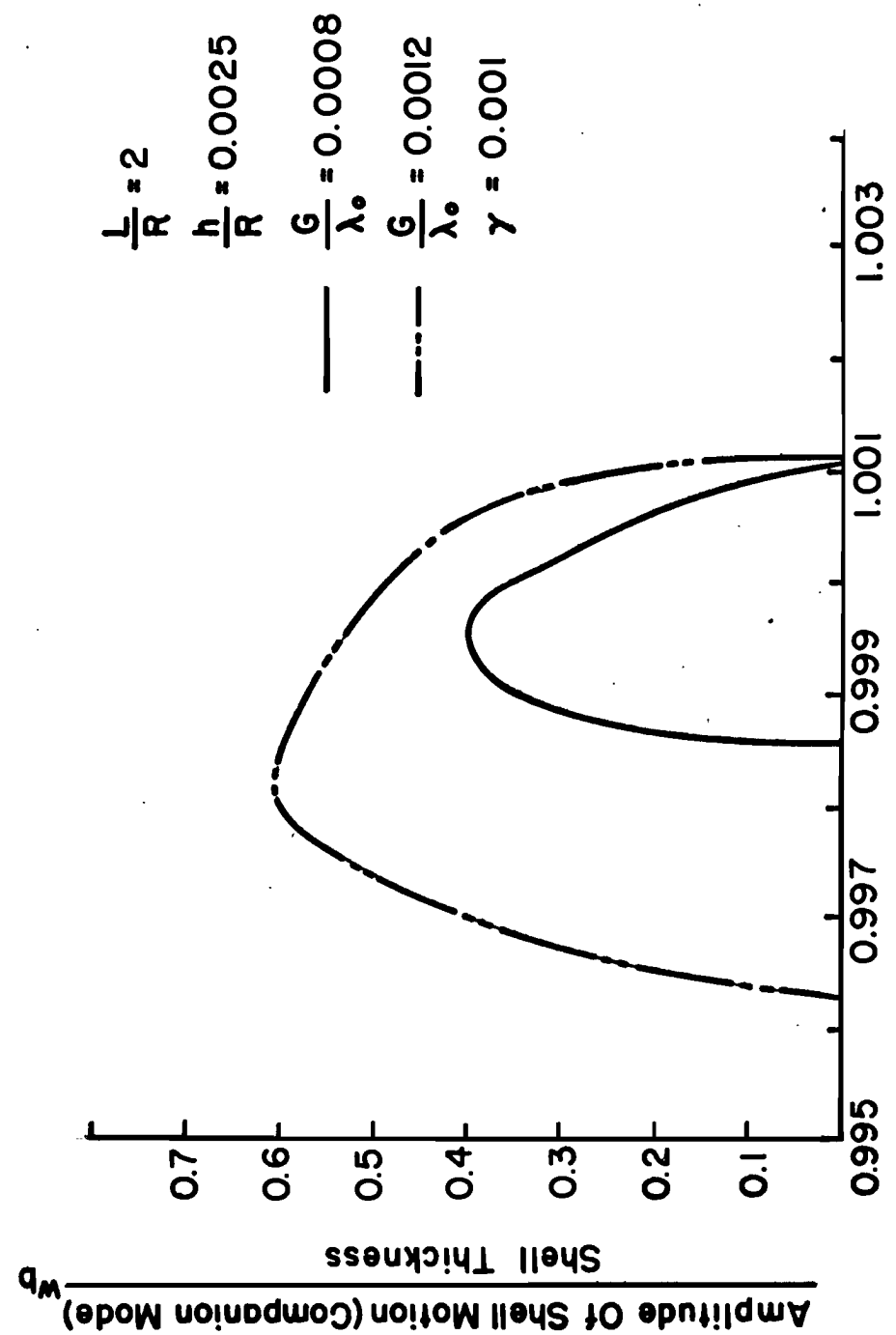

FIG.14 RESPONSE - FREQUENCY RELATIONSHIP OF COMPANION MODE m = 1, n = 6

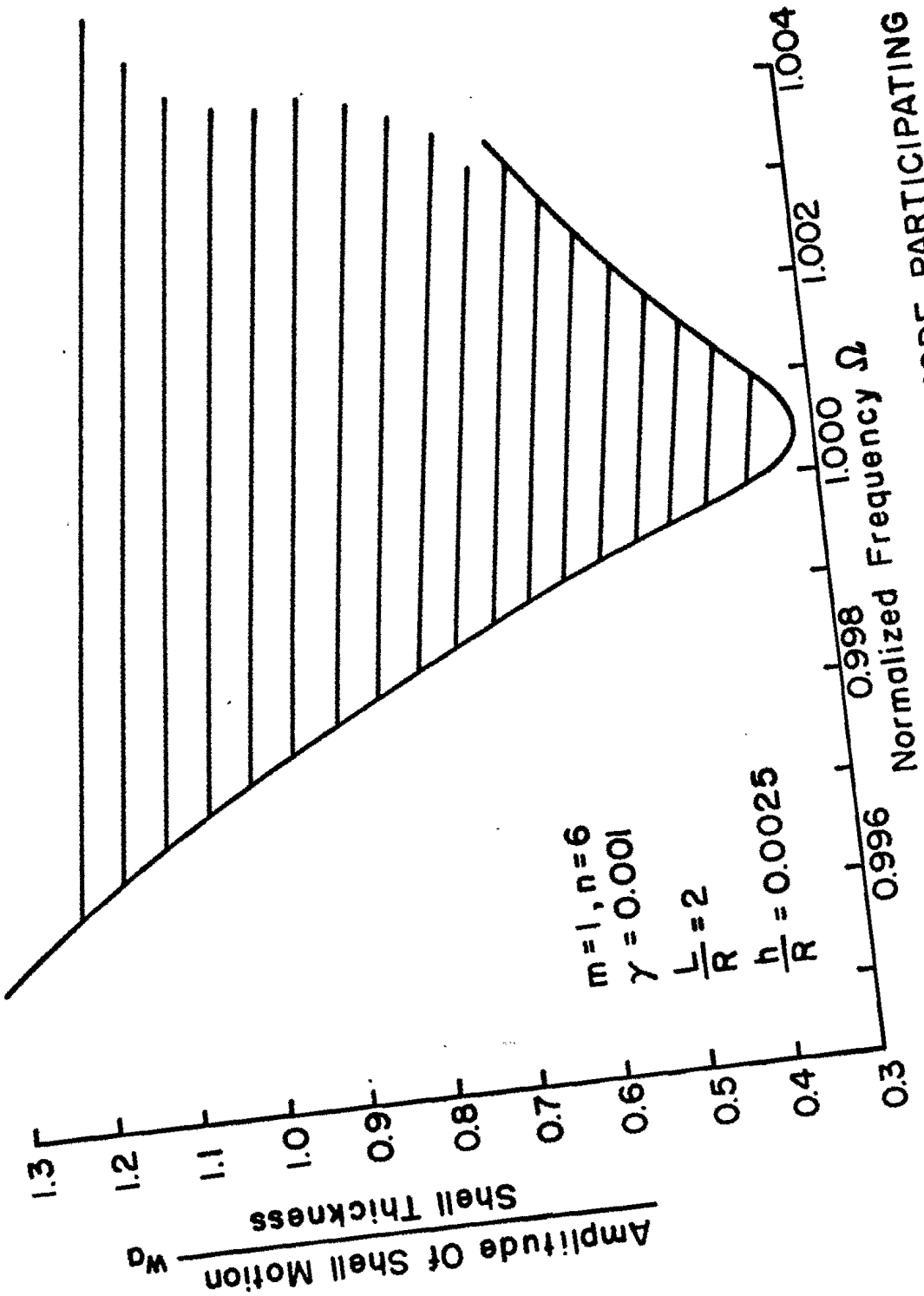

FIG. 15 REGION OF COMPANION MODE PARTICIPATING

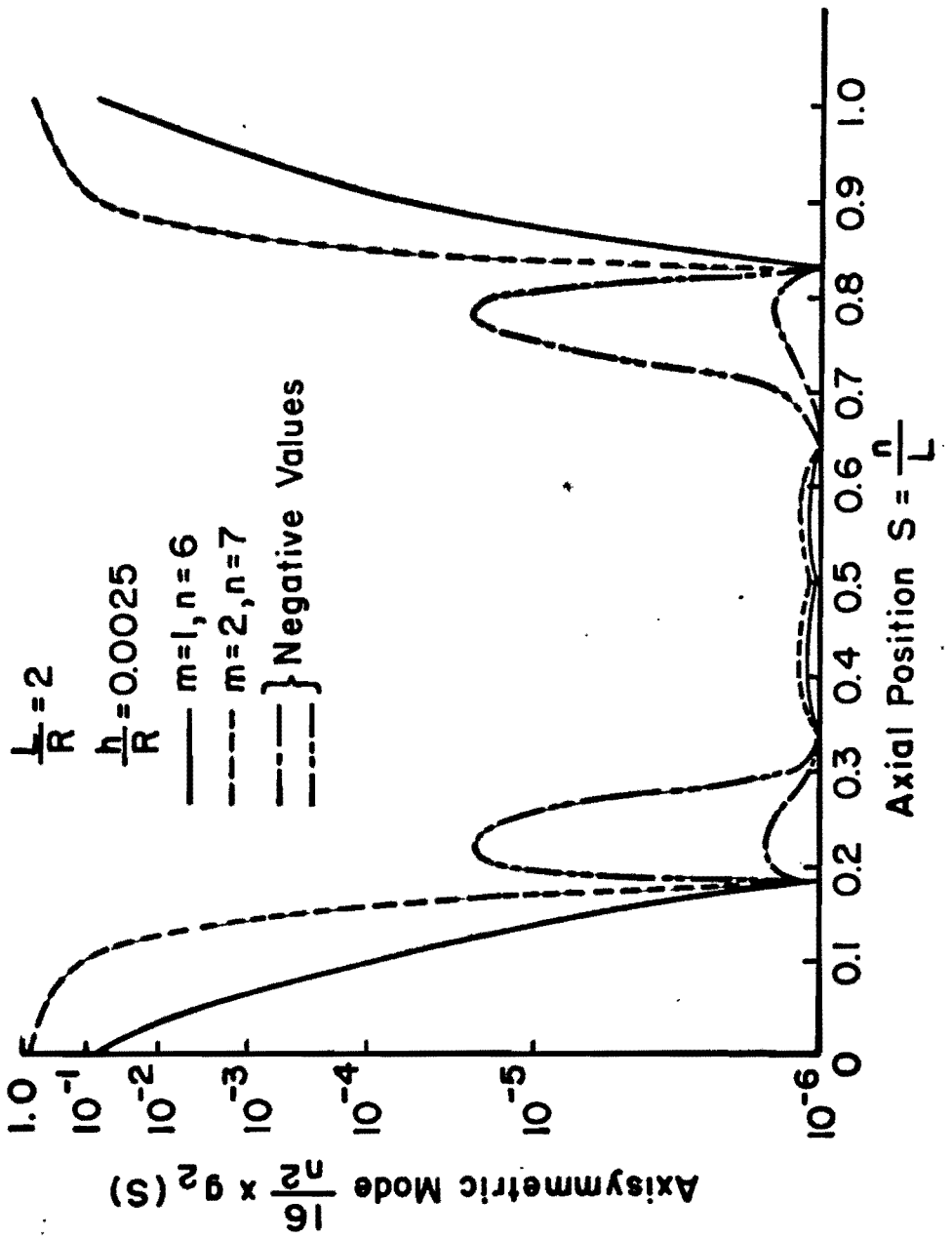

FIG.16 AXISYMMETRIC MODE $g_2(S)$

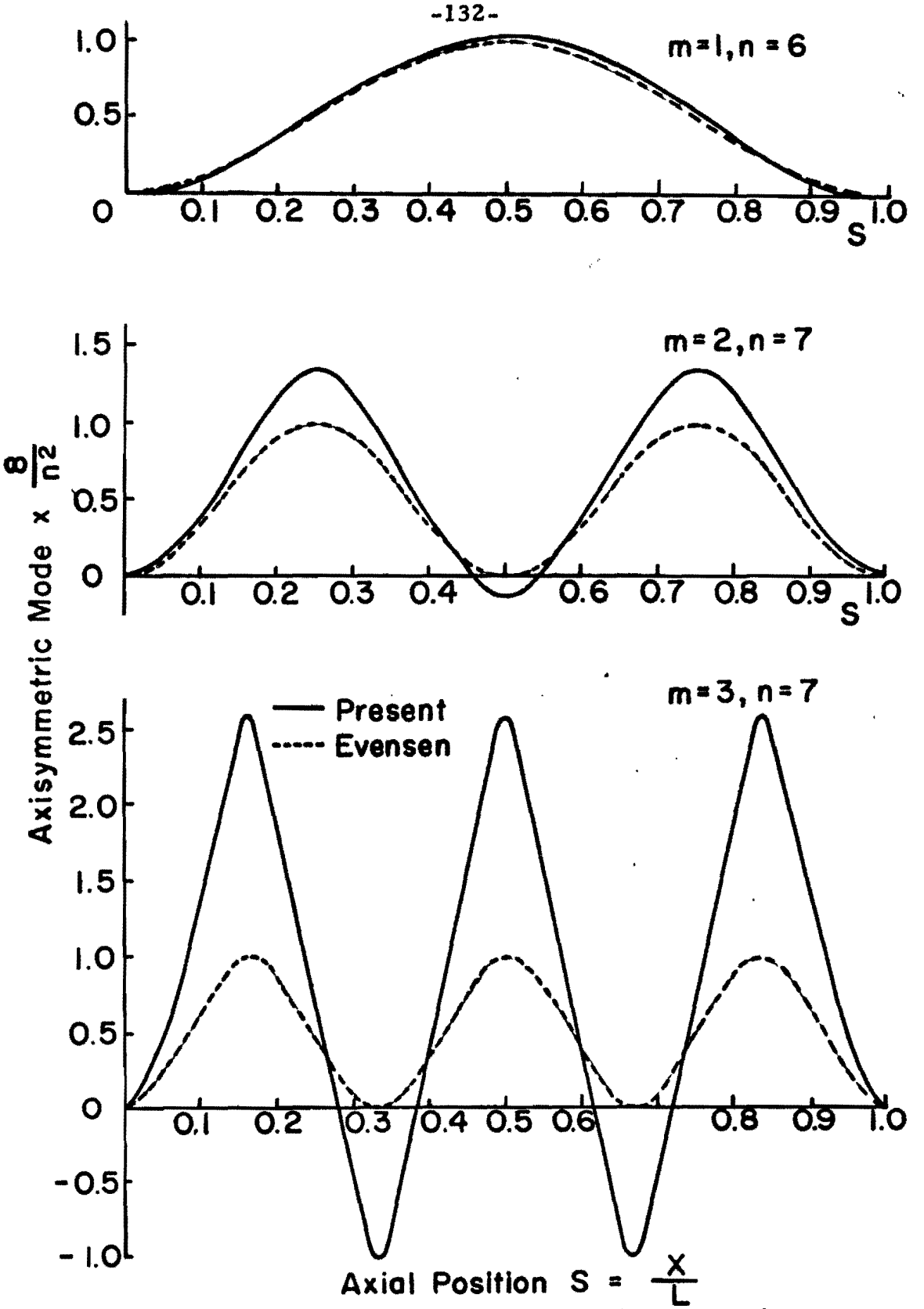

FIG. 17 AXISYMMETRIC MODE FOR $\frac{L}{R}$ = 2, $\frac{h}{R}$ = 0.0025

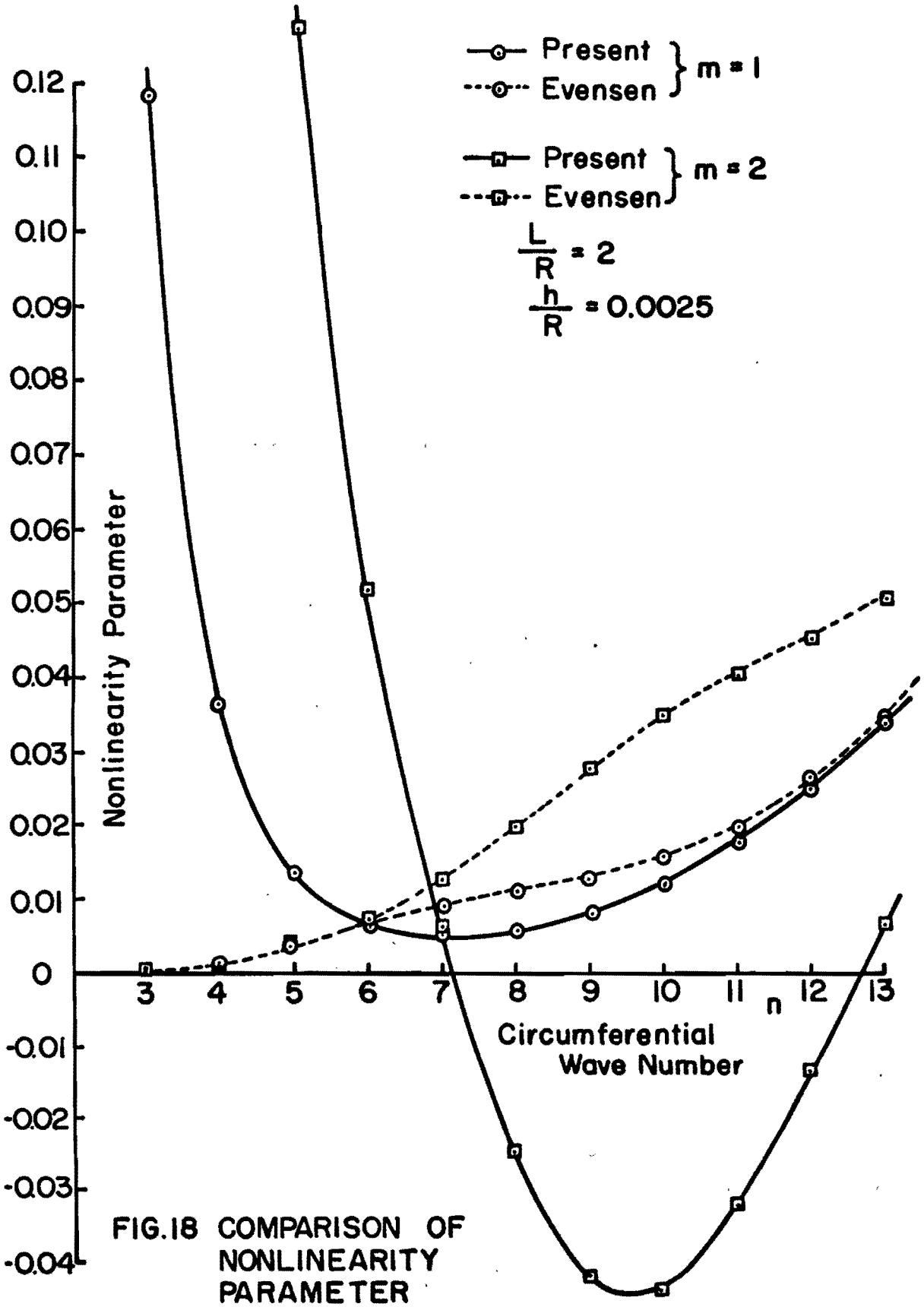

FIG. 18 COMPARISON OF NONLINEARITY PARAMETER

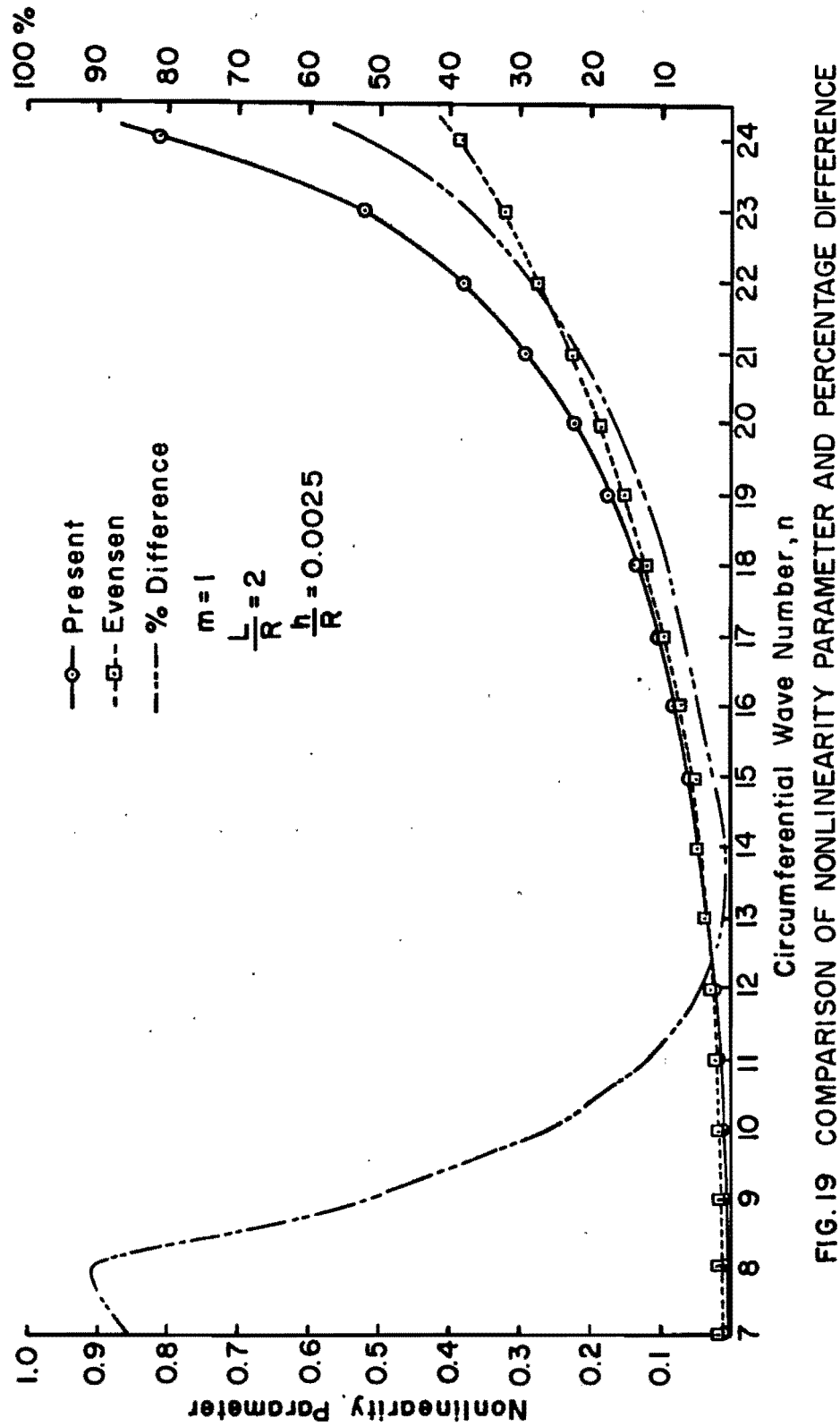

FIG. 19 COMPARISON OF NONLINEARITY PARAMETER AND PERCENTAGE DIFFERENCE

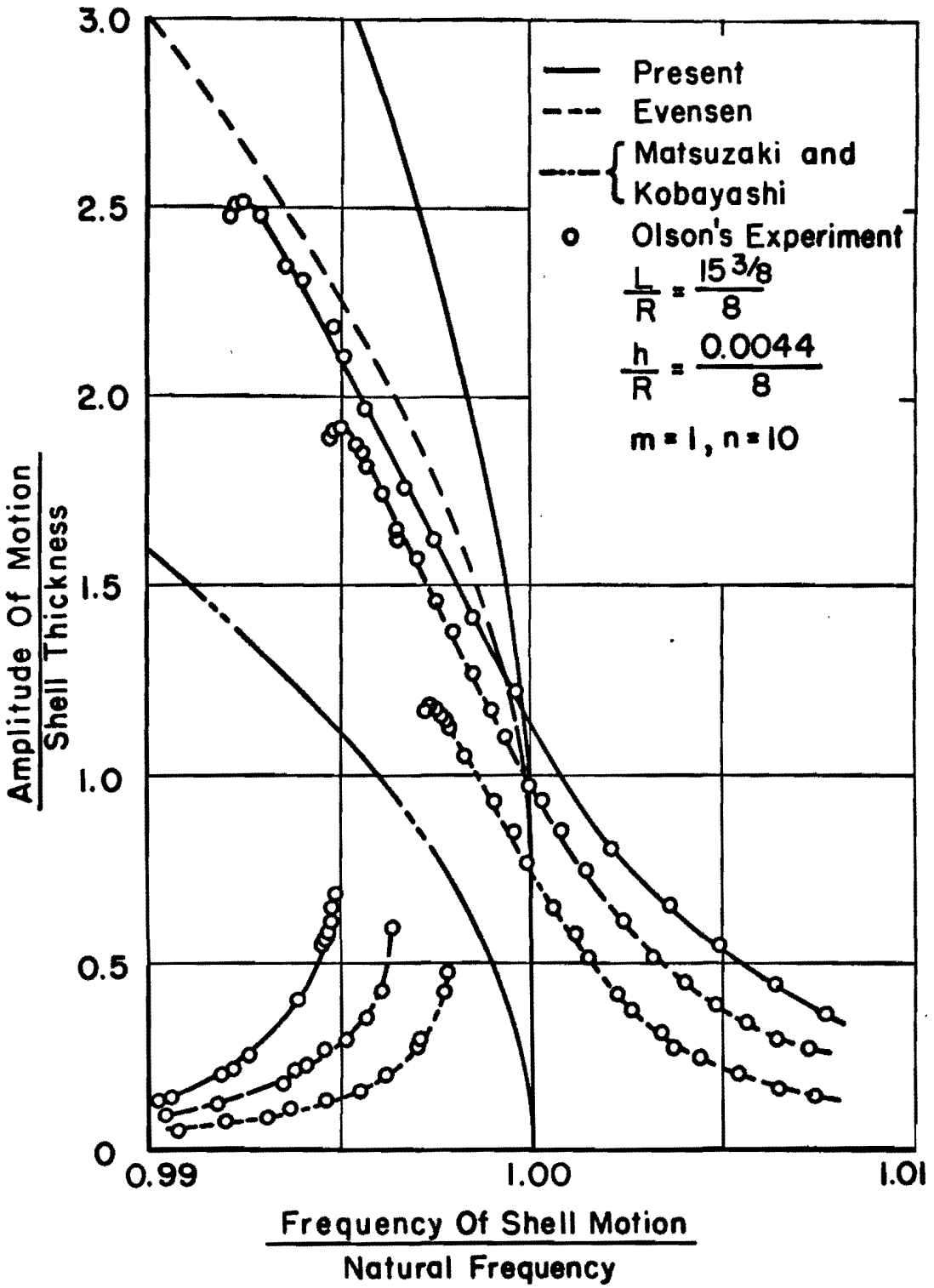

FIG. 20 COMPARISON OF NONLINEARITY

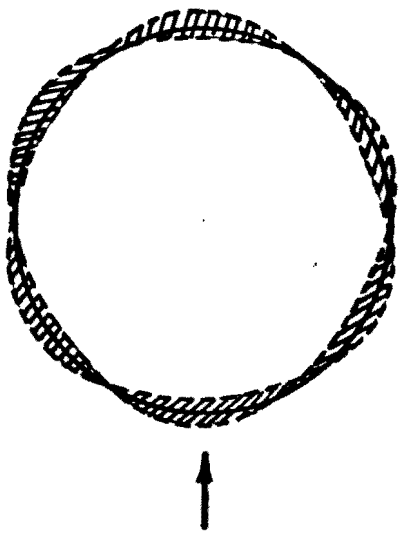

$W(\theta,t) = a \cos n\theta \cos \omega t$

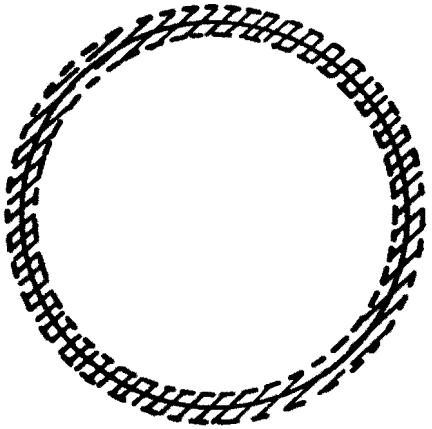

$W(\theta,t) = a \cos n\theta \cos \omega t + b \sin n\theta \sin \omega t$

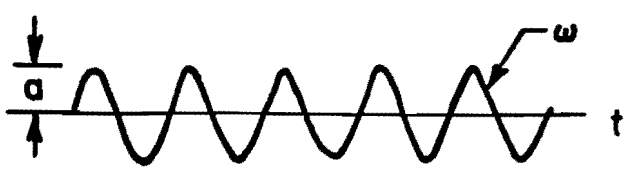

Standing Wave

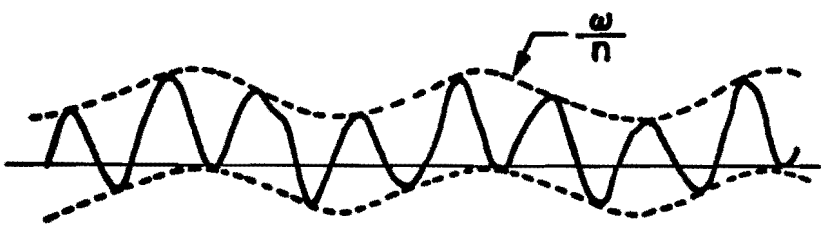

Traveling Wave

FIG. 21 STANDING AND TRAVELING WAVE RESPONSE

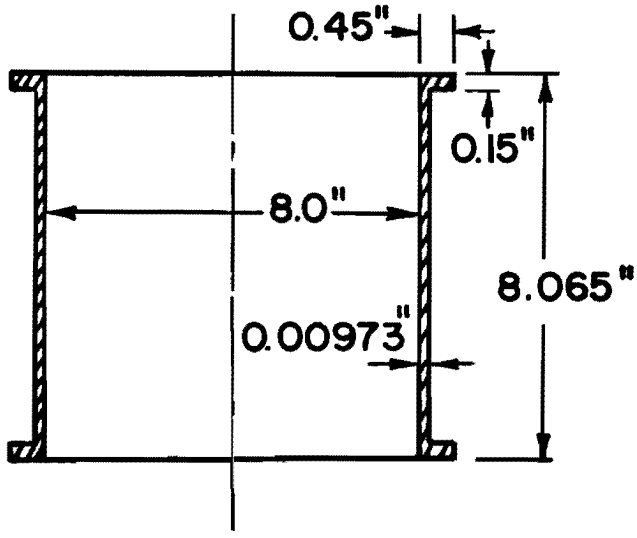

Density $\rho = 0.101$ lb./in.^{3}

Young's Modulus $E = 10.3 \times 10^6$ psi

Poisson's Ratio $\nu = 0.31$

FIG. 22 PROPERTIES OF SHELL-RING SPECIMEN

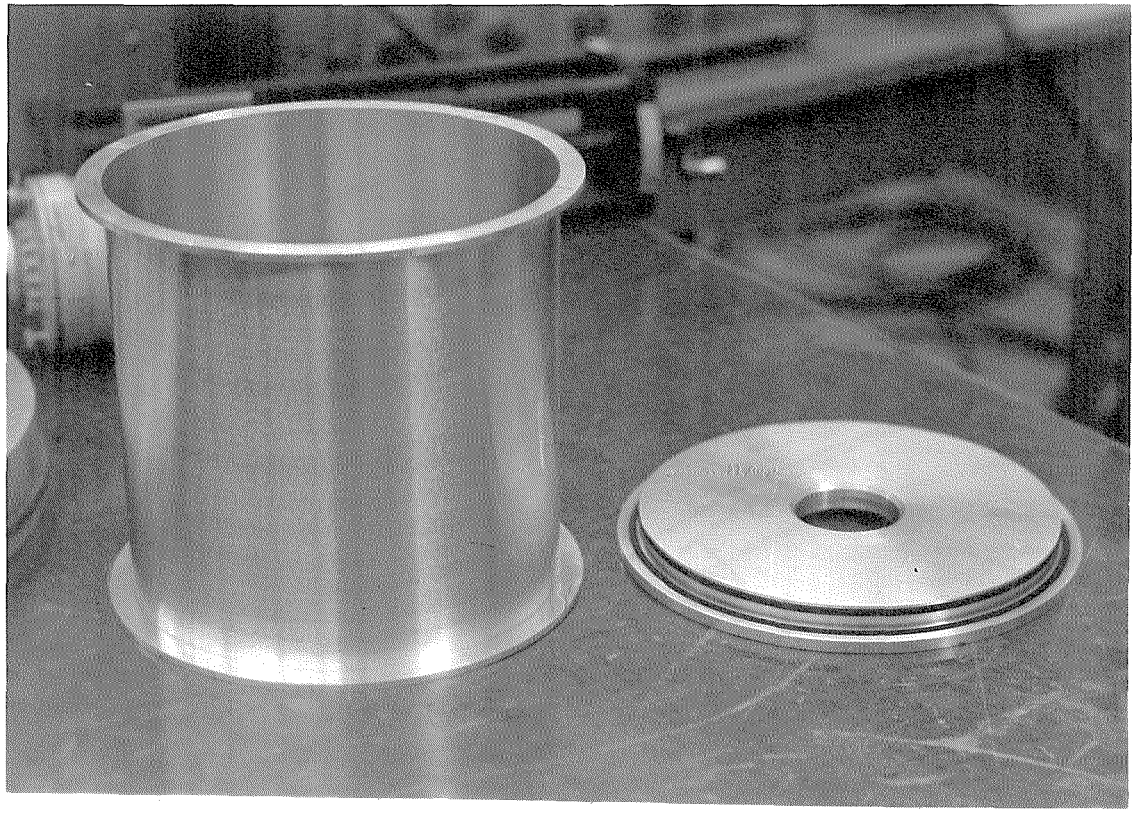

FIG. 23 SHELL SPECIMEN AND SUPPORT PLATE

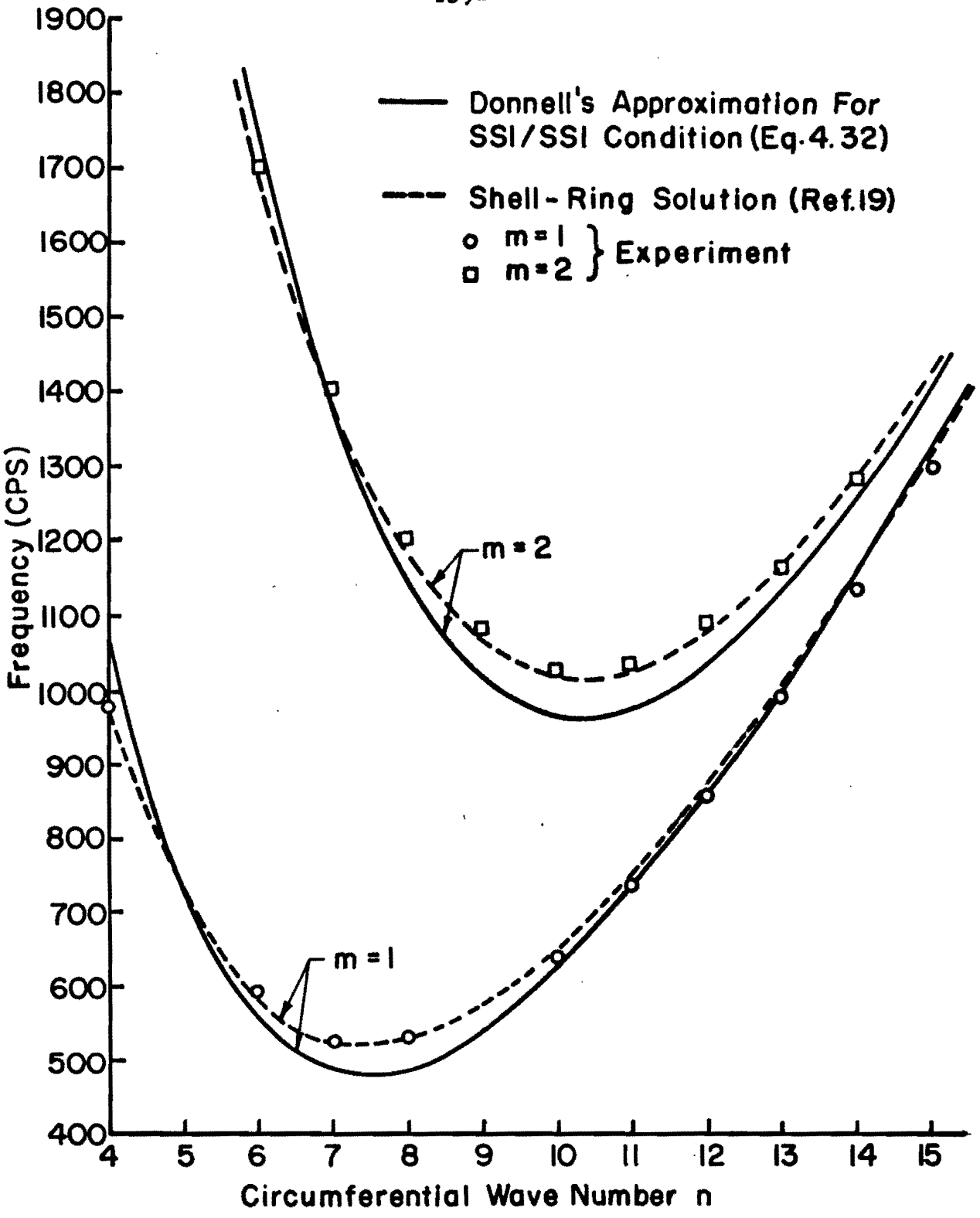

FIG. 24 FREQUENCY SPECTRUM OF SHELL SPECIMEN

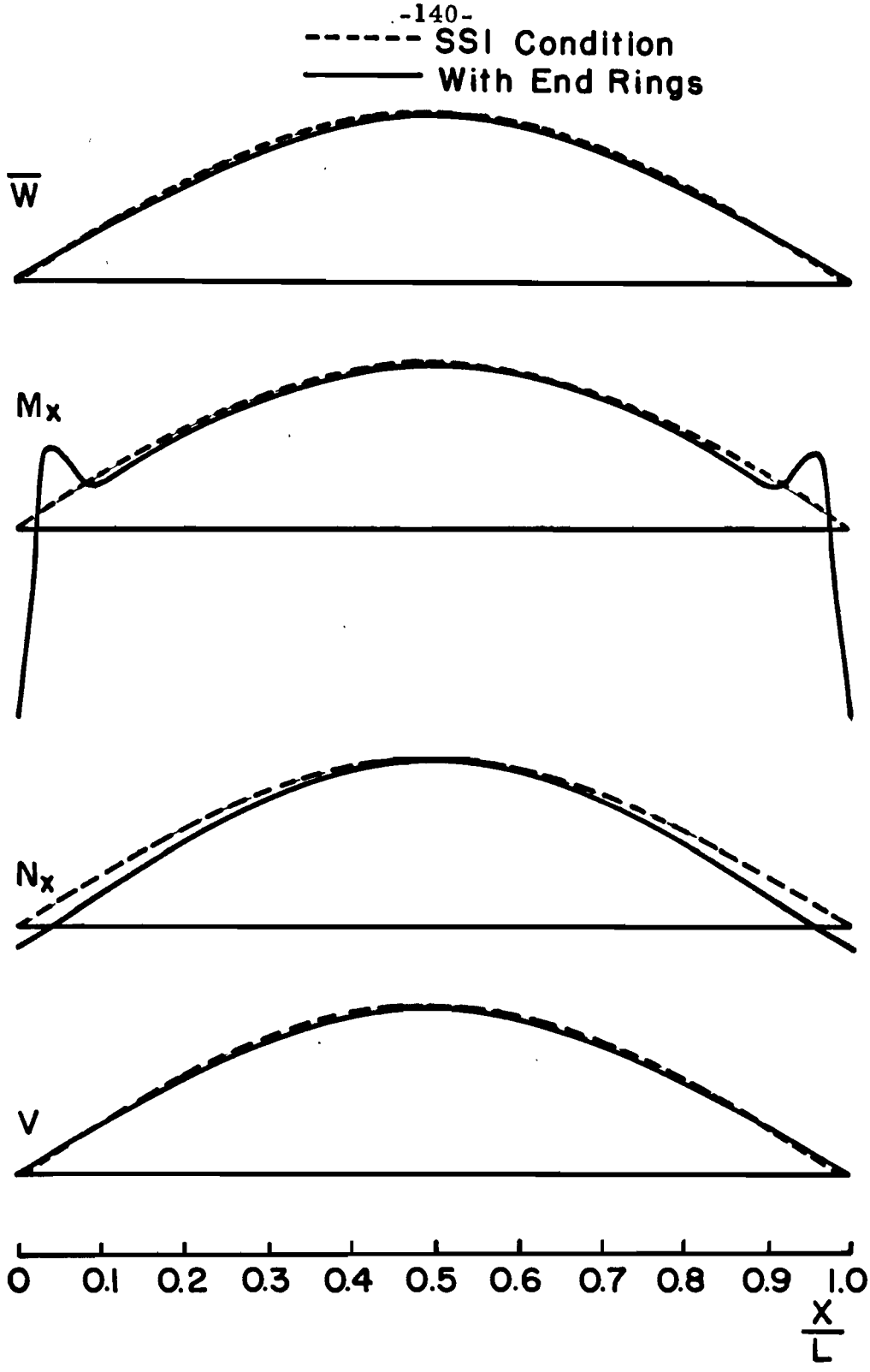

FIG. 25 CALCULATED AXIAL MODE SHAPES OF SHELL SPECIMEN

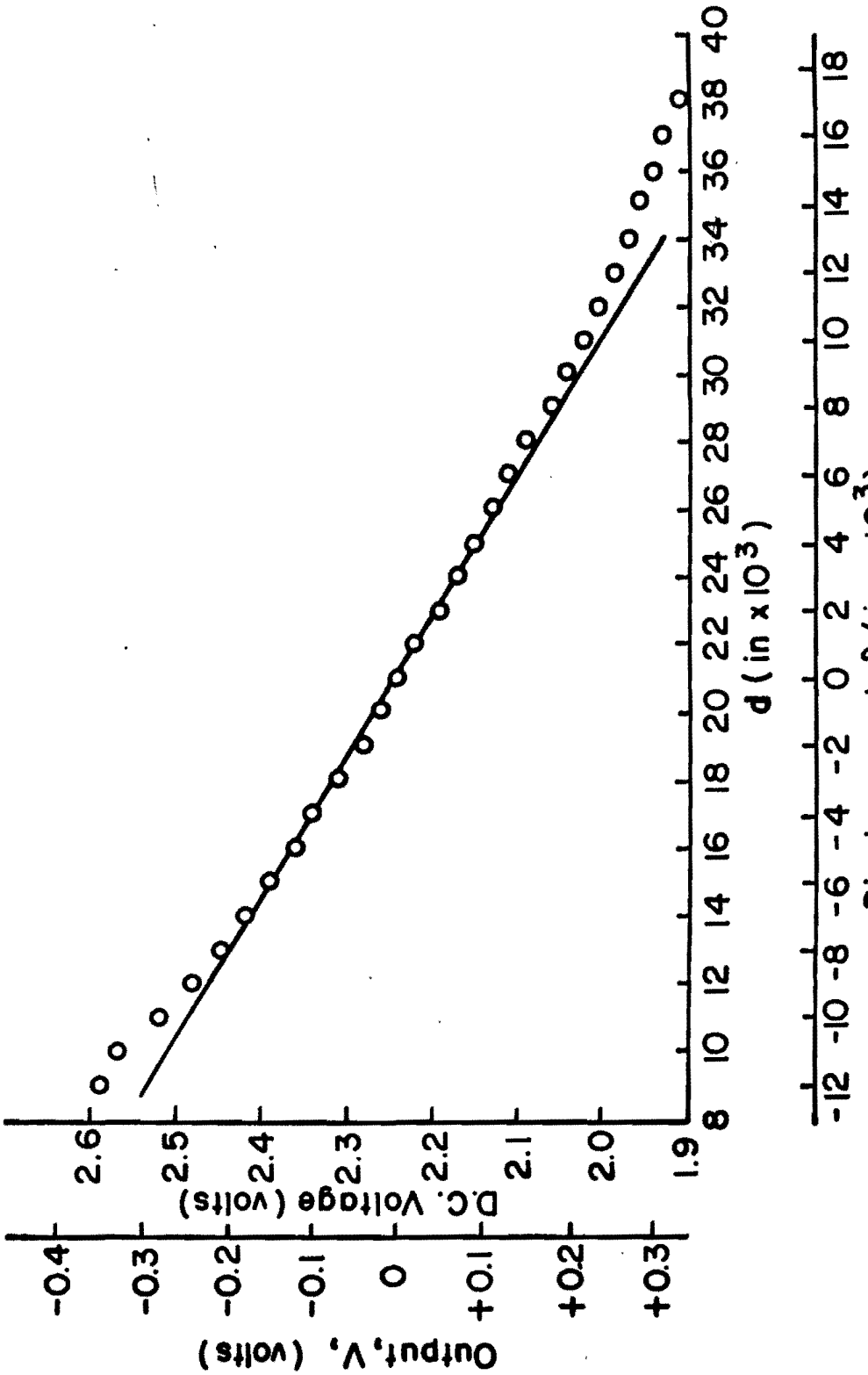

FIG. 26 CALIBRATION OF RELUCTANCE PICK UP

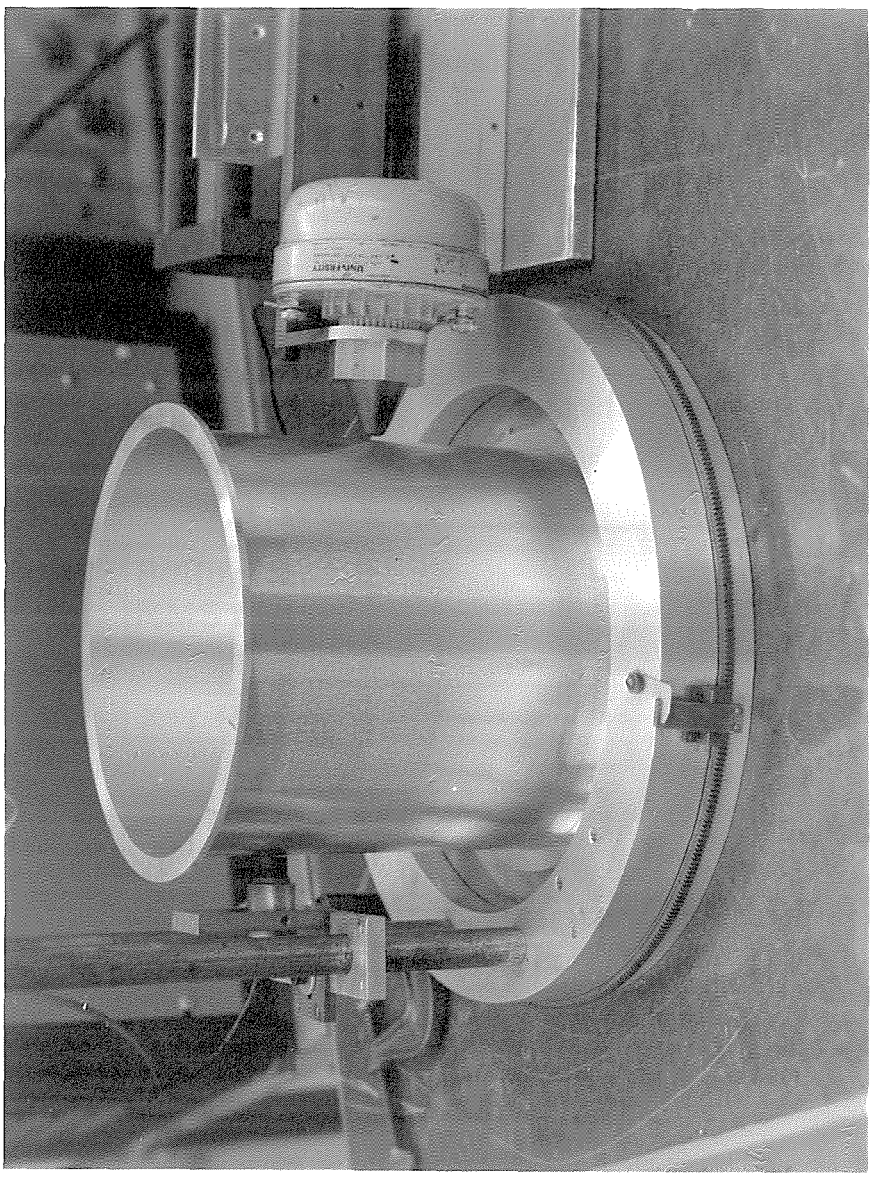

FIG. 27 ARRANGEMENT OF ACOUSTIC DRIVER AND RELUCTANCE PICKUP

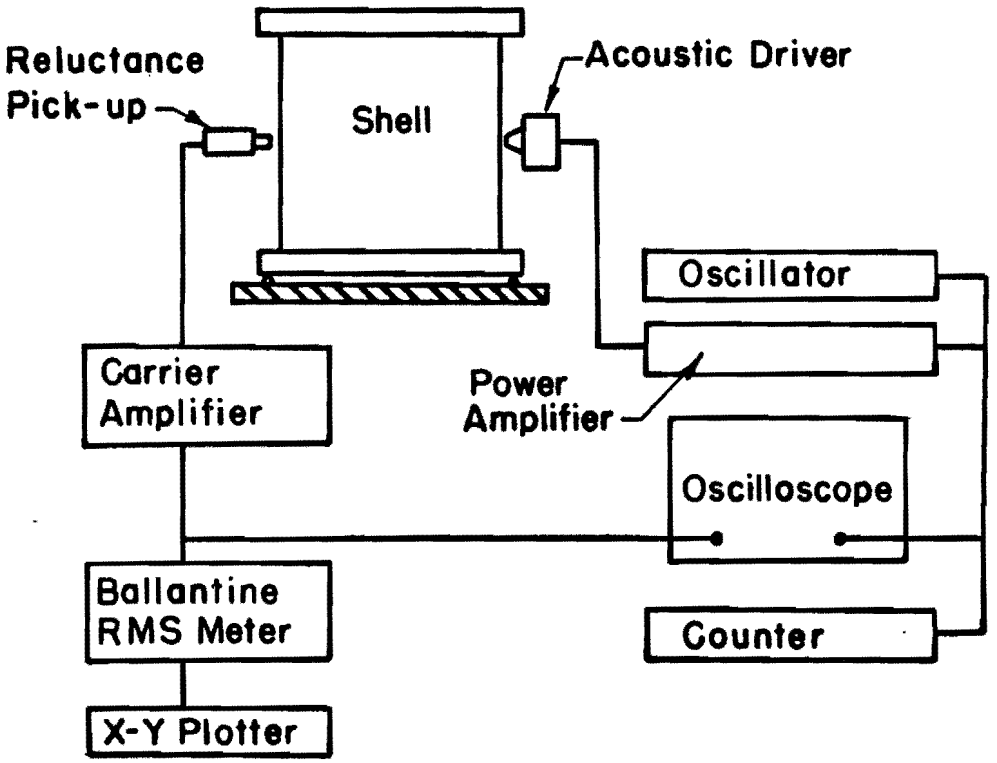

FIG. 28 SCHEMATIC DIAGRAM OF INSTRUMENTATION ARRANGEMENT

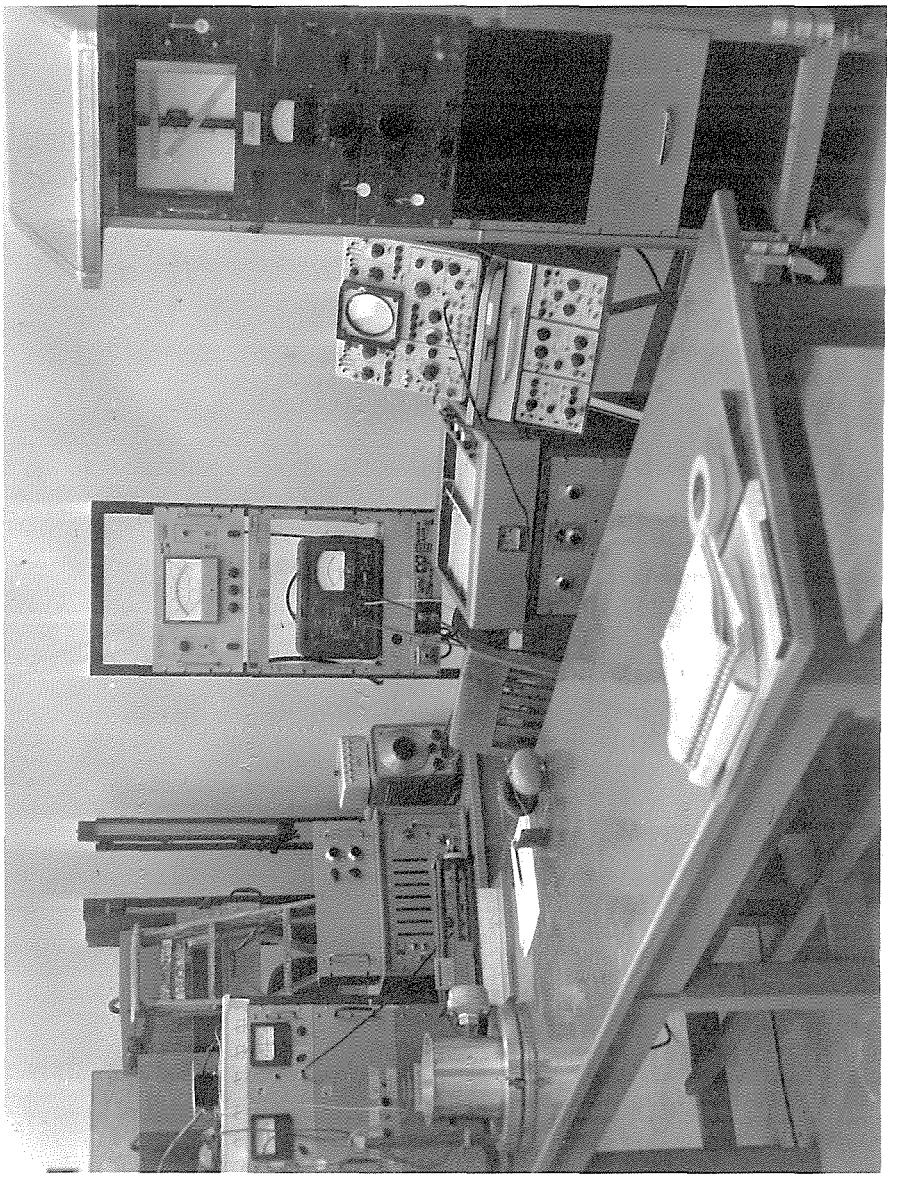

FIG. 29 INSTRUMENTATION SET-UP

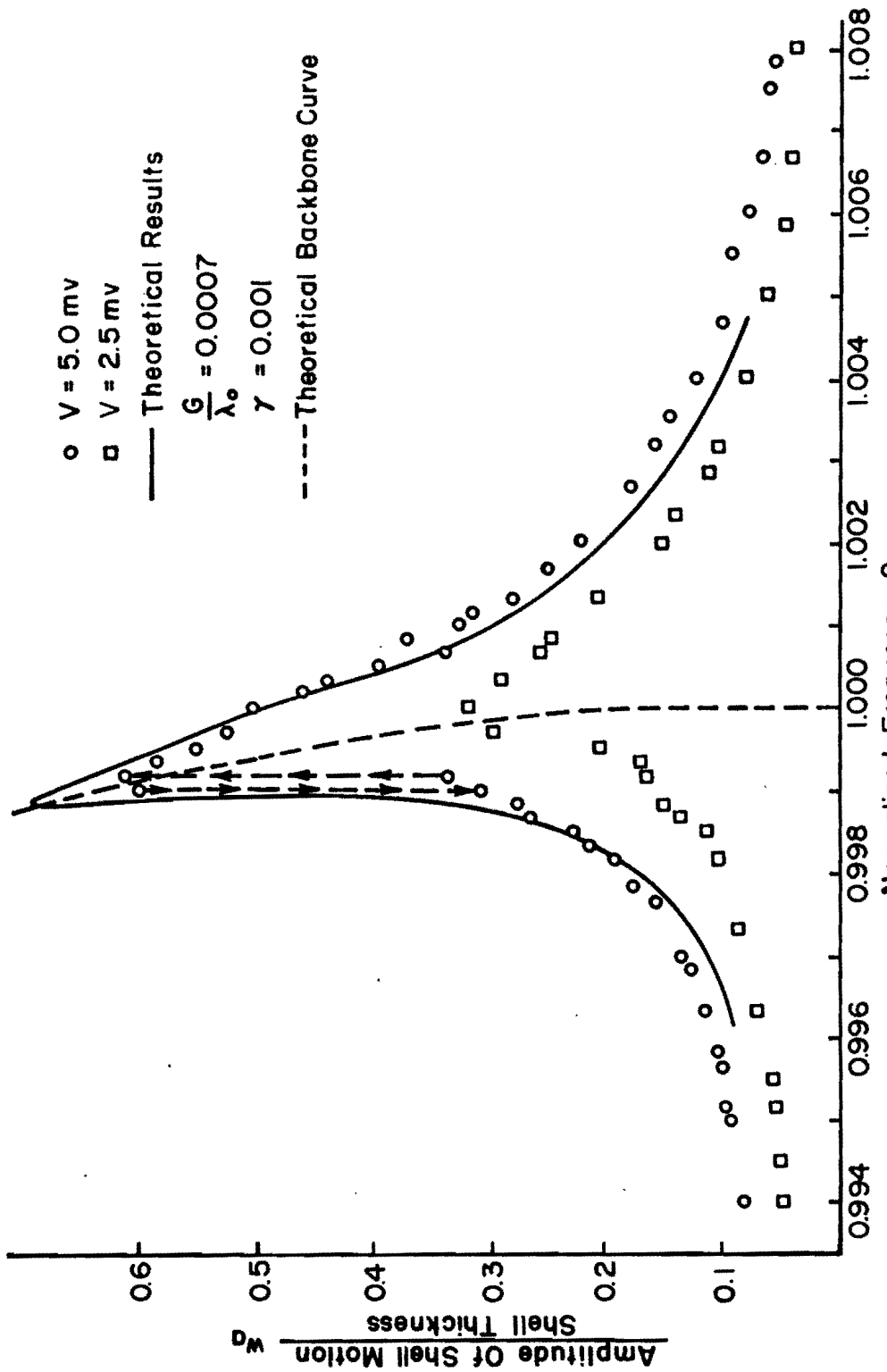

FIG. 30 RESPONSE-FREQUENCY RELATIONSHIP OF DRIVEN MODE m = 1, n = 6

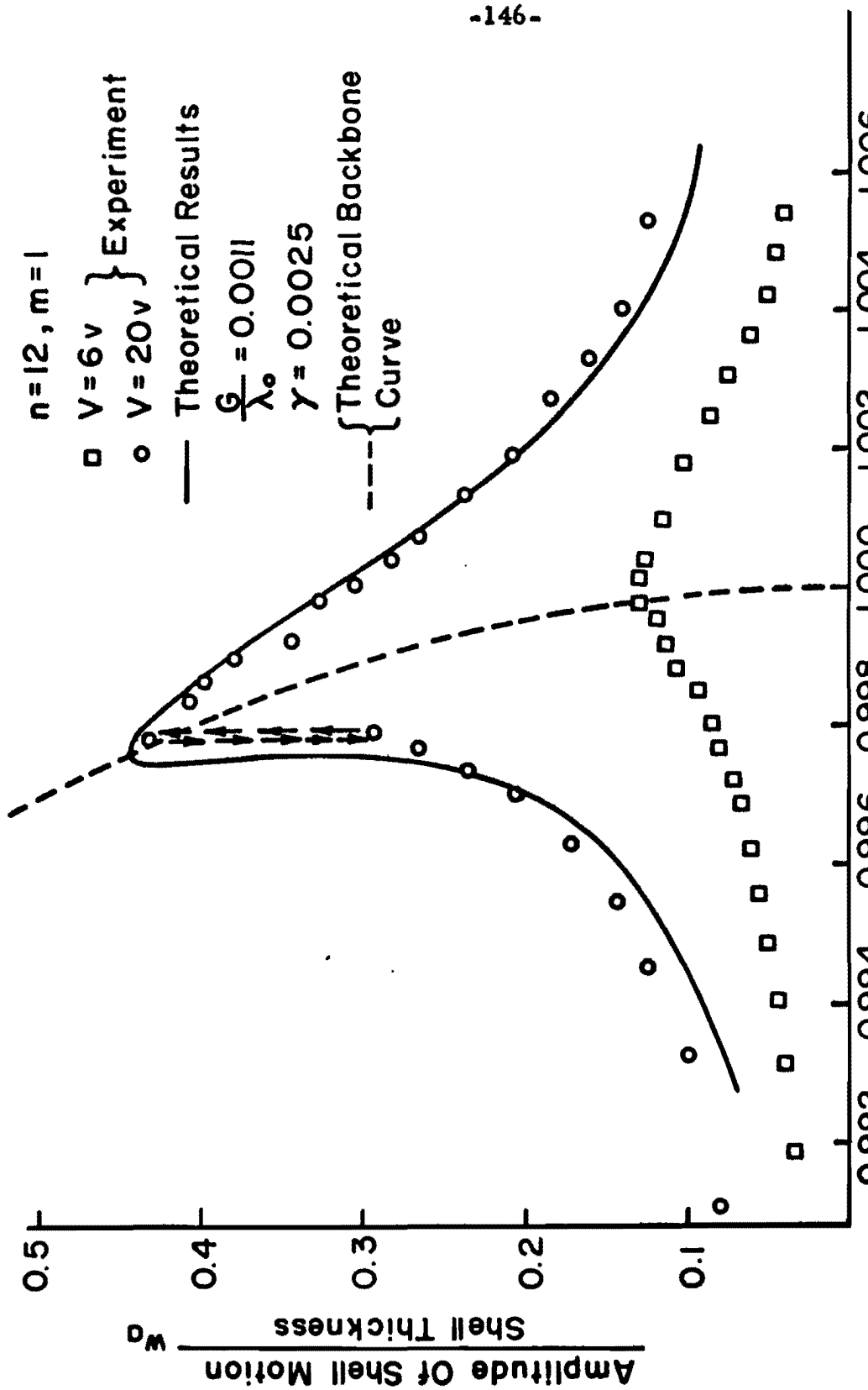

FIG. 31 RESPONSE-FREQUENCY RELATIONSHIP OF DRIVEN MODE

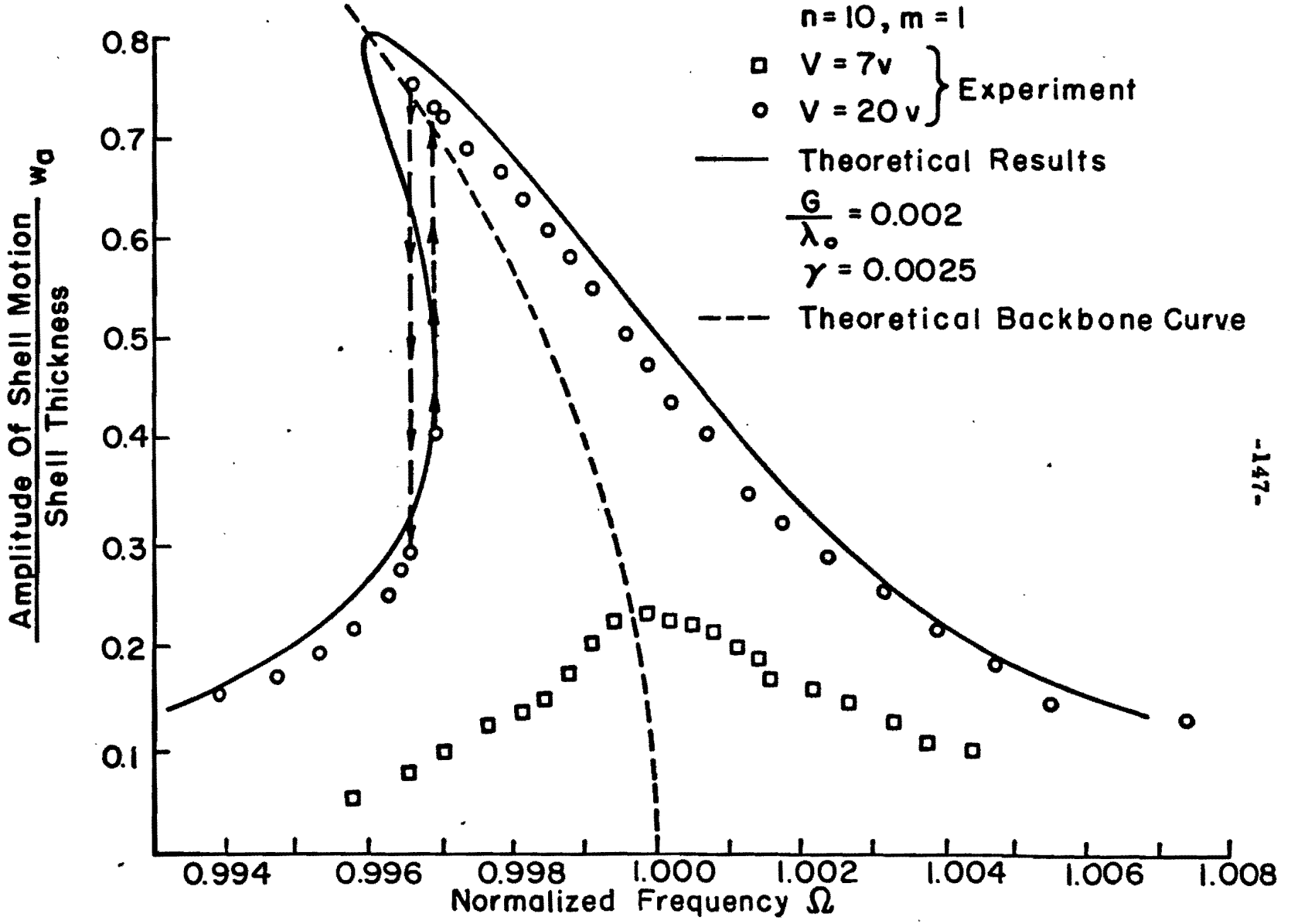

FIG. 32 RESPONSE-FREQUENCY RELATIONSHIP OF DRIVEN MODE

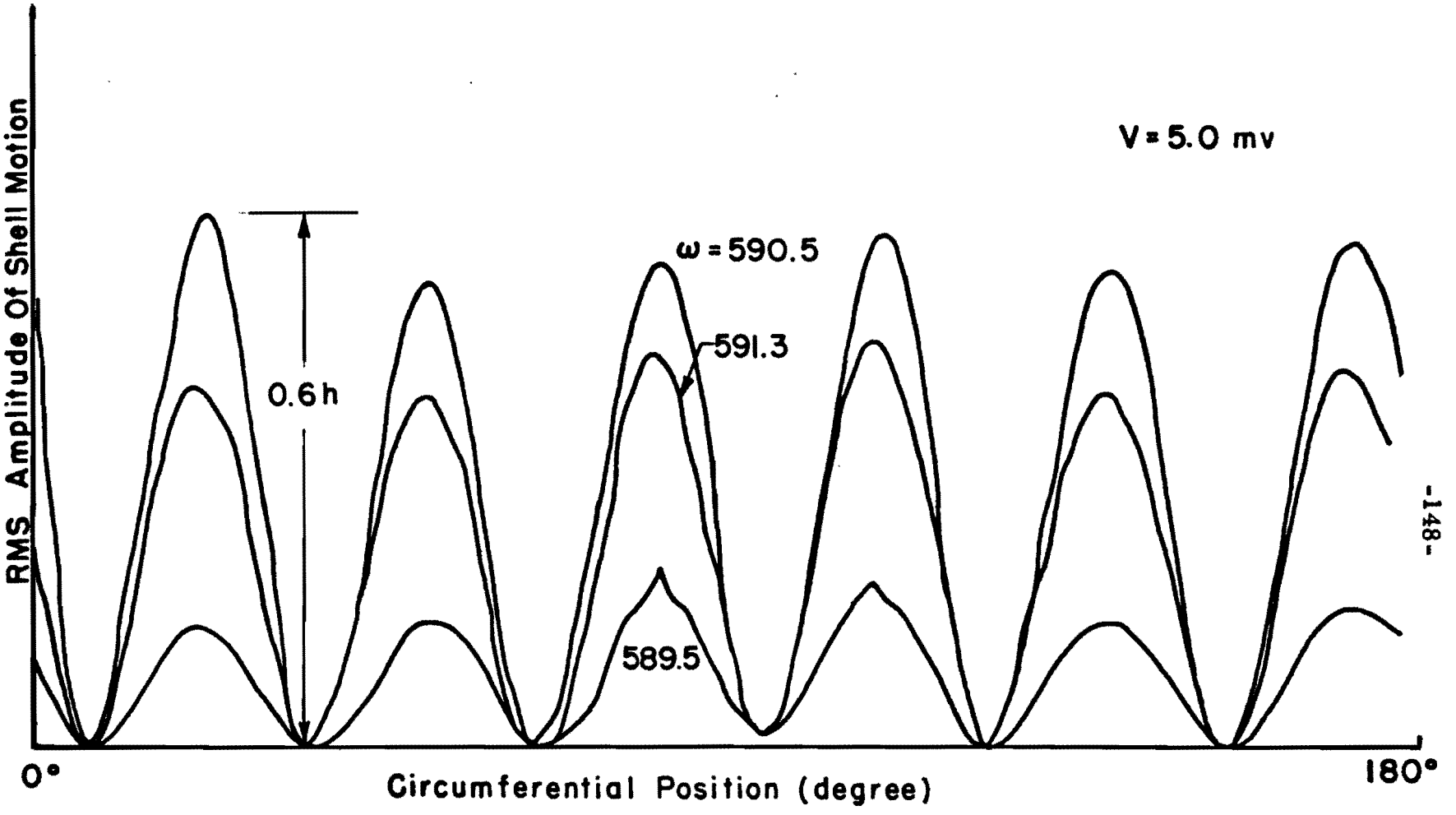

FIG.33 MODE SHAPES FOR m = 1 , n = 6

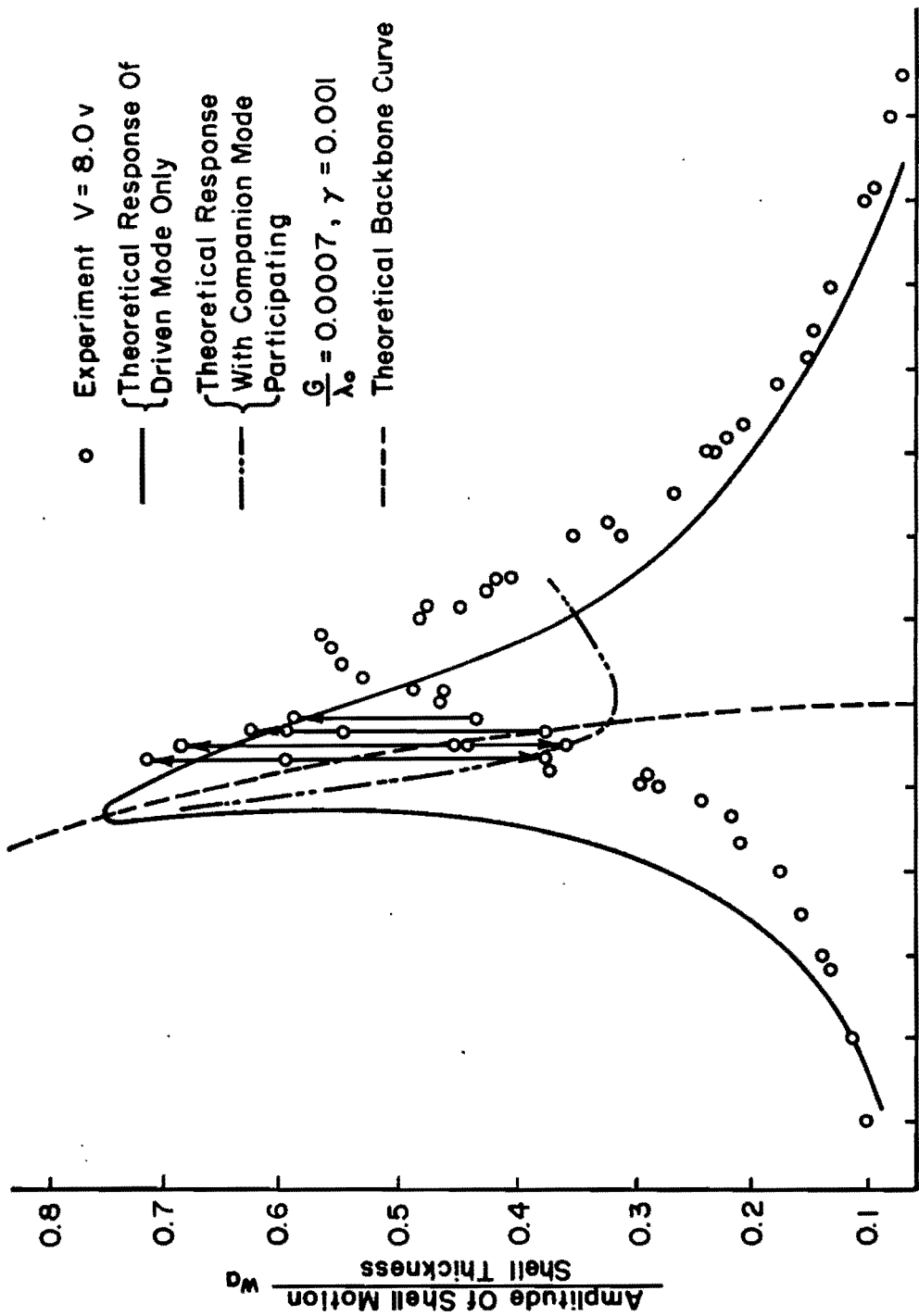

FIG.34 RESPONSE-FREQUENCY RELATIONSHIP OF DRIVEN MODE m = 1, n = 6

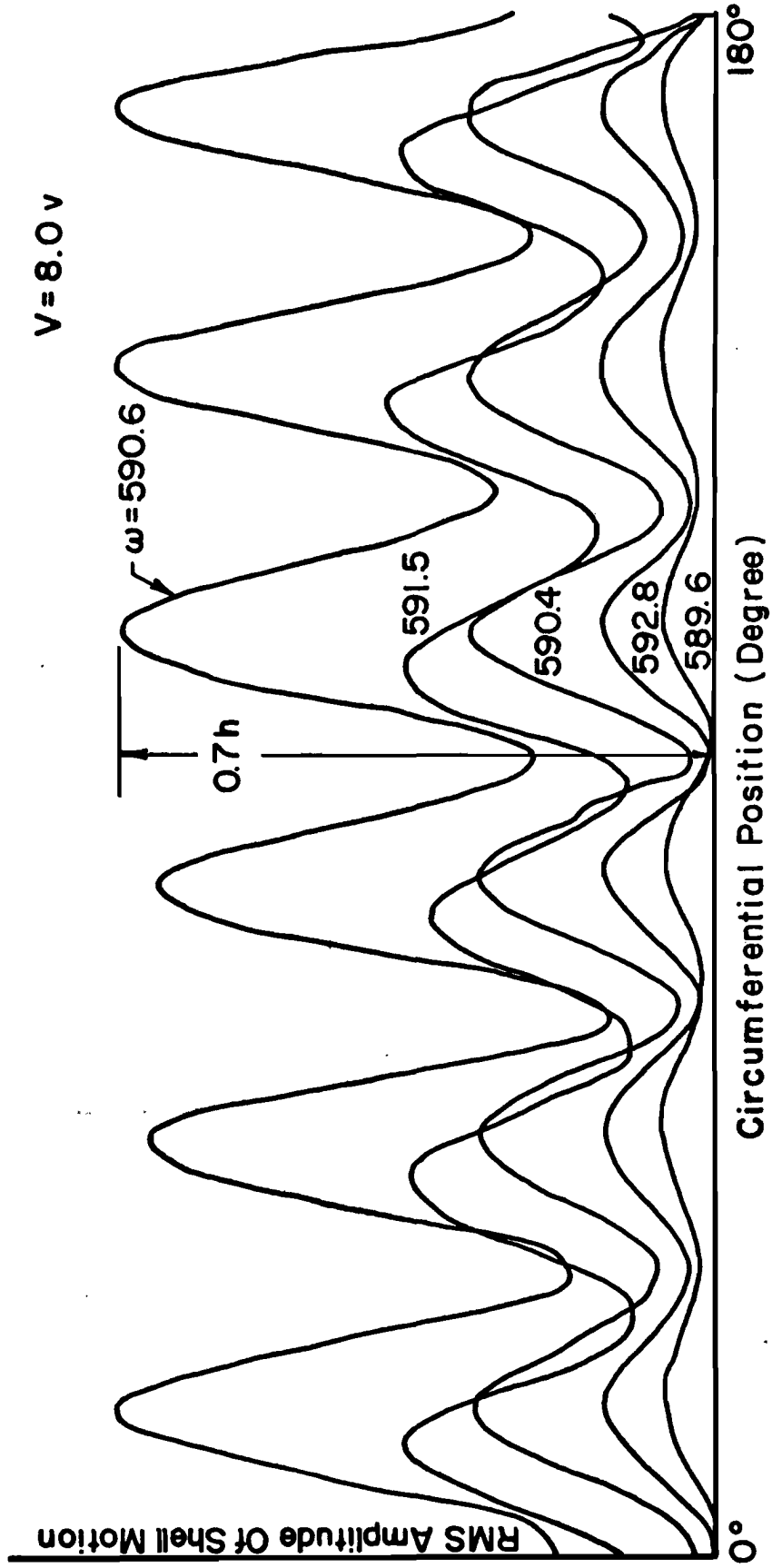

FIG. 35 MODE SHAPES FOR m = 1, n = 6

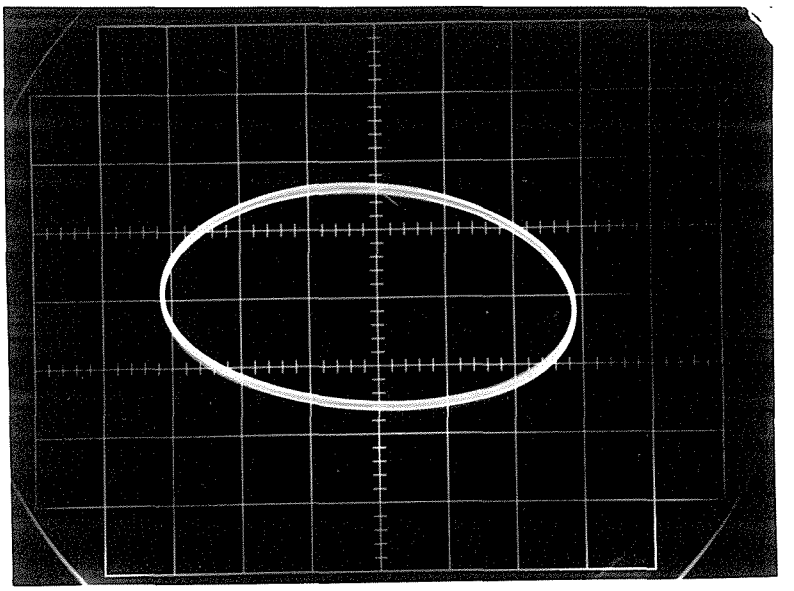

FIG. 36 LISSAJOUS FIGURE AT ANTINODE OF COS(nθ)

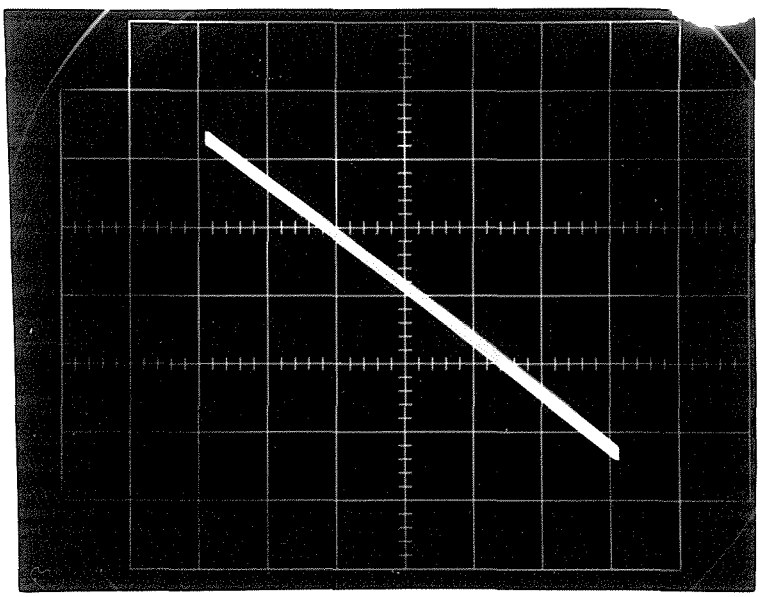

FIG. 37 LISSAJOUS FIGURE AT NODE OF COS(nθ)

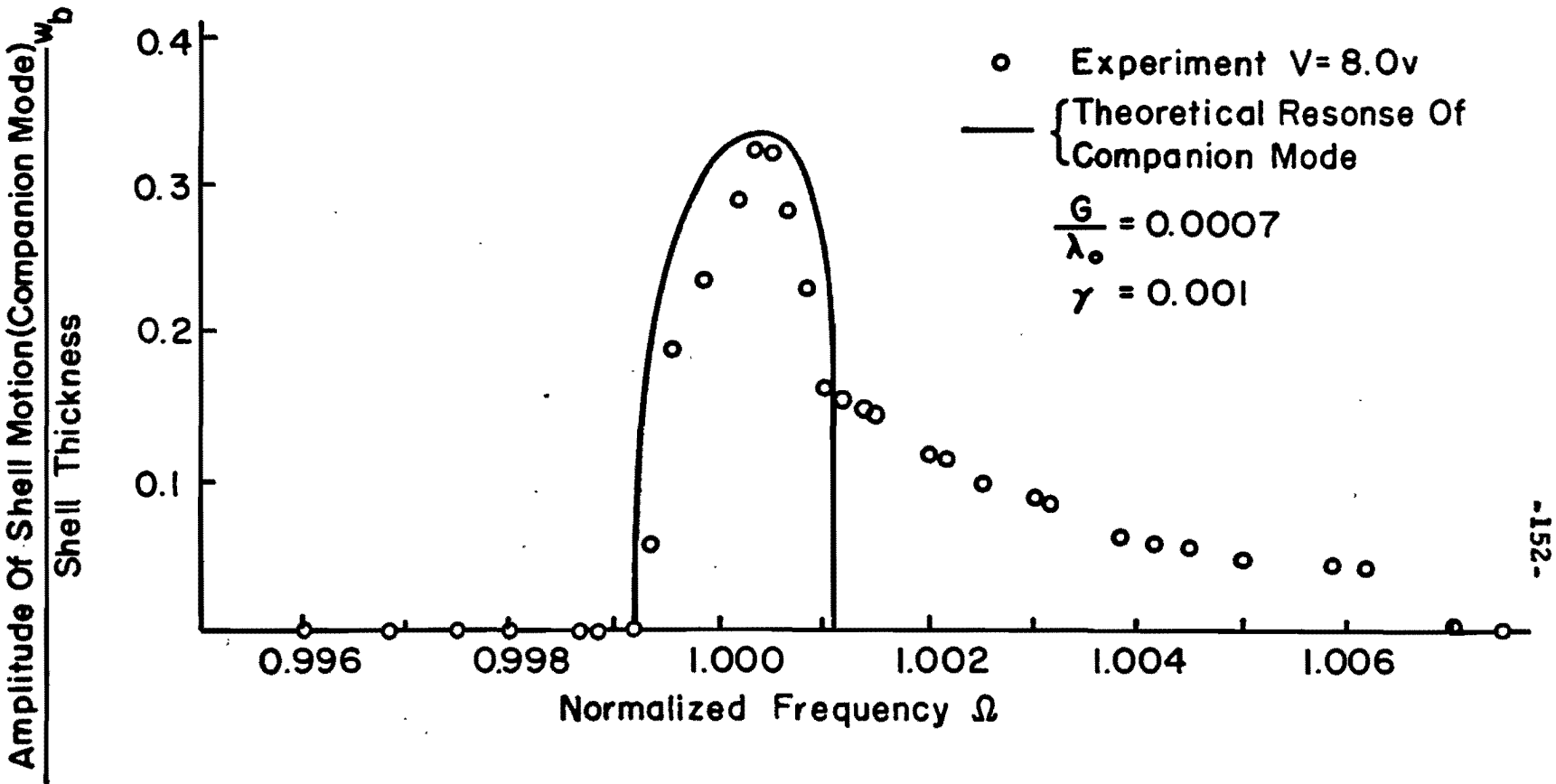

FIG. 38 RESPONSE-FREQUENCY RELATIONSHIP OF COMPANION MODE m=1, n=6

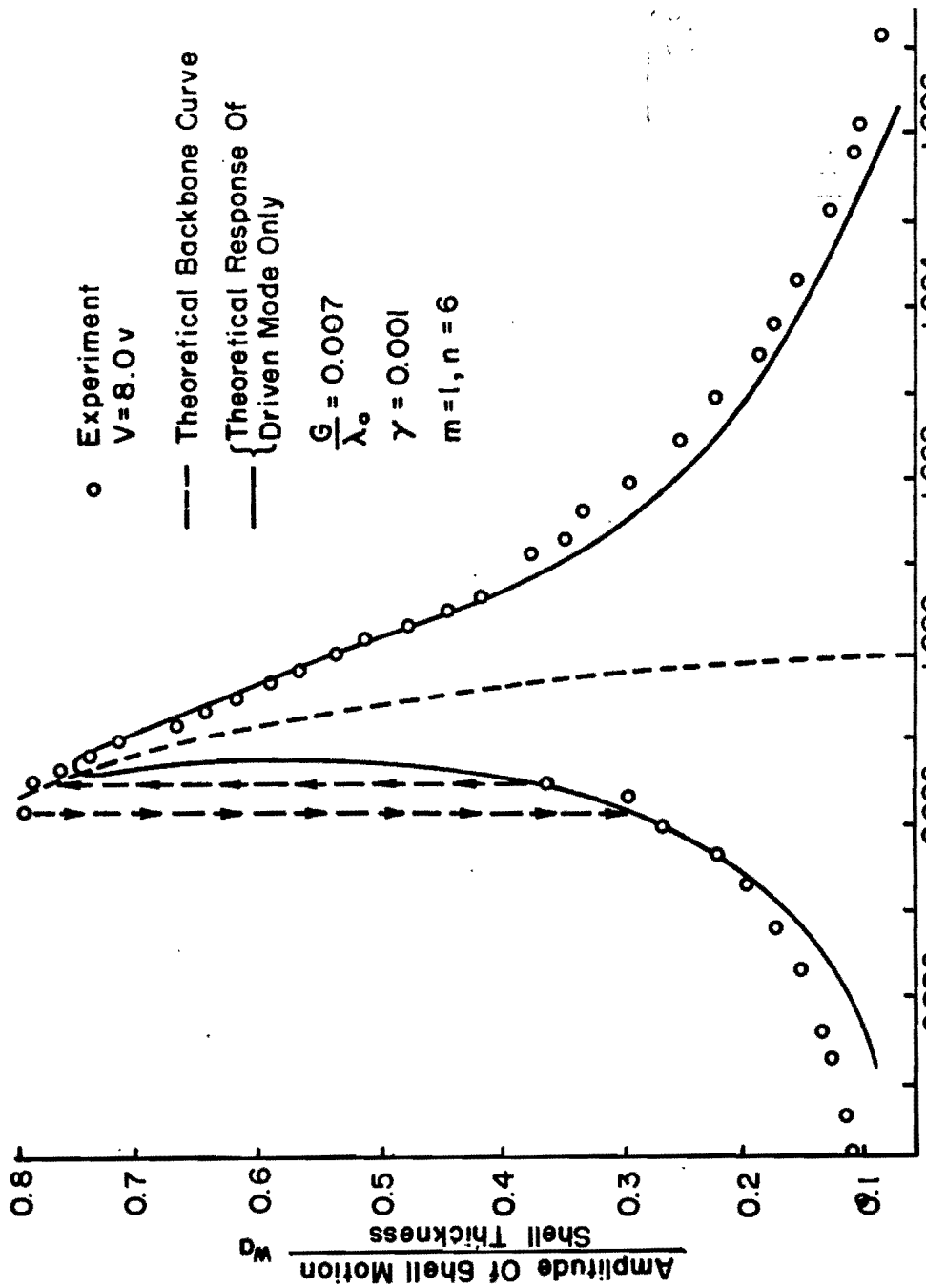

FIG.39 RESPONSE-FREQUENCY RELATIONSHIP OF DRIVEN MODE WITH ADDITIONAL CONSTRAINT

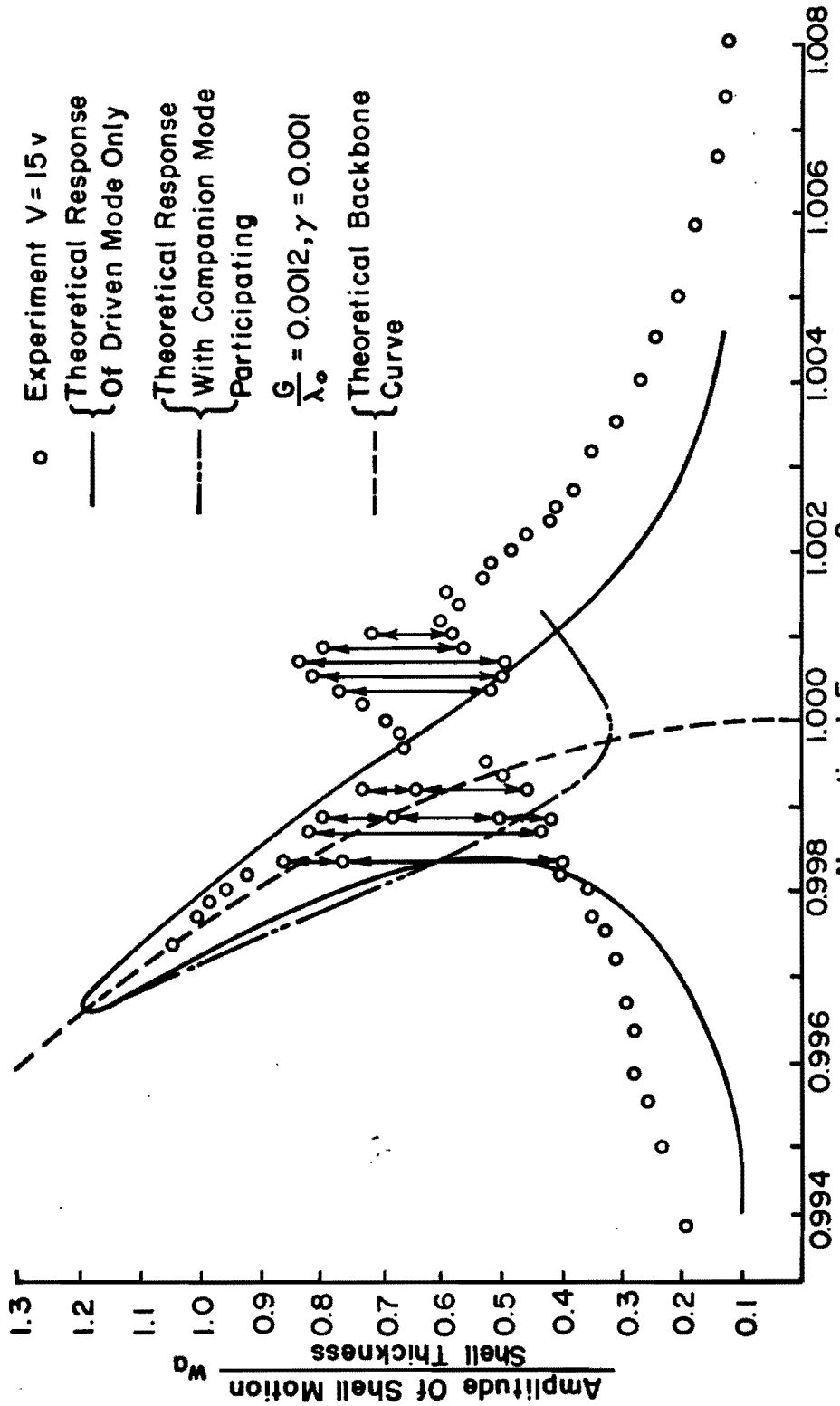

FIG. 40 RESPONSE-FREQUENCY RELATIONSHIP OF DRIVEN MODE m=1, n=6

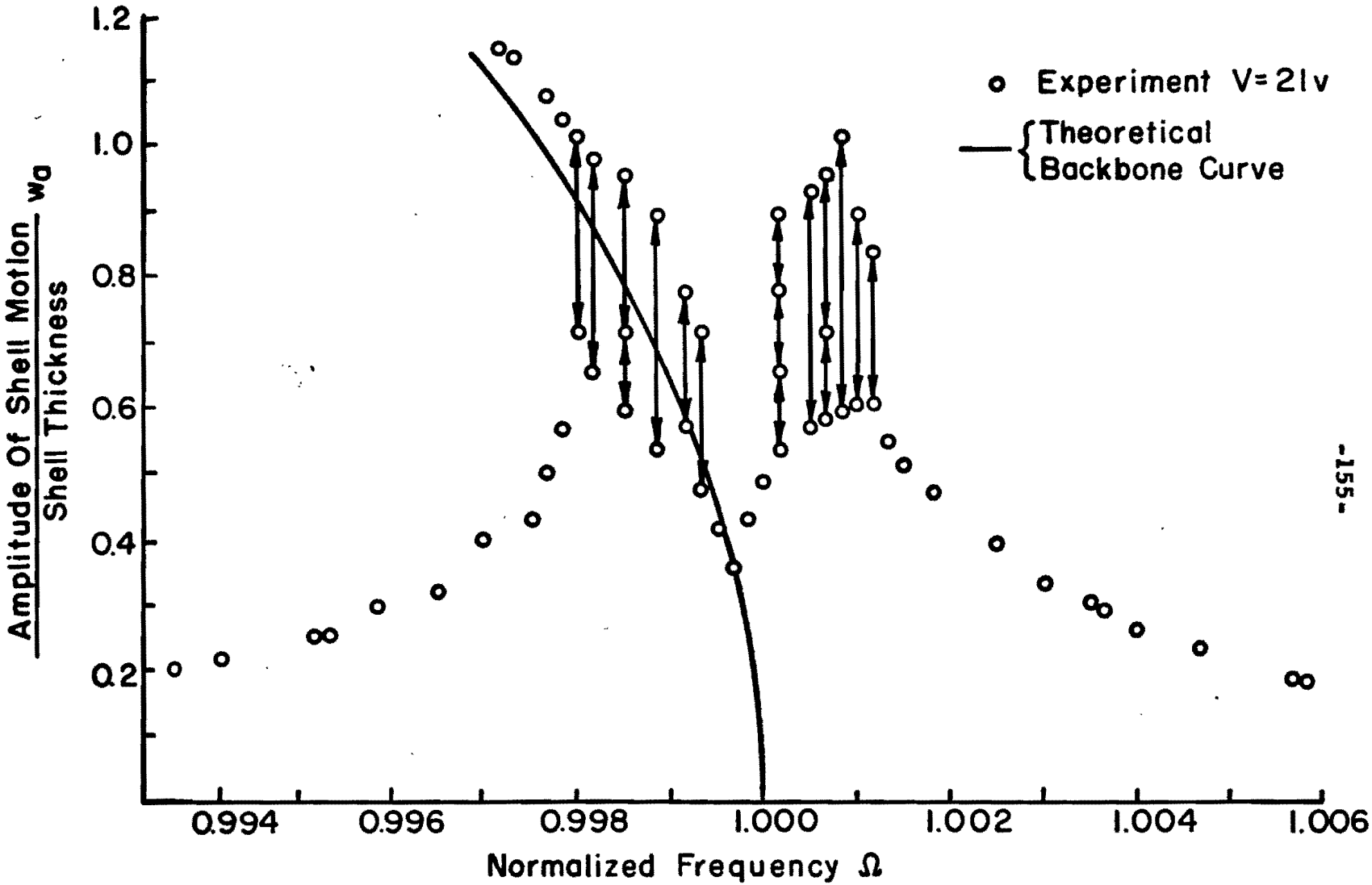

FIG. 41 RESPONSE-FREQUENCY RELATIONSHIP OF DRIVEN MODE m=1, n=6

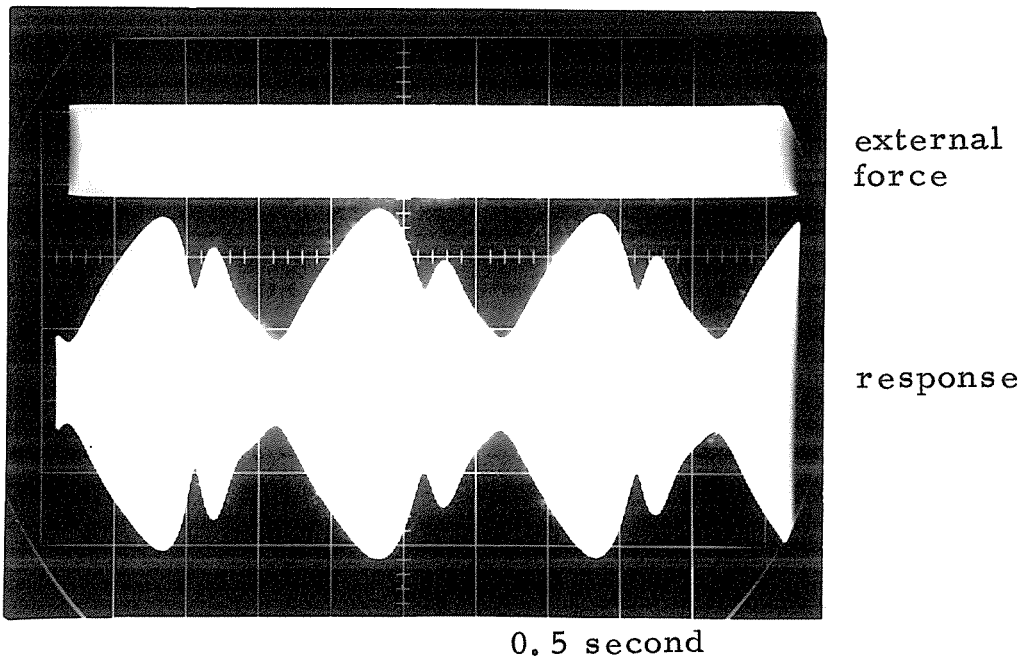

FIG. 42 DRIFTING PHENOMENON OF RESPONSE

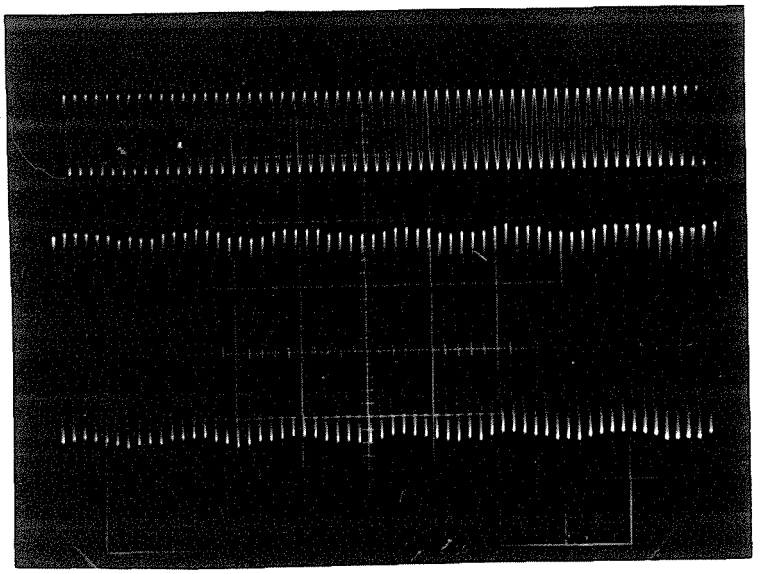

frequency = 590.7 cps

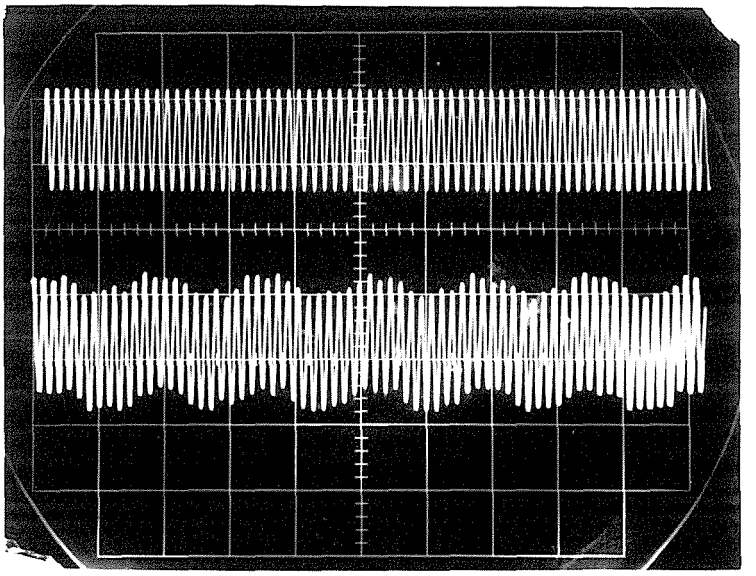

frequency = 591.2 cps

FIG. 43 TRAVELING WAVE PHENOMENON

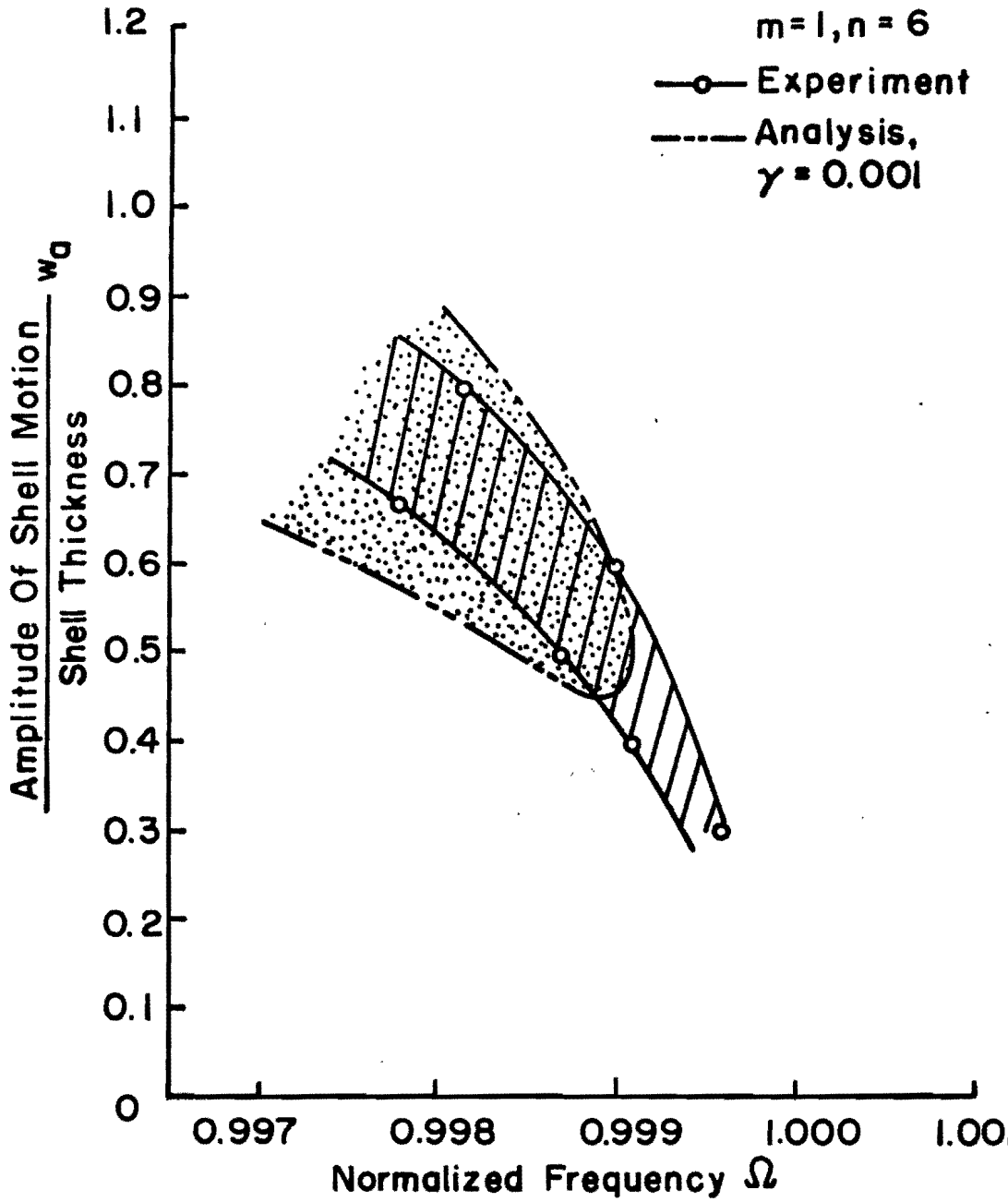

FIG. 44 REGION OF JUMP PHENOMENA

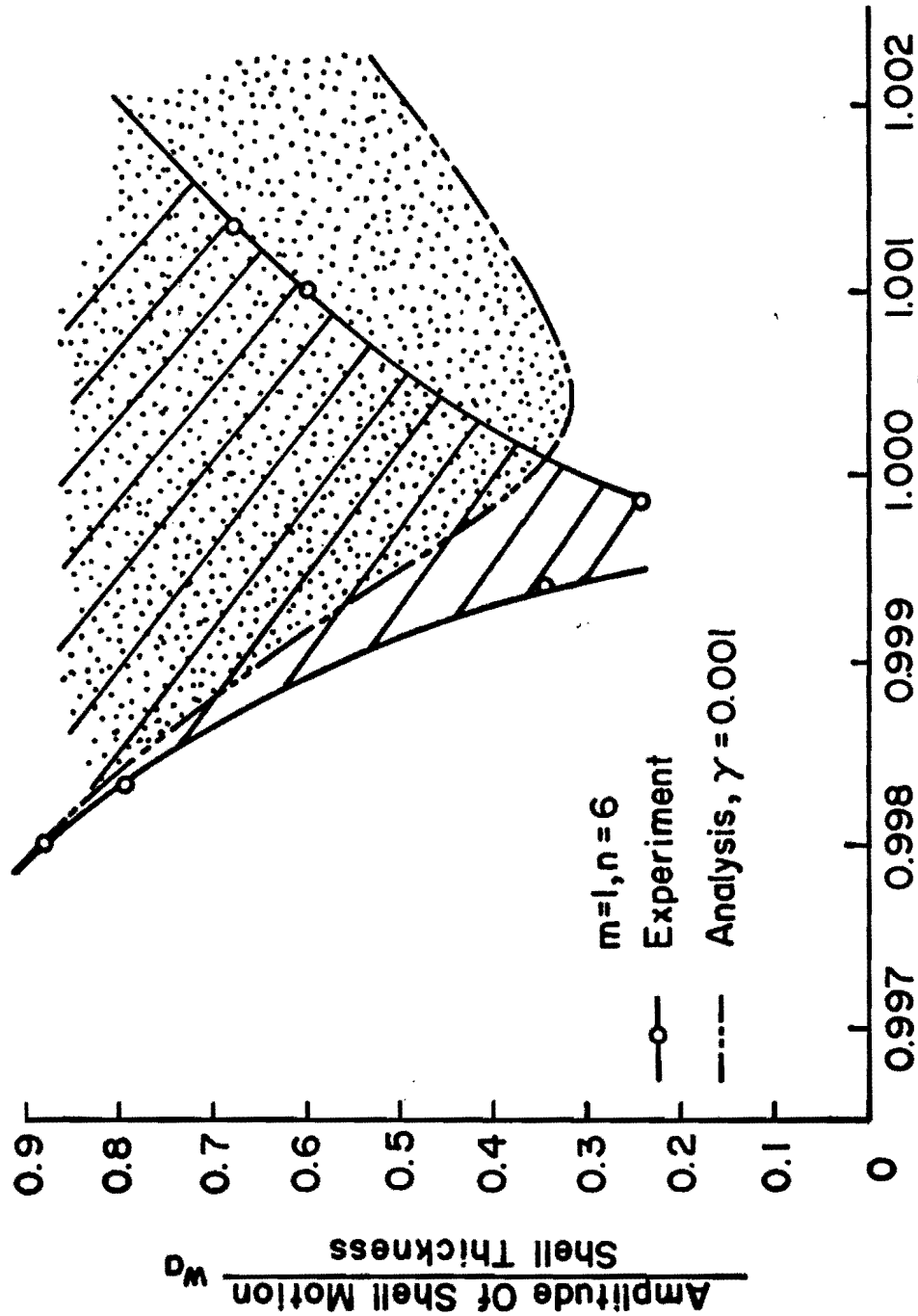

FIG. 45 REGION OF COMPANION MODE PARTICIPATION